Carl von Ossietzky

Universität Oldenburg

Masterstudiengang Biologie

Masterarbeit

Expression of cpCx43.4 and cpCx47.6 in the carp retina.

vorgelegt von Nicole Seggewiß

Betreuende Gutachterin: Apl. Prof. Dr. Ulrike Janssen-Bienhold
Zweite Gutachterin: Dr. Karin Dedek

Oldenburg, den 18.10.2010

Summary

Gap junctions represent the most common form of intercellular communication in vertebrates. A single gap junction channel is composed of two integral membrane protein complexes, called connexons, which consist in turn of six connexins. By screening zebrafish connexins, 37 putative connexin genes were identified in this specie (Eastman et al., 2005). Some of these connexins, e.g. zfCx27.5, zfCx35, zfCx43, zfCx52.6 and zfCx55.5 were first found in the retina. Due to the fact that the vertebrate retina is strictly layered and has a relatively small number of neurons with various types of interconnections, the retina is ideally suited as a model to study the role of gap junctions in the central nervous system.

Within this study two carp connexins cpCx43.4 and cpCx47.6 were analyzed. By means of fluorescence in situ hybridization combined with indirect immunofluorescence, the expression of both connexins was identified in GABAergic amacrine cells. Whereas cpCx43.4 was expressed in amacrine cells in the INL and in displaced ones in the GCL, cpCx47.6 expression was exclusively found in amacrine cells in the proximal INL. Further characterization of these cells indicated that the GABAergic amacrine cells, expressing either cpCx43.4 or cpCx47.6 even contain nitric oxide as second neurotransmitter. For cpCx47.6 expressing cells there was also evidence of a co-expression of acetylcholine.
By expression studies of both connexins in N2A cells, it was evidenced that an antibody against the cytoplasmic loop of the homologous mouse connexin mmCx45 cross-react with cpCx43.4 and cpCx47.6. Putative gap junction plaques were detected by the antibody, indicating a correct expression of functional connexins which were integrated into the membrane. Due to the fact, that cpCx43.4 expressing N2A cells started to die after transfection and that the cell death was abolished by enhanced calcium there was evidence that cpCx43.4 forms functional hemichannels.

A second project dealt with the specificity of an antibody against the cytoplasmic terminal of cpCx53.8. The specificity of cpCx53.8 antibody was analyzed in the case of detecting two related zebrafish connexins zfCx52.7 and zfCx52.9. No zebrafish connexin was labeled upon expression in N2A cells, which ruled out the specificity of the cpCx53.8 antibody.

Table of contents

I   List of abbreviations

AC	amacrine cell
Amp	ampicillin
AP	alkaline phosphatase
APS	ammonium persulfate
BCIP	5-bromo-4-chloro-3-indolylphosphate
β-ME	β-mercaptoethanol
bp	base pair
BSA	bovine serum albumin
cAMP	cyclic adenosin-3´-5´-monophosphate
cDNA	complementary DNA
CF	cytosolic fraction
CL	cytoplasmic loop
CMV	*cytomegalovirus*
cp	carp (*Cyprinus carpio*)
cRNA	complementary RNA
Cx	connexin
Da	Dalton
ddH2O	double distilled water
DEPC	diethyl-pyro carbonate
DIG	digoxiginin
DKS	donkey serum
DMEM	Dulbecco´s Modified Eagle Medium
DNA	desoxyribonucleotide acid
DNAse	desoxyribonuclease
dNTPs	2´-desoxyribonucleosid-5-triphosphate
	(dATP, dCTP, dGTP und dTTP)
DTT	dithiothreitol
ECL	Enhanced Chemiluminescence
EDTA	ethylendiamintetraacetat
EGTA	ethylenglycol-bis-(2-aminoethyl)-tetraacetat
EGFP	*enhanced green fluorescent protein*
et al.	et alii
EtBr	ethidium bromide

FCS	fetal calf serum
FISH	fluorescence *in situ* hybridization
g	gravity (speed)
GCL	ganglion cell layer
gDNA	genomic DNA
HC	horizontal cell
hm	human
H$_2$O	water
HP2	homogenisation buffer
HRP	horse radish peroxidase
INL	inner nuclear layer
IPL	inner plexiform layer
IPTG	isopropyl-β-D-thiogalactoside
IRES	internal ribosome entry side
ISH	*in situ* hybridization
Kan	kanamycin
kb	kilo base pairs
kDa	kilo Dalton
LB	Luria Bertani, medium for bacteria
MCS	multiple cloning side
mHz	membrane fraction of mouse heart
mm	mouse (*mus musculus*)
mRNA	messenger RNA
NBT	nitroblue-tetrazoliumchloride
NGS	normal goat serum
OD	optical density
ONL	outer nuclear layer
OPL	outer plexiform layer
OS	outer segments
P1	crude membrane fraction
P2	membrane fraction
PAGE	polyacrylamid-gelelectrophoresis
PB	phosphate buffer
PBS	phosphate buffered saline
PCR	polymerase chain reaction
PFA	paraformaldehyde

pH	negative logarithm of the molar concentration of dissolved hydronium ions
RNA	ribonucleic acid
RNase	ribonuclease
rpm	rounds per minute
RT	reverse transcriptase or room temperature
SDS	sodiumdodecylsulfate
SSC	saline-sodiumcitrate-solution
SWF	small wide-flied amacrine cell
TBE	tris-boric acid-EDTA-electrophoresis buffer
TBST	tris-saline buffer with Tween-20
TH	total homogenate
TSA	tyramide signal amplification
U	unit
X-Gal	5-bromo-4-chloro-3-indoyl-b-D-galactoside
zf	zebrafish

II   List of figures and tables

1. Introduction

The coordinated interaction between cells is a prerequisite for the maintenance of a multicellular organism. During evolution, various channels of communication between organs, tissues and cells have developed. This includes interactions that are mediated via neuronal or endocrine mechanisms over long distances. There are also interactions, which were based on direct physical contact or cell-cell contacts. A common mechanism of intercellular communication is the formation of gap junctions between adjacent cells (Revel and Karnovsky, 1967; Makowski *et al.*, 1977). Gap junctions are clusters of specific channels, providing an equal distribution of ions and metabolites, a rapid spread of information and a coordinated effort between the connected cells in order to form a synchronized cell organization (Perkins *et al.,* 1997). The importance of contact-dependent communication in a tissue is illustrated by the nearly ubiquitous distribution of gap junctions in multicellular organisms. With the exception of red blood cells, platelets, sperm cells and differentiated skeletal muscle cells, all vertebrate cells are connected via gap junctions to each other and for this reasons gap junctions attend a variety of functions depending on the tissue (Gilula et al, 1987; Evans and Martin, 2002; Eastman et al., 2005). The physiological properties of gap junctions are strongly influenced by the gap junction forming proteins, so-called connexins. To date, 20 connexin genes in the mouse genome and 21 in the human genome have been described (Söhl and Willecke, 2003; Söhl et al., 2005). In the zebrafish 37 connexins have been identified, classified and compared to those in higher vertebrates (Eastman et al., 2005, Dermietzel et al., 2000). Despite the great diversity of connexins, only a few were characterized according to their tissue specificity and their physiological properties. The comparison of the sequences and properties of connexins with other homologous species offers the possibility of fundamental insights into the working mechanisms of the channels. In this context, fish, such as zebrafish or carp, provide an ideal model organism for extensive studies of identifying and characterizing different connexins because of their rapid generation and development time.

1.1 Role and function of gap junctions in the retina

As a network of highly specialized neurons, the retina is a part of the central nervous system (CNS). Electrophysiological measurements and dye injections have demonstrated gap junction-mediated coupling in all neural cell types of the retina.

The diversity of these couplings is the highest of the whole CNS (Cook and Becker, 1995; Söhl et al., 2005). Because of the combinatorial and physiological diversity of connexins in retinal neurons, the structural organization of the retina and the experimental accessibility, the vertebrate retina has been an ideal model system for the analysis of gap junction-mediated communication in the CNS.

The retina has a highly organized laminar structure (Bloomfield and Völgyi, 2009; cf. Figure 1). Five classes of neural cells: photoreceptors (PR; rods and cones), bipolar cells (BC), horizontal cells (HC), amacrine (AC) and ganglion cells (GC), form three anatomically clearly defined cell body layers separated by two synaptic layers. Visual perception starts in the outer segments of the PR. Their somata form the outer nuclear layer (ONL), which is neighboured by the outer plexiform layer (OPL) in which the photoreceptors interact with horizontal and bipolar cells. The inner nuclear layer (INL) is formed by the somata of horizontal cells, bipolar cells and amacrine cells. The inner plexiform layer (IPL) summarizes the synaptic connections of the bipolar cells, amacrine cells and the ganglion cells. Latter are organized in the proximal layer of the retina, in the ganglion cell layer (GCL), where they pool their axons to the so called optic nerve to send light information in form of electrical impulses to the brain.

Gap junction-mediated coupling mainly takes place in the plexiform layers of the retina. In the IPL, homologous gap junctions between neighbouring cones (Feigenspan et al., 2004) and heterologous gap junctions between cones and rods are formed consisting of Cx36. Dang et al. (2004) have shown that rods do not express Cx36, indicating that the corresponding connexin protein of the rods, which is involved in the heterologous coupling with cones, is still unknown. Basically, it is proposed that retinal electrical synapses composed of Cx36 are essential for scotopic vision (Demb and Pugh, 2002). Furthermore, rods are coupled to each other via homologous gap junctions. The respective connexin protein is as well still unknown (Tsukamoto et al., 2001). Furthermore, horizontal cells are strongly coupled to each other by their dendrites in the OPL. In the mammalian retina the coupling of horizontal cells is mediated by the Cx50 in rabbit (O'Brien et al., 2006) and in axonless horizontal cells by the Cx57 in mouse (Hombach et al., 2004).
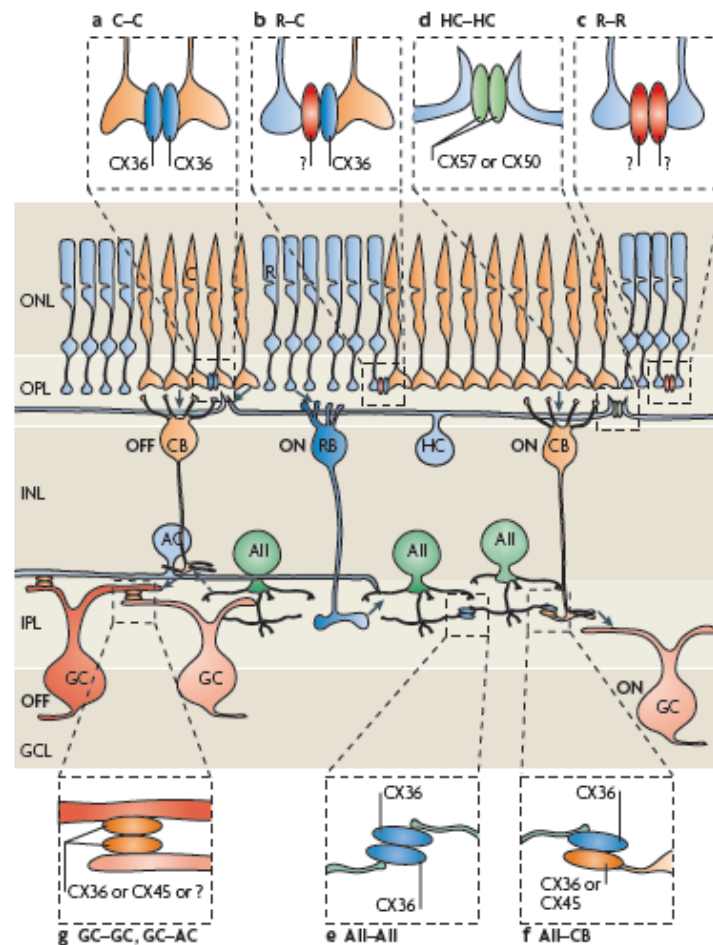
Figure 1: Gap junctions expressed by retinal neurons. a) Homotypic gap junctions (Cx36/Cx36) between cones (C) b) Heterotypic gap junctions (Cx36/?) between cones and rods (R). The connexin expressed by the rod remains unknown. c) The connexin which builds homotypic rod–rod gap junctions is also unknown. d) Homotypic gap junctions (Cx57/Cx57 (mouse) & Cx50/Cx50 (rabbit)) between horizontal cells (HC). e) Homotypic gap junctions (Cx36/Cx36) between AII amacrine cells (AII). f) Homotypic (Cx36/Cx36) and heterotypic gap junction (Cx36/Cx45) between AII amacrine cells and ON cone bipolar cells (CB). g) Homotypic gap junction (Cx36/Cx36 or Cx45/Cx45) between ganglion cells (GL) and homotypic (Cx36/Cx36) and heterotypic gap junction (Cx36/Cx45) between ganglion cells and amacrine cells (AC). GCL: ganglion cell layer; INL: inner nuclear layer; IPL: inner plexiform layer; ONL: outer nuclear layer; OPL: outer plexiform layer; RB, rod bipolar cell (Bloomfield and Völgyi, 2009).

In the carp retina, homologous gap junctions are formed by Cx53.8 (Janssen-Bienhold et al., 2007). AII amacrine cells form two different types of gap junctions in the IPL. Gap junctions between AII amacrine cells are homotypic and consist of homomeric Cx36 hemichannels (Feigenspan et al., 2001). On the other hand AII amacrine cells and ON-cone bipolar cells are coupled homotypic (Cx36/Cx36) and heterotypic (Cx36/Cx45) (Feigenspan et al., 2001; Mills et al., 2001; Dedek et al., 2006). Ganglion cells are coupled by Cx36 and Cx45-containing gap junctions with each other and also with neighbouring amacrine cells (Schubert et al, 2005 a; 2005 b; cf. Figure 1). Moreover, Cx45-mediated coupling was demonstrated between

bistratisfying ganglion cells in the mouse retina (Schubert et al., 2005b). Recent studies on the expression of Cx45 showed that this connexin is expressed in two types of amacrine cells in the mouse retina (Pérez de Sevilla Müller et al. 2007). The rod A17 amacrine cell type seems to form homologous coupling (Cx45) to other A17 amacrine cells. The SWFAC (small wide-field amacrine cell) type is apparently homologously coupled with other SWF amacrine cells (Cx45) and also heterologously coupled with an unknown amacrine cell type (Pérez de Sevilla Müller et al., 2007). Other studies suggest that an interplexiform amacrine cell, expressing Cx45, is a potential coupling partner. This cell type is most likely a medium wide-field amacrine cell (Dedek et al., 2009).

After the years of monoculture in the spectrum of model organisms, mainly the zebrafish but also goldfish and carp were established as new model organisms next to mouse. Fish have the advantage of high material yield, rapid generation and development time and a good accessibility and ease of management conditions. In contrast to mouse retina, in fish new characteristics in the morphology and classification of neural cell types were identified. In a publication by Marc and Cameron (2001) seven cone classes with different morphology are described for zebrafish. The same study characterized four different horizontal cell types, 18 bipolar cell types, about 70 types of amacrine cells and 15 ganglion cell types. In contrast, Connaughton et al. (2004) described only seven different amacrine cells and 17 bipolar cells in the retina of the zebrafish. The increased number of retinal neurons in fish heightens the number of possible cell coupling. The screening of all zebrafish connexins carried out by Eastman et al. (2005) approved that, because of previous gene duplication in evolution, more connexins are expressed in zebrafish than in mammals. Therefore it is likely, that more fish connexins are available because of the increased number of neuronal cells in the retina of fish.

Compared to human (n = 21) or mouse (n = 20) Eastman et al. (2005) have identified 37 putative connexin genes of the zebrafish by phylogenetic analysis. Comparing the connexin gene families of the mouse, human and zebrafish to each other, 23 zebrafish connexins are related to 16 mammalian connexins pointing out that 14 of the known zebrafish connexins are unique and are solely found in its genome (Eastman et al., 2005). Although the zebrafish genome contains almost twice the amount of connexins compared to the mammalian genome, not all of the zebrafish connexins are orthologous to human connexins (Eastman et al., 2005). According to Eastman et al. (2005) the connexins Cx44.2, Cx45.1, Cx44.6 and Cx43.4 are fish specific. In addition, they have shown that the zebrafish genome

contains duplications and tandem duplications of genes and consequently the complexity of the connexin family could still enlarge.

1.2 Structure of gap junctions

Structural and functional, gap junctions belong to the class of ion channels. Each gap junction channel consists of two hemichannels (so-called connexons) of intercommunicating cells, which are held together through homophilic interactions (Krüger et al., 2000). A connexon is in turn composed of six connexins, and thus forms an amphiphilic pore with a pore size of about 1-1.5 nm (Kumar and Gilula, 1996), connecting the cytoplasm of adjacent cells and allowing a passive diffusion of small molecules (e.g. ions, glutathione), macromolecular substrates (nucleotides, amino acids, small polysaccharides) and second messengers such as cAMP, cGMP, Ca^{2+} and IP3 (Kumar and Gilula, 1996; Güldenagel et al., 2000; Söhl et al., 2005). The permeability of gap junctions has been described for molecules up to 1200 kDa and is therefore relatively non-selective (Simpson et al., 1977). The permeability of the channels is influenced by the combination of different connexins (Elfgang et al., 1995; Cao et al., 1998; Steinberg et al., 1994).
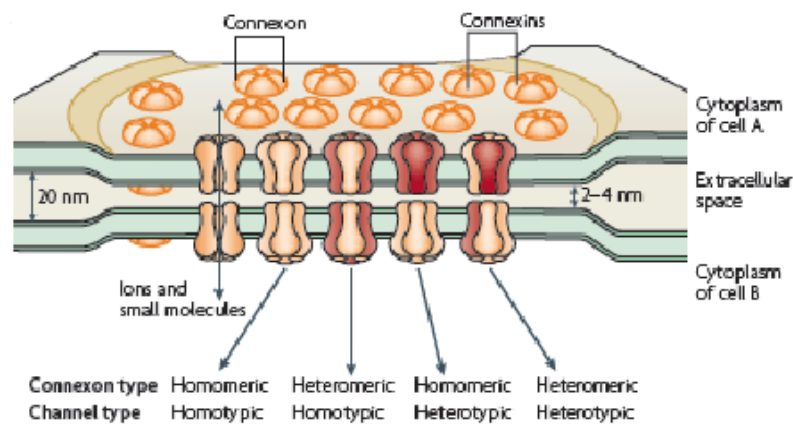
Figure 2: Structure and diversity of gap junctions. Hemichannels in the membranes of adjacent cells form a gap junction channel. An extended field of these channels form a gap junction plaque. Each hemichannel (connexon) is comprised of 6 connexins which form a central pore. This central pore serves as a conduit for ions and low-molecular-mass molecules of up to 1000 Da. Four different types of gap junction channels are shown: (1) homomeric / homotypic, (2) heteromeric / homotypic, (3) homomeric / heterotypic and (4) heteromeric / hetero-typical (Bloomfield and Völgyi, 2009).

The existence of different connexins in one cell amplifies the variety of possible combinations. This results in the association of identical or different connexins to the emergence of homomeric or heteromeric hemichannels (Figure 2). The diversity of gap junction channels is also significantly increased by the coupling of different

connexons. The assembly of two identical or different connexons results in the formation of homotypic or heterotypic gap junction channels (Bloomfield and Völgyi, 2009; Figure 2). Connexons also can exist as unpaired functional hemichannel in the plasma membrane (Janssen-Bienhold et al., 2001, Goodenough et al., 2003). This combinatorial diversity enables a complex regulation of intercellular communication.

Similar to other known plasma membrane proteins, connexins are transported through the intracellular secretory transport to the plasma membrane (Pfeffer and Rothman, 1987). Compared to other multimeric membrane proteins, connexins are properly folded and assembled in the trans-Golgi after leaving the ER (Falk et al., 1997). In hemichannel conformation, they are integrated in already existing gap junction plaques (Gaietta et al., 2002). Gap junction channels may occur singly or as aggregates of up to several thousands. In a density greater than approximately 10^4 channels per membrane area [µm], it is called a gap junction plaque (Lowenstein, 1981).

1.3 Connexins: gap junction-forming proteins

Connexins are gap junction-forming proteins and belong to a multigene family of proteins with similar structure (Bruzzone et al., 1996; Goodenough and Paul, 2003). Using alignments of protein sequences of individual representatives of the connexin multigene family, the existence of highly conserved and divergent domains in the connexin proteins were identified. Each connexin isoform forms channels with different specific biophysical properties.

1.3.1 Molecular structure of connexins

All connexins present an identical topology with four hydrophobic α-helical transmembrane domains, two extracellular loops (E1 and E2) and three cytoplasmic domains: an amino terminal domain (NT), a cytoplasmic loop (CL) between the second and third transmembrane domain and a carboxy-terminal region (CT) (cf. Figure 3).

The N-terminus, the transmembrane domains and the extracellular loops (E1 and E2) are the most conserved regions of the connexins. The third transmembrane domain has an amphipathic character, it has both, hydrophobic and hydrophilic side chains. In the α-helix of the M3, the hydrophilic side chains are distributed in a way

that they only cover one side of the transmembrane domain and thus are involved in the lining of the channel pore.
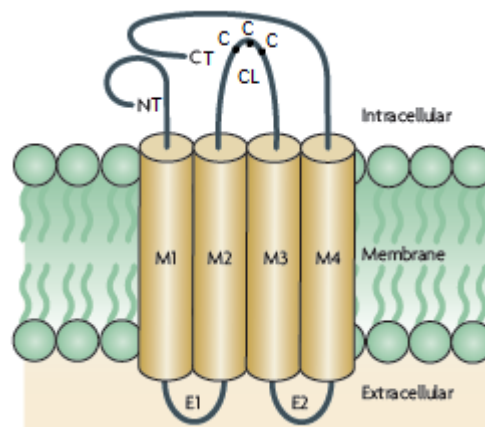
Figure 3: Molecular organization of a connexin protein. Each connexin contains four transmembrane domains (M1-M4), an amino-terminale (NT) and a carboxyter-minal domain (CT) on the cytoplasmic side of the membrane. In addition, each connexin has two extracellular loops (E1 and E2) with three cysteine residues and a cytoplasmic loop (CL) between M2 and M3 (modified from Bloomfield and Völgyi, 2009).

Six of these transmembrane domains are engaged in channel pore formation of one connexon (Kumar and Gilula, 1996). The two extracellular loops (E1 and E2) contain three conserved cysteines (E1: CX_6CX_3C and E2: CX_5CX_4C) (Kumar and Gilula, 1992). The cysteines form intramolecular disulfide bonds between the two loops of opposite connexins and for this reason are involved in the formation and stabilization of gap junction channels (Kumar and Gilula, 1996; Dahl et al., 1991).

1.3.2 Physiological properties of connexins

Gap junction channels underlie dynamic conformation. They are not constitutively opened. As dynamic structures, their reversible conformation is depending on cellular signals. As a response, the channels open or close (Bruzzone et al., 1996). The functional properties of gap junction channels vary, depending on the respective connexin isoforms and can be modulated, as in other ion channels, through a variety of physiological factors and substances. As a result, a synchronous and coordinated response of a cell association on extracellular stimulation of a single cell is possible (Söhl et al., 2005; Dermietzel et al., 2000). Slow regulatory mechanisms are based on the change in the amount of gap junction channels in the cell membrane (Goodenough, 2010). The availability of connexins is controlled via the transcription, the stability of the transcript, intracellular transport of vesicles, distribution, and the half-life of proteins, for example in the case of mmCx32 less than 5h (Fallon and

Goodenough, 1981). Rapid regulatory mechanisms influence the opening state of the gap junction channel, which can be controlled by different mechanisms. First, the opening state can be modified electrically by a voltage difference between two cells, or second, chemically, which is referred to as gating (Harris et al., 1981). In addition, a change in the pH, the concentrations of Ca^{2+} and cyclic nucleotides in the intracellular medium affect the coupling between the cells and the permeability of the channels (Spray et al., 1981; Rose et al., 1977; Bevans and Harris, 1998). Furthermore, most connexins are subject of posttranslational modification by phosphorylation of serine, tyrosine or threonine in the C-terminus and in the intracellular loop (Lampe and Lau, 2000, 2004). In the vertebrate retina known modulating substances are dopamine, retinoic acid and nitric oxide which regulate the gap junction coupling (Pottek et al., 1997; Weiler et al., 2000).

1.3.3 Classification and nomenclature of connexions

For the nomenclature of connexins two alternative systems exist. The first is based on the molecular weight of the connexins. The name of the respective connexin is a combination of the abbreviation "Cx" for connexin and the suffix of the corresponding theoretical molecular weight in kilo Dalton (kDa) (Beyer et al., 1987). In this work, the nomenclature of Beyer is used. If necessary, the appropriate species specific prefixes (e.g. "mm" for mouse, "zf" for zebrafish," cp "for carp) are added in front.

In the second system connexins are classified according to the sequence homology and length of the cytoplasmic loop into three categories: α, β, and γ-subgroup (Risek et al., 1990; Söhl and Willecke, 2003). Connexins, having the same number of amino acids in the cytoplasmic loop (50-55 AS) as mmCx43, correspond to the α-subgroup. Connexins with a shorter cytoplasmic loop (30-35 AS), according to the mmCx32 are in the β-subgroup and connexins with a long cytoplasmic loop (AS 80-105) similar to mmCx36 are summarized in the γ-subgroup. In the new δ-subgroup, all connexins are summarized, having neither a similarity to the connexins of α-, β- and γ-group nor a similarity to one another (Söhl et al., 1998). In this nomenclature connexins are abbreviated as "Gj" for gap junction protein. The assignment of the connexins is used and numbered chronologically by the date of their discovery. Cx43 was the first protein of the α-subgroup of connexins and the corresponding gene is known as Gjα1 (Hsieh et al., 1991).

1.4 Objectives and question

Gap junctions represent the most ubiquitous form of intercellular communication in vertebrates. Since it is known, that the physiological properties of gap junction channels are depending on their connexins, there is great interest in resolving the identity of connexins, forming retinal gap junctions. Due to characteristics of the retina as a part of the CNS, the highly organized laminar structure and the fact that almost all subtypes of retinal neurons are coupled via gap junctions, the vertebrate retina is an excellent model system to study the expression patterns of connexins.

Cx45 is a connexin, which is expressed in bipolar cells (Maxeiner et al., 2005), amacrine cells (Schubert et al., 2005b) and ganglion cells (Maxeiner et al., 2005) leading to the assumption that this connexin is important for the connection of different cells (see above). In the Department of Neurobiology two carp connexins (Cx43.4 and Cx47.6) have been identified by means of RT-PCR which are homologous to the mouse connexin Cx45. Expression analysis, using multiple tissue RT-PCR, have revealed the highest level of cpCx43.4 expression in carp brain, kidney and heart, only weak expression in retina, liver and muscle and no expression in lens (Diploma thesis, Beermann, 2006). In comparison, cpCx47.6 has shown the highest expression level in carp retina and brain, low expression in kidney and heart, but no expression in lens, liver and muscle (Diploma thesis, Beermann, 2006). The analysis of the expression patterns of both connexin transcripts within the carp retina using ISH and FISH have revealed mRNA expression in putative amacrine cells. Furthermore, by means of immuno-FISH cpCx47.6 expression was excluded for glycinergic-, calbindin- or caldendrin-expressing amacrine cells (Diploma thesis, Beermann, 2006).

The first goal in this study was dedicated to reproduce the present results of ISH and FISH in order to establish RNA probes for further hybridization experiments. Next, connexin expression was characterized in putative amacrine cells by means of Immuno-FISH. The combination of indirect immunofluorescence and FISH allowed the characterization of cpCx43.4 and cpCx47.6 expressing amacrine cells by co-localization of the detected connexin specific mRNA by FISH and the detected amacrine cell specific proteins by immunofluorescence.

Another aspect of this study focussed an expression of functional cpCx43.4 and cpCx47.6 proteins in mouse neuroblastoma N2A cell lines. pIRES2-EGFP plasmid constructs of both connexins were cloned. Because of the high sequence similarity of both connexins to mmCx45, possible cross-reactions of the mmCx45 antibody which was prepared by the Department of Neurobiology with the expressed

cpCx43.4 and cpCx47.6 proteins were examined. The epitope of this antibody is a part of the cytoplasmic loop of mmCx45, so that a cross-reaction with the present connexins is possible and desired. By means of immunocytochemistry and protein biochemistry the functional expression of the connexins and the cross-reactivity with mmCx45 antibody was aimed to be analyzed.

In another project that has emerged during this study, possible cross-reactions of the cpCx53.8 with the zebrafish connexins zfCx52.7 and zfCx52.9 were analyzed antibody, which was also prepared by the Department of Neurobiology. Because of high sequence similarities of connexins of similar molecular weight, cross-reactions of this antibody were conceivable. For this reason it was advantageous to prove its specificity. Cross-reactions were examined by protein expression of connexins in neuroblastoma N2A cell lines because of existing connexin-plasmid constructs. Further analysis was done by immunocytochemical as well as protein biochemical techniques.

2. Methods

A listing of all used equipment and chemicals is given in the appendix (see section 6). Special reagents and solutions are listed at the beginning of the protocols.

2.1 Preparation of carp retina

For experiments, carp (*Cyprinus carpio*) was used, that was obtained from a breeding facility in Visbek. The carp was decapitated with a knife. After transection of the optic nerve, the eyes were removed, freed from surrounding connective tissue and fat and stabbed in the transitional zone of the cornea-conjunctiva. Through a circular cut along the ora serata, the optic cup was opened. The cornea, together with the lens and the vitreous were carefully removed and for subsequent preparation of frozen sections, the retina was fixed directly in the eyecup. For the isolation of nucleic acids and for crude subcellular fractionation, the fish was dark adapted 2h before preparation and the retina was extracted of the eyecup.

2.2 Preparation of frozen sections

For the preparation of frozen sections, the prepared eyecups (see Section 2.1) were immediately fixed for 20 min (2 x 10 min) in 2% paraformaldehyde (PFA) at room temperature (RT). After washing in 0.1 M phosphate buffer (PB; 3 x 10 min; RT) the preparations were incubated in a 30% succrose solution for cryoprotection overnight at 4°C. Then the eyecups were embedded in TissueTek ® at -20°C. By using a cryostat microtome, 20 µm thin vertical retina sections were produced. These were recorded by Poly-L-lysine-coated slides and dried for 15 min at 37°C on a hot plate.

2.3 Preparation of coding connexin DNA from carp retina

2.3.1 RNA isolation

The efficient isolation of intact DNA-free RNA is an important precondition for further analysis of gene expression and the cloning of genes. This is especially important for mRNA. One of the most important aspects of RNA isolation is therefore the prevention of RNA degradation by ribonucleases (RNases). For this reason, all

experiments were performed by using gloves and sterile RNase free materials. All solutions and buffers were prepared with diethylpyrocarbonate (DEPC)-H_2O and stored in baked glass materials (5h, 200°C) before use.

The total RNA from the carp retina was isolated using the NucleoSpin ® RNA II kit (Macherey-Nagel) according to the manufacturer. After the preparation (see Section 2.1), the retina was mechanically homogenized with a sterile syringe in the presence of high concentrations of chaotropic salts (eg guanidine thiocyanate) and β-mercaptoethanol. For reducing the viscosity of the homogenate, it was drawn through a filter. Under optimal conditions, all nucleic acids were bound by a silica membrane in an affinity column. The genomic DNA was eluted after several washing steps of the silica membrane. For significantly reduction of contamination with genomic DNA from the column matrix, it was treated directly with DNase. After several washing steps, the total RNA was eluted from the silica membrane. A detailed description of RNA isolation is provided in the appendix section 6.3.1.

After RNA elution, the RNA has repeatedly been treated with DNase to reduce DNA contamination. The purified total RNA was, if necessary, stored at -80°C or directly used for cDNA synthesis (see next section or appendix section 6.3.2).

2.3.2 Reverse transcription

The first step of cloning a specific DNA sequence is to create a single-stranded, complementary DNA copy (cDNA) of the selected mRNA using reverse transcriptase (RT). Reverse transcriptase is a DNA-dependent RNA polymerase and requires, like all DNA polymerases, a primer with a free 3'-hydroxyl group (3'-OH). Because all mRNA molecules have a polyadenylate sequence (polyA) at their 3´end (Rapley and Manning, 1998), a short oligodesoxythymidinsegment (oligo (dT)) was used as a primer.

In order to transcribe RNA molecules from the total RNA preparation into cDNA molecules and to amplify them, the reverse transcriptase SuperscriptTM III RT (Invitrogen) was used according to the manufacturer. For transcription one µg total RNA was taken directly after DNase digestion (see Section 2.3.1) and was treated with a reverse transcriptase for one hour (detailed protocol see appendix section 6.3.2). After inactivation of the RT, the cDNA was finally stored at -80°C or used as template for amplification of selected DNA sequences. To analyze the purity of the cDNA, a PCR (see 2.3.3) with intron-spanning carp ß-actin primer was made to visualize possible contaminations. The purity was verified by the length of the amplified DNA segments on an agarose gel (see section 2.3.5).

2.3.3 Polymerase chain reaction (PCR)

A polymerase chain reaction (PCR) is a technique to amplify a selected DNA sequences based on a given DNA template (Mullins et al., 1986). The method relies on thermal cycling, consisting of cycles of repeated heating and cooling of the reaction, for melting and enzymatic replication of the DNA. The target region is defined by two synthetic oligonucleotides (primers), each complementary to one 3´end of the sense and anti-sense strand of the target DNA. A thermo resistant DNA polymerase uses these primers as a starting point for synthesis of complementary daughter strands. The PCR consists of a series of 20-40 repeated temperature changes, so-called cycles, with each cycle commonly consisting of three discrete temperature steps. In the first step the reaction is heated to 94-98°C for denaturation of the template DNA by disrupting the hydrogen bonds between complementary bases. In the second step, the annealing step, the temperature is lowered to 50-65°C. This temperature allows binding of the primers to the complementary single-stranded DNA template. In the last step, the elongation step, the temperature is raised to 72°C. The DNA polymerase synthesizes a new DNA strand, complementary to the template strand by adding dNTPs in 5' to 3' direction, complementary to the template nucleotides.

The length of each step depends on the length of the target DNA and on the GC percentage of the primers. Some DNA polymerases need to be activated by heating the reaction for 5-10 minutes to 94-98°C before the cycling starts. After 30-40 cycles the PCR is finished by a final elongation at 72°C for 10 minutes.

All primers used in this work were manufactured by Eurofins MWG GmbH (Ebersberg). The oligonucleotides were supplied as lyophilisate and directly added to ddH2O (RNase free). A summary of all used primer, their sequences and annealing temperatures is given in the appendix (see section 6.1; Table 9). For amplification of selected sequences, the HotStar Taq Polymerase (Qiagen) was used according to the manufacturer. The corresponding reaction mixtures were prepared as follows:

5 µL	10x PCR buffer
1 µL	dNTPs (10µM)
2 µL	Primer forward (10 µM)
2 µL	Primer reverse (10 µM)
0,25 µL	HotStar Taq polymerase (250 U/µL)
38,75 µL	ddH2O (RNase free)
1 µL	template

As PCR template, cDNA or plasmid DNA was used, depending on the purpose. For HotStar Taq Polymerase the PCR cycles were performed under optimized conditions (see table 1)

Table 1: Used PCR program.

step	temperature [°C]	time [min]	cycle
activation	95	5	1
denaturation	94	0.5	
annealing	50-65	1	36
elongation	72	2	
final elogation	72	10	1

2.3.4 Quantification of nucleic acids

The concentration of DNA or RNA was measured by photometry with the BioPhotometer (Eppendorf). Nucleic acids in solution have an UV-absorption with a maximum of 260 nm. The concentration of a given solution is proportional to the measured absorbance. An absorbance of 1.0 corresponds to 40 g/mL RNA or 50 g/mL DNA. In addition to the concentration and the absorbance at 260 nm, three other wavelengths (230, 280 and 320 nm) were calculated. The ratio E260/A280 is an indicator of the purity of the nucleic acid sample. For further use, the ratio for DNA should lie in the range of 1.8-2.0 and for RNA in the range of 1.9-2.0. At a ratio of 1.8-2.0 the purity of the DNA is 70-95% (Mülhardt, 2003). In case of insufficient purity, the DNA was purified by using the QIAquick PCR Purification Kit (Qiagen) according to the manufacturer for removing excess proteins. RNA was discarded and was isolated again.

2.3.5 Agarose gel electrophoresis

For the analysis of DNA fragments by PCR (see Section 2.3.3), restriction (see Section 2.4.1) and plasmid isolation (see Sections 2.4.4 and appendix section 6.3.4), the process of agarose gel electrophoresis was used. In this procedure, negatively charged DNA molecules are divided in an electric field, depending on their size and conformation (linear, supercoiled, circular, single-strand). Depending on the expected fragment size, 1-2% agarose gels were used. The agarose gels were prepared with TBE. After boiling and a short cooling, the solution was transferred

into a horizontal gel carrier. The DNA probes were charged with coloured loading dye (Qiagen) to enhance the density of the molecules and filled into the slots. As a length standard, a standard DNA ladder (Peqlab) was pipetted into the gel slots. After polymerisation in a horizontal gel chamber (Biometra), the electrophoretic separation of the molecules was performed for 45-90 min at 120 V. Subsequently, the DNA was stained (30 min, RT) with an ethidium bromide solution (EtBr). EtBr bound to DNA, intercalates into the guanine-cytosine pairs, so that DNA fragments glow under ultraviolet (UV) light. The DNA lanes were excited with a UV transilluminator and documented with the UV-Alpha Imager documentation system (Biozym).

2.4 Cloning of connexin DNA in different plasmids

For further experiments like the expression of connexins in N2A cells or in situ hybridization, it was necessary to create plasmids, which contain the full length of the coding sequence of the connexin of interest or even a part of it. Depending on the experiment, a plasmid with adequate characteristics like different promoters, restriction sites, fluorescent proteins etc. was selected. For expression of a functional connexin protein in N2A cells the plasmid pIRES2-EGFP was chosen. This plasmid has a mammalian promoter, allowing the expression of proteins in mammalian cells, a gene for expression of the enhanced green fluorescent protein (EGFP), which allows the detection of transfected cells by EGFP signal and an IRES sequence between the multiple cloning site (MCS), the connexin integration region, and the EGFP for separated translation of both proteins from a single mRNA. This sequence guarantees, that the connexin of interest is going to be expressed without a disruptive tag. For in situ hybridization, a plasmid was needed to create DIG labeled RNA probes of a highly variable part of the sequence of the connexin of interest, differerent from other connexins. For this reason, a plasmid called pBluescriptII KS+ was chosen, in which the MCS, where the part of the connexin sequence will be cloned, is flanked by two different transcription start points for RNA polymerases (T3, T7). On the one hand it is important for RNA production from DNA and on the other hand it allows creating a positive and a negative RNA probe for hybridization.

Before the sequences were cloned into the selected plasmids, they were first sub cloned by the pGem-T-Easy Vector System (Promega). This plasmid arrived in an open cycled form with a thymine overhang at the 3'ends. The target sequence can

easily be inserted into the plasmid, because the polymerases used for PCR have the property, adding adenosine to the 3' ends of the synthesised fragments, so that no restriction is needed. Before cloning into another plasmid, the sequence was analyzed, because the insert can be integrated in any direction.

2.4.1 DNA restriction

To cut the target connexin sequence out of the pGem-T-Easy plasmid, special restriction endonucleases (Roche) were needed, which flank the connexin sequence and have no restriction side within the sequence. Another criterion was that the target plasmid possesses these cutting sides and allows an insertion of the sequence in the right direction (important for protein expression). Used restriction enzymes are shown in table 2.

Table 2: Cloned vector constructs.

further research	target sequence	target plasmid	enzymes
expression of cpCx43.4	cpCx43.4 (full length)	pIRES2-EGFP	XhoI, EcoRI
expression of cpCx47.6	cpCx47.6 (full length)	pIRES2-EGFP	XhoI, EcoRI
hybridization of cpCx43.4 RNA	cpCx43.4 (part)	pBluescriptII KS+	EcoRI, HindIII
hybridization of cpCx47.6 RNA	cpCx47.6 (part)	pBluescriptII KS+	XhoI, EcoRI

After restriction and before insertion of the sequence, the DNA was purified and separated from the rest of the plasmid. This was performed by extraction of the sequence from agarose gels (see next section).

Restriction enzymes were also used for analysing the success of insertion of the DNA fragments into the plasmids after amplification (see section 2.4.4). To get all restriction sides of a target sequence or even to know restriction enzymes, which do not cut the inserted DNA, the program NEBcutter V2.0 was used (*tools.neb.com/NEBcutter2/index.php).*

2.4.2 Extraction of DNA fragments from agarose gel

After the agarose gel electrophoresis of the restricted plasmid and the EtBr staining, the desired fragments were cut out of the gel under UV light. DNA was extracted by using the QIAEX II Gel Extraction Kit (Qiagen) according to the manufacturer. Here

16

the gel was melted in a buffer with high salt concentration. Subsequently, the DNA was bound by a silica matrix and after some washing steps, eluted in water.

2.4.3 DNA ligation

Ligation is a process, by which double-stranded DNA molecules are linked together. The enzyme DNA ligase catalyses, under consumption of adenosine triphosphate (ATP), the formation of covalent phosphate diester bonds between adjacent 3'-hydroxyl and 5'-phosphate groups of the complementary cohesive ends of two DNA molecules. In this study the pGem-T-Easy Vector System (insertion of target DNA into pGem-T-Easy plasmid) or the Rapid DNA Ligation Kit (Roche) was used for ligation. The application was made according to the respective manufacturer. To increase the rate of incorporation of the insert into the plasmid, a plasmid-insert molar ratio of 3:1 was chosen. The amount of the vector DNA was 50 ng. Depending on the fragment size, the amount of insert DNA was determined by using the following formula:

$$\frac{\text{ng of vector} \times \text{kb size of insert}}{\text{kb size of vector}} \times \text{insert:vector molar ratio} = \text{ng of insert}$$

After ligation, the reactions were used for the transformation in bacteria (see next section).

2.4.4 Amplification of plasmid DNA

For amplifying the DNA-plasmid, the reaction was used for transformation of One Shot™ Top10 chemical competent *E.coli* cells (transformation protocol see appendix section 6.3.3). After transformation, the bacteria were plated onto agar plates with added antibiotics (kanamycin for pIRES2-EGFP; ampicillin for pBluescriptII KS+). For pBluescript also X-gal and IPTG were added, allowing a blue/white screening of colonies. The plates were incubated at 37°C overnight for the growth of colonies. To monitor the success of the DNA insertion, only little DNA is needed. For this reason, colonies of the transformed bacteria were picked and cultivated in 5 mL LB medium at 37°C overnight to do a minipreparation (peqGOLD Plasmid Miniprep Kit I; PEQLAB). After sequence analysis of the picked clones, a correct clone was picked again and cultivated in 200 mL LB medium overnight at

37°C to do a midipreparation, achieving a high copy of target plasmids (PureYield™ Plasmid Midiprep System; Promega). For a detailed description of DNA isolation protocols see appendix section 6.3.4.

After quanti- and qualification of plasmid DNA by restriction analysis and gel electrophoresis and after DNA purification (if needed), the plasmids were used for further experiments. During this study the following plasmids were created:

cpCx43.4-pIRES2-EGFP

cpCx47.6-pIRES2-EGFP

Cx43.4-pBluescriptII KS+

Cx47.6-pBluescriptII KS+

Sequencing of the created plasmids or even PCR products was performed by LGC genomics (formerly AGOWA genomics). The analysis of the sequencing results was carried out by using the program Chromas (http://www.agowa.de). Furthermore, for sequence analysis and sequence comparisons the following databases were used: the NCBI BLAST server (National Center for Biotechnology Information, http://www.ncbi.nlm.nih.gov) and the program Clustal W (http://www.ebi.ac.uk/Tools/clustalw/).

2.5 Transfection of mouse neuroblastoma neuro-2A cell line (N2A cells) for connexin expression

In order to analyze cross-reactions between the respective connexins and different antibodies and to analyze the channels properties by electrophysiology (not in this study), the connexin-plasmid constructs were transfected to N2A cells for protein expression. For efficient transfection of eukaryotic cells a transfection of DNA in liposomes (small, membrane-bounded bodies) was selected. Their structure is in some ways similar to the structure of the transfected cell and can actually fuse with the cell membrane, releasing the DNA into the cell.

All work with cell cultures was performed under a sterile working bench (Holten Laminair) and all working solutions were sterile filtrated to reduce contamination and cell death. The cell line was cultivated in DMEM and as transfection reagent attractene (Qiagen) was used. Depending on the subsequent experiment, cells were grown at different densities and in different environment. For immunocytochemistry 50.000 cells were planted on coverslips for transfection. For protein biochemical

experiments, cells were grown in 6 cm dishes with a density of 500.000 cells. Transfection was carried out by using 0.4 µg DNA for coverslips and 4 µg DNA for 6 cm dishes. 48h after transfection the cells were analyzed by immunocytochemical or protein biochemical techniques (see next sections). A detailed protocol of cultivating and planting N2A cells is shown in the appendix section 6.3.5. The N2A cells were transfected with the following DNA:

cpCx43.4-pIRES2-EGFP
cpCx47.6-pIRES2-EGFP
cpCx53.8-pIRES2-EGFP
zfCx52.7-pIRES2-mRFP
zfCx52.9-pIRES2-EGFP

2.5.1 Immunocytochemical analysis

For immunocytochemical analysis of transfected cells, indirect immunofluorescence was used. After binding to the protein, a primary antibody is detected by a secondary, to which a fluorescent molecule is bound. As the primary antibody has multiple binding sites for secondary antibodies, the signal is amplified by the second antibody. Because the protein is not directly requested by the first, but is detected only on the second antibody, this method is called indirect immunofluorescence. It was used for analyzing cross-reaction of over-expressed proteins with the selected antibody and for analyzing the allocation of the expressed connexins in the mammalian cells. The evaluation of the experiment was carried out by confocal microscope.

In order to analyze cross-reactions between the expressed proteins and different antibodies the following antibodies were used:

Table 3: Primary antibodies used to analyze possible cross-reaction.

expressed protein	primary antibody	concentration
cpCx43.4	anti-mmCx45 serum 3	1 : 1.000
	preimmune serum 3	1: 10.000
cpCx47.6	anti-mmCx45 serum 3	1 : 1.000
	preimmune serum 3	1: 10.000
cpCx53.8	anti-cpCx53.8 serum 1	1 : 750
zfCx52.7	anti-cpCx53.8 serum 1	1 : 750
	anti-zfCx52.7	1 : 100
zfCx52.9	anti-cpCx53.8 serum 1	1 : 750
	anti-zfCx52.9	1 : 250

Depending on the expressed fluorescent protein (red or green) a secondary antibody was chosen. For a detailed protocol see 6.3.5.1.

2.5.2 Protein biochemical methods

For analysing the expressed proteins in detail, crude subcellular fractions of the transfected N2A cells were examined by SDS-gel electrophoresis and Western blot. The separated and transferred proteins were finally visualized by enhanced chemiluminescence-mediated immunodetection (ECL).

2.5.2.1 Crude subcellular fractionation

For crude subcellular fractionation, the transfected N2A cells were entered by using a cell scraper in 100 µL homogenization buffer (HP2). With the help of a glass homogenizer the N2A cells were homogenized mechanically. The included protease inhibitors in HP2, such as PMSF, leupeptine and aprotinine should prevent the degradation of proteins. By means of different centrifugation steps, the total homogenate of the N2A cells was separated into a nuclear fraction (P1), a cytosolic fraction (C) and membrane fraction (P2). The explicit process of the crude subcellular fractionation is shown in appendix section 6.3.5.2.

2.5.2.2 Bradford protein assay

For identifying the protein concentration of the different fractions, the Bradford protein assay was performed. Coomassie Brilliant Blue G-250 binds non-specifically to hydrophobic side chains of proteins, leading to the displacement of the absorption maximum of 465 to 595 nm. This allows, by measuring the absorbance at 595 nm, a protein detection up to 0.05 µg/mL (Lottspeich and Zorbas, 1998). To determine the protein concentration of each fraction, 2 µL of each sample were mixed with 3 mL Bradford reagent. After 15 minutes incubation at RT, the absorption of the protein solution was measured at a wavelength of 595 nm and compared to reference absorptions of BSA solutions with defined concentrations. For avoiding measurement errors, each sample was measured twice.

2.5.2.3 SDS polyacrylamide gel electrophoresis

For the analysis of protein fractions, the SDS polyacrylamide gel electrophoresis (SDS-PAGE) was performed in modification to Laemmli (1970). Proteins were separated under denaturing conditions according to their apparent molecular weight. 30 µg of each fraction was used for SDS-PAGE. The respective sample volumes were adjusted to 30 µL with HP2. After adding 15 µL 3x SDS sample buffer, the samples were boiled in water for 3 min and after a short centrifugation (3 min, 6000 rpm, RT), applied to a polyacrylamide gel with a gradient from 8-10% of acrylamide. The whole gel consists of two different parts: the upper part, the stacking gel, forming the slots and defines the lanes, where the proteins are going to run and the second part, the resolving gel, by which the proteins get separated. The composition of the gels is shown in table 4. As protein standards, a high molecular weight marker (HMW, Sigma) and low molecular weight marker (LMW, Sigma) and/ or a staining marker (SM, BioRad) were used according to the manufacturer. The gel electrophoretic separation of proteins was performed for 120 min at a constant voltage of 160 V.

Table 4: Pipetting scheme for SDS-gel

stacking gel		resolving gel		
ingredients		ingredients	8 %	10%
ddH$_2$O [mL]	2.9	ddH$_2$O [mL]	4.35	3.75
38% acrylamide [mL]	0.75	38% acrylamide [mL]	2.40	3.00
0.5 M Tris/HCl pH 6.8 [mL]	1.25	1.5 M Tris/HCl pH 8.8 [mL]	2.25	2.25
10% APS [µL]	40.00	10% APS [µL]	20.00	20.00
TEMED [µL]	20.00	TEMED [µL]	20.00	20.00

2.5.2.4 Western blot analysis

For subsequent detection of the proteins, the Western blot method (Towbin et al., 1979) was used, by which the proteins are transferred from the SDS gel to a nitrocellulose membrane. Again, the proteins migrate in an electrical field to the anode and are bound to the membrane, forming the same distribution patterns of proteins on the nitrocellulose as on the gel. The transfer was carried out in a Mini Trans-Blot Cell (Bio Rad) at 40 V overnight. The proteins bound to the nitrocellulose membrane and were finally detected by using the indirect immunofluorescence in combination with the ECL detection system. The secondary antibodies used for this approach were linked with the enzyme horseradish peroxidase (HRP). By using the Pierce ECL detection system, a light response was detected by a radiographic film. The explicit protocol is shown in the appendix section 6.3.5.2.

2.6 *In situ* hybridization

In situ hybridization is a technique, allowing the detection of mRNA expression in tissue sections and is therefore an analysis of gene expression in a topographic context (Rapley and Manning, 1998). The principle of this method is based on specific binding of labeled RNA probes to complementary mRNA sequences in the tissue, followed by a detection of the used probes. As a part of this work, in situ hybridization was performed to localize the transcription of cpCx43.4 and cpCx47.6 mRNA in the carp retina.

2.6.1 Production of DIG labelled RNA

In order to produce DIG labeled RNA, complementary to a very specific part of the connexin of interest, special plasmids were created, containing the specific part of the connexin (see appendix section 6.2). For RNA production, the two plasmids Cx43.4-pBluescriptII KS+ and Cx47.6-pBluescriptII KS+ were used. The inserted DNA sequence was flanked by two promoters for RNA polymerases (T3 and T7) and a number of different restriction sites. In two different approaches each vector was cut with two different restriction enzymes. The first enzyme cut in front of the insert, in the second reaction another enzyme cut behind the insert. For the following in vitro transcription it was necessary to use a RNA polymerase, which transcription started on the opposite side of the insert as the restriction side was. To label the RNA with digoxigenin (DIG), the DIG-UTP RNA Labeling Mix (Roche) was used for in vitro transcription. After transcription of DNA into RNA, the DNA was removed by using DNaseI (Roche) and the RNA was purified by ethanol precipitation. The explicit protocol is shown in the appendix section 6.3.6.

2.6.2 Conventional *in situ* hybridization (ISH)

For conventional in situ hybridization, fresh produced cryosections of carp retina were used and fixed again in 4% PFA fixative. After several washing steps (PBS buffer) and ethanol treatment, the membranes of cells were permeabilized by 0.1 M hydrochloric acid. This step ensured that the RNA probes were able to diffuse into the cells. Ensuring that the negatively charged RNA probe bind to the negatively charged mRNA, the basic amino groups were acetylated by different reagents. At the same time this step prevented potential non-specific binding. Subsequently, a dehydration of the cryosections was performed, using different concentrated ethanol solutions. After dehydration the sections were dried in the air, followed by the incubation with the prehybridization buffer. Finally, the actual incubation with the RNA probes started overnight at high temperature in a humid chamber. The RNA probes were diluted in hybridization buffer. Further stringency washes at high temperature in different solutions followed the next day, reducing non-specifically bound RNA probes. After the subsequent blocking of nonspecific binding with MBM, the sections were incubated with anti-DIG antibodies linked with alkaline phosphatase (AP) overnight, which bind to the labelled probes. The alkaline phosphatase catalysed in combination with 5-bromo-4-chloro-3-indolyphosphat

(BCIP) and nitroblue tetrazolium (NBT) a reddish-brown dye. This dye was visible under the light microscope and was used for detection of mRNA in the retina. After the desired colour intensity was achieved on retina sections, the reaction was stopped by different washing steps. Finally, the sections were embedded in Fluoromount (Serva). For a detailed protocol see section 6.3.7.

2.6.3 Fluorescence *in situ* hybridization (FISH)

In addition to conventional ISH, the fluorescence in situ hybridization was performed in this study. This method offers a higher spatial resolution and better facilities for the differential representation of target sequences than ISH. Furthermore, this method can be extended by different essays, for example by hybridization with a second RNA probe, so called Double-FISH, or by indirect immunofluorescence, so called Immuno-FISH. Depending on the question, the FISH can be combined with a high number of different techniques or essays (Volpi and Bridger, 2008), which make this method very advantageous and versatile. In this study the Immuno-FISH was used for further characterization of mRNA expressing cells in the carp retina (see next section).

The FISH was performed by using the TSA Plus Fluorescence System (Perkin Elmer). Until the hybridization, the preparations were processed as in conventional ISH. For hybridization, the same DIG-labeled probe was used as in conventional ISH. Detailed information on washing and incubation can be found in the appendix section 6.3.8. After SSC and PBS washing steps, the endogenous peroxidase activity was stopped with 2% H_2O_2 in PBS the next day. After blocking of non-specific bindings by MBM, the detection of the applied RNA probes were performed. For this reason the DIG antibody, coupled with horse-radish peroxidase (HRP) was selected. After washing in TNT buffer, the signal development was carried out in a sealed incubation chamber, using the TSA system. This system is based on the use of tryramide molecules. Each molecule is coupled with a specific fluorochrome (e.g. Cyanine 3, Cyanine 5 or fluorescein) and reacts with the HRP. In the used TSA fluorescein system (green) a dilution of 1:50 of the Tyramide Plus Amplification Diluent and the fluorescein was necessary. The enzyme reaction was stopped after 5 to 7 minutes by washing in TNT buffer, whereby the non-precipitated tyramide molecules were removed. For further analysis the preparations were embedded in Vectashield (Vector Laboratories, Inc.Burlingame) and sealed with nail varnish.

FISH-treated sections were evaluated by confocal microscopy. The detailed protocol for the implementation of FISH is in the appendix section 6.3.8.

2.6.4 Combination of FISH and indirect immunofluorescence (Immuno-FISH)

The Immuno-FISH is a combination of FISH and indirect immunofluorescence, allowing the characterization of the mRNA positive cells of the cryosections. For further analysis of the putative amacrine cells, different antibodies against amacrine cell specific proteins were selected for visualizing possible co-localizations.

After the evaluation of the FISH, the cover of the microscope slides was removed and the sections were repeatedly washed in 0.1 M PB. Subsequent to the blocking the unspecific binding sides with normal goat or donkey serum (NGS / DKS; depending on the host of the second antibody), the sections were incubated with the primary antibody overnight. Several washing steps in 0.1 M PB were followed by the incubation of sections with the second antibody for 2 hours. Finally, after washing in 0.1 M PB, the sections were embedded in Vectashield and evaluated by confocal microscopy (detailed protocol see appendix section 6.3.9). In detail, the following primary and secondary antibodies were selected:

Table 5: Antibodies used for Immuno-FISH

	description	host	blocking reagent	dilution	manufacturer
1st ab	anti-bNOS	rabbit		1:500	Sigma
2nd ab	anti-rabbit Alexa 568 conj.	goat	NGS	1:600	Molecular Probes / Invitrogen
1st ab	anti-Chat	goat		1:100	Chemicon
2nd ab	anti-goat Cy3 conj.	donkey	DKS	1:600	Chemicon
1st ab	anti-GABA	rabbit		1:2000	Chemicon
2nd ab	anti-rabbit Alexa 568 conj.	goat	NGS	1:600	Molecular Probes / Invitrogen
1st ab	anti-Gycin	rat		1:2000	ImmunoSolution
2nd ab	anti-rat Cy3 conj.	goat	NGS	1:600	Chemicon
1st ab	anti-TH	mouse		1:100	Boehinger Mannheim
2nd ab	anti-mouse Alexa 568 conj.	goat	NGS	1:600	Molecular Probes / Invitrogen

3. Results

3.1 Comparison of cpCx43.4 and cpCx47.6 mRNA expression patterns on sections of the carp retina by means of ISH and FISH

The conventional ISH allows the detection of specific nucleic acid sequences directly in tissues (in situ) using complementary RNA probes. The detection of mRNA-RNA-hybrids was carried out by anti-digoxigenin antibodies which interact with the bound digoxigenin labeld RNA probe. The bound antibody was visualized via an enzyme reaction of the alkaline phosphatase, conjugated with the antibody.

To produce specific RNA probes, a highly variable region of the connexin was chosen. For localization of Cx43.4 transcripts, a 351 nucleotide sequence from the cytoplasmic terminal were selected to create a pBluescriptII KS+ construct. To generate the Cx47.6 construct, a 225 nucleotide sequence of the cytoplasmic terminal were chosen. The parts of the sequences are compared in Figure 4. By aligning the two sequences, the most variable region was picked out to create the RNA probes. The selected regions have a sequence similarity of 50.2 %.

```
Cx43.4    CGTGCACGACACCACAGTGTTGCACGACCCCGTGGCGCCATAAGCAGACAGGTGCCCACG    60
Cx47.6    -------------------------CCTGGTGGTTAAATCTGAAAA-ACCGGGTCGCG      32
                                   **  ****    **  * * * *    *  * **

Cx43.4    GCCCCGCCAGGGTACCACACTGCACTGAAAAAAGACAAGCTGTCCATGGGATTGAAACCG    120
Cx47.6    TTCCCAACAGCAT----CATCATACAGGACCAGAACATGC----------------CCA     71
            ***  ***  *      **    ** * *  *  *** **                 **

Cx43.4    GAGTATAACCTGGACTCGGGTCGGGAGTCTTTTGGTGACGAGTCGTCATCGCGAGATATT    180
Cx47.6    GAGTGCTGCCTGAACA-GCATTGCACAAGTCCTGATGA-GAATATTCCCTCTGACCTGGC    129
          ****     **** **  *   * *        *  ** *** ** *  **     ** *

Cx43.4    GACCGCCTGCGTAGACACCTAAAACTGGCCCAGCAGCATCTGGATATGGCCTATCAGA-A    239
Cx47.6    TACA--CTGCACCATCATTTACGAGTAGCTCAGGAACAACTTGACATGGCGTTTCAGACA    187
            **    ****     **   **   * * **  *** * ** ** ** ***** * ***** *

Cx43.4    TG-AGGAGAGCAGTCCTTCACGCAGCAGCAGCCCAGAGTCCAACGGCACTGCTGTCGAGC    298
Cx47.6    TATAACACAAAAAACACTCAGATCTCCAGAGCTAGCAG--------------------     225
            *   *   *   *   *   *  ***    *    ***    **

Cx43.4    AGAACAGACTCAACTTCGCTCAGGAGAAGCAGGGAAGCACATGTGAA                345
Cx47.6    ------------------------------------------
```

Figure 4: Alignment of the chosen sequences of cpCx43.4 and cpCx47.6 to create RNA probes for hybridization. Both regions were located in the cytoplasmic terminal of the coding sequences of both connexins, a highly variable region. By comparing these two sequences, this region was the most variable one. Sequence similarity is 50.2%. "*" = identical in all sequences in the alignment.

Both sequences were short enough to enter the tissue without an alkaline hydrolysis of the RNA probes, aiming that their specificity remains conserved.

The results of the hybridization of cpCx43.4 RNA antisense probes on vertical sections of carp retina showed dark brown labeled cells in the proximal INL and in the GCL (Figure 5; A). RNA probes were used in a concentration of one ng/µL. The signal was developed by colour reaction of AP and NBT in 45 minutes. The cpCx43.4 mRNA positive cells in the proximal INL showed large and round somata with large nuclei. The position right to the border to the IPL and their appearance suggested the expression of Cx43.4 in amacrine cells. The cells, stained in the GCL, possessed a smaller and oval soma. Information about their nuclei was not given by this image. These cells were assumed to be ganglion or even displaced amacrine cells. The sense probes as a negative control showed no labelling (Figure 5; B).
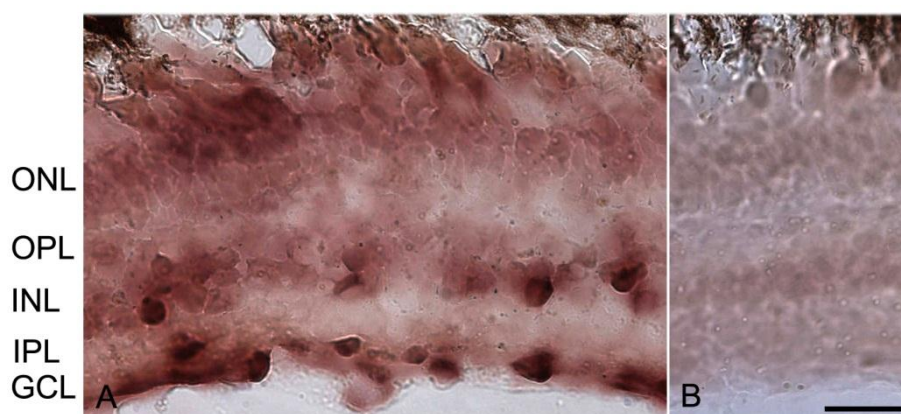
Figure 5: Detection of cpCx43.4 mRNA expression in retinal cells of carp by means of ISH. A) By hybridization of Cx43.4 antisense probes [1 ng/µL] large cells with large nuclei in the proximal INL (putative amacrine cells) and small to large oval cells in the GCL (ganglion or displaced amacrine cells) were detected. B) Hybridization of Cx43.4 sense probes [1 ng/µL], testing the specificity of the probes showed no labeling. GCL: ganglion cell layer; INL: inner nuclear layer; IPL: inner plexiform layer; ONL: outer nuclear layer; OPL: outer plexiform layer. Scale: 20 µm.

By means of FISH, results similar to ISH were achieved (Figure 6). The same RNA probes were used in equal concentrations. The detection of bound RNA was performed by digoxiginin antibodies conjugated with HRP. The fluorescent signal was amplified by a TSA System within seven minutes for cpCx43.4 RNA probes.

Like ISH, the FISH showed expression of cpCx43.4 transcripts in the proximal INL and in the GCL of carp retina (Figure 6, B; white arrows) where amacrine cells are located. The cells, in which cpCx43.4 mRNA were localized, possessed relatively large somata with large nuclei. As expected, because of the better spatial resolution, FISH signal showed a different intensity of fluorescence in the labeled cells. There were so-called hot spots. A high intensity was found round the nuclei in the rough

endoplasmic reticulum, where connexins are formed to membrane proteins. By contrast, in the periphery of the nuclei only a low fluorescence was observed. This faint signal could be explained by the non-specific background. The sense probes showed no positive cells (Figure 6, D).

Figure 6: Detection of cpCx43.4 mRNA expressing retinal cells of carp by means of FISH. A) Overview of the retinal layers. B) Detection of cpCx43.4 mRNA expressing cells. Large cells with large nuclei in the proximal INL and GCL were stained by the antisense probes (white arrowheads). C) Overlay of the projection and the transmission picture evidenced the position and the character of the cells. D) Incubation of tissue with sense probes showed no signal. GCL: ganglion cell layer; INL: inner nuclear layer; IPL: inner plexiform layer; ONL: outer nuclear layer; OPL: outer plexiform layer. Scale: 20 µm.

For localizing cpCx47.6 transcripts on vertical sections of carp retina by means of ISH, a concentration of one ng/µL of RNA probes was used. Five hours were needed for visualizing a dark brown signal. cpCx47.6 transcripts were localized in the proximal INL. Positive cells in the GCL were seen sporadically (Figure 7; A). All positive cells possessed large and round somata with large nuclei and were therefore putative amacrine cells. The poor spatial resolution allowed no detailed description of the labeled cells. The negative control showed no staining (Figure 7; B).
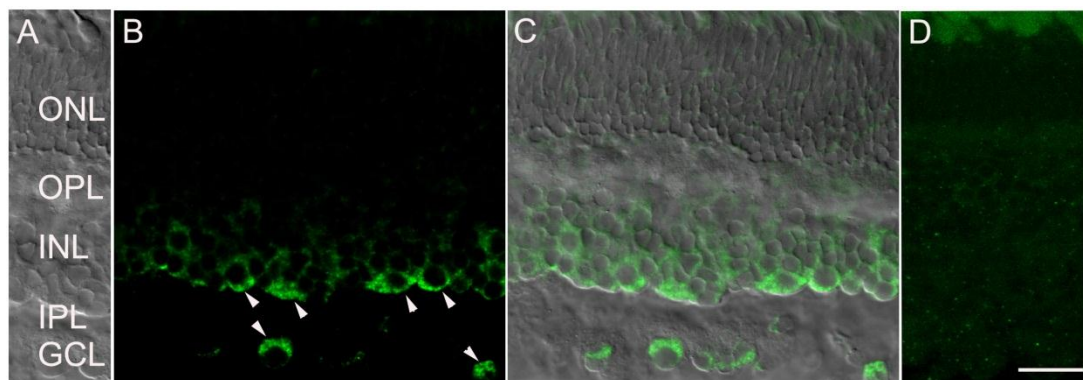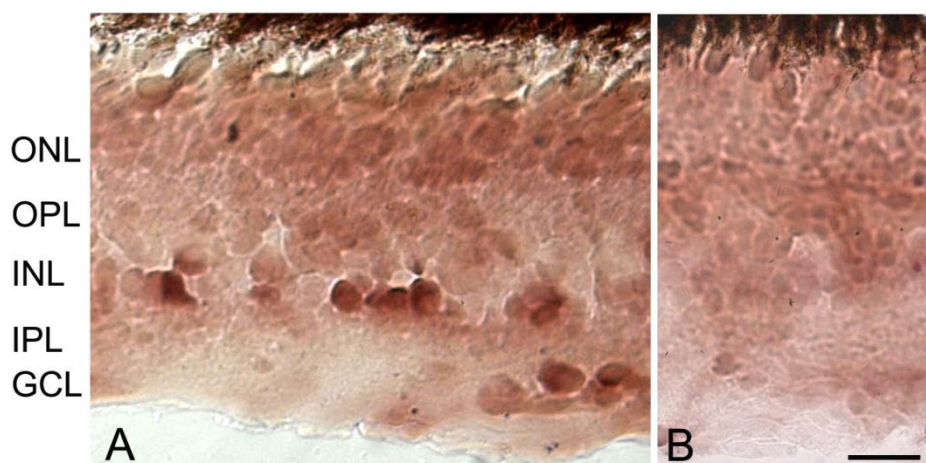
Figure 7: Detection of cpCx47.6 mRNA expression in retinal cells of carp by means of ISH. A) By hybridization of Cx47.6 antisense probes [1 ng/µL], large cells with large nuclei in the proximal INL (putative amacrine cells) and cells in the GCL (ganglion or displaced amacrine cells) were detected. B) Hybridization of Cx47.6 sense probes [1 ng/µL] evidencing the specificity of the probe. No staining was found. GCL: ganglion cell layer; INL: inner nuclear layer; IPL: inner plexiform layer; ONL: outer nuclear layer; OPL: outer plexiform layer. Scale: 20 µm.

By FISH, a better spatial resolution was achieved. Big round cells with large nuclei showed cpCx47.6 mRNA expression in the proximal INL. Like before, hot spots around the nuclei, probably in the rough ER, were seen in which connexins reach their proper formation (Figure 8, B; white arrowheads). No cells in the GCL were stained. By sense probes, no detection of cpCx47.6 transcripts was found (Figure 8, D).
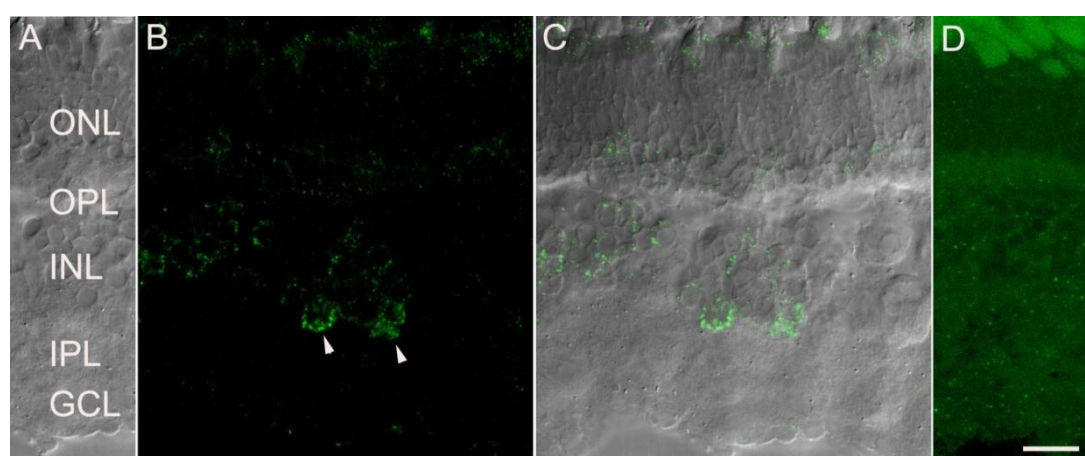
Figure 8: Detection of cpCx47.6 mRNA expressing retinal cells of carp by means of FISH. A) Overview of retinal layers. B) Detection of cpCx47.6 mRNA expressing cells. Large round cells with large nuclei in the proximal INL were stained by the antisense probes (white arrows). C) Overlay of the projection and the transmission picture showed the position and the character of the cells. D) Incubation of tissue and sense probes showed no labeling. GCL: ganglion cell layer; INL: inner nuclear layer; IPL: inner plexiform layer; ONL: outer nuclear layer; OPL: outer plexiform layer. Scale: 20 µm.

3.2 Characterization of cpCx43.4 and cpCx47.6 expressing cells

Subsequent to the FISH, the retina sections were incubated with different antibodies in order to characterize the cpCx43.4 and cpCx47.6 expressing cells. Assuming that the connexin positive cells are likely to be amacrine cells, antibodies detecting amacrine cell-specific proteins were selected. Because all amacrine cells of the vertebrate retina possess either the inhibitory neurotransmitter γ-aminobutyric acid (GABA) or the inhibitory neurotransmitter glycine, antibodies against both neurotransmitters were chosen (Marc et al., 1994). For further classification, antibodies for cholinergic ACs (anti-ChAT), dopaminergic ACs (anti-tyrosine hydroxylase) and ACs which express the brain nitric oxide synthase (anti-bNOS) were picked out.

3.2.1 Comparison of cpCx43.4 and cpCx47.6 expression patterns with GABA immunoreactivity

For analyzing cpCx43.4 and cpCx43.4 expression in GABAergic amacrine cells, FISH was combined with immunodetection of GABA. Figure 9 presents the results achieved by cpCx43.4 Immuno-FISH. The transmission image (Figure 9; A) served for navigation through retinal layers. By FISH, cpCx43.4 transcripts were detected in the proximal INL (Figure 9; B). Because of tangential sections, the GCL is not shown, but there were detected cells, either. By indirect immunofluorescence GABAergic cells were detected (Figure 9; C). Positive cells were localized in the middle and proximal INL and in the GCL (are not shown because of tangential sections). Labeled cells possessed large and round somata with large nuclei like the cells detected by FISH. The overlay of FISH and the GABA immunoreactivity indicated a co-localization of cpCx43.4 expressing cells and GABAergic amacrine cells (Figure 9; D; white arrowheads). Even the cells located in the GCL showed a co-localization (not shown). The results provided evidence that cpCx43.4 is expressed in GABAergic amacrine cells. Because not all GABA positive cells matched with cpCx43.4 FISH signal, cpCx43.4 may be expressed by a subtype of GABAergic ACs.
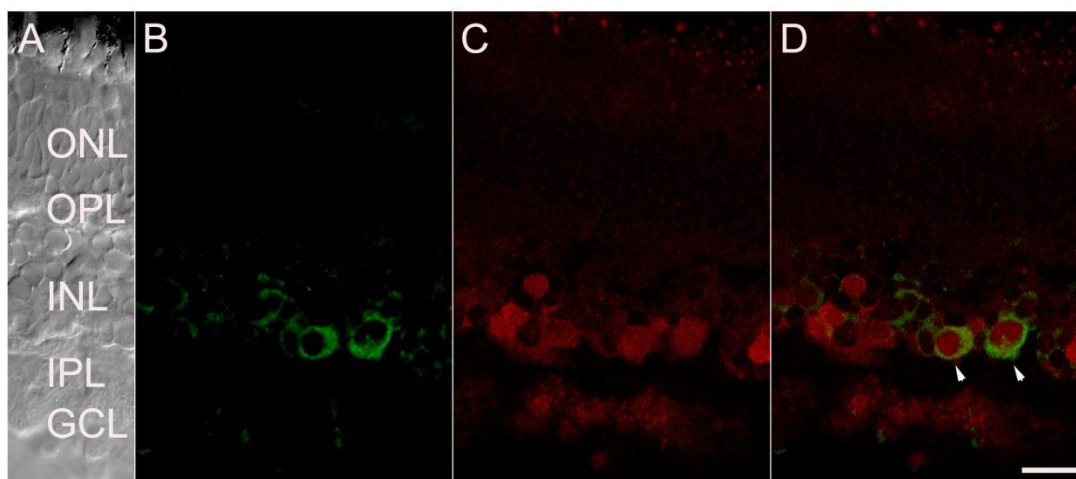
Figure 9: Co-localization of cpCx43.4 mRNA expressing cells and GABA immunoreactivity. A) Overview of the retinal layers. B) Detected cpCx43.4 mRNA expressing cells in the proximal INL. C) Immunoreactivity of GABAergic amacrine cells in the proximal INL. D) Overlay of cells detected by FISH and Immunofluorescence. Co-localization in the case of two cells indicated cpCx43.4 mRNA expression in GABAergic amacrine cells (white arrowheads). GCL: ganglion cell layer; INL: inner nuclear layer; IPL: inner plexiform layer; ONL: outer nuclear layer; OPL: outer plexiform layer. Scale: 20 µm.

Figure 10 presents the results for cpCx47.6 Immuno-FISH. The transmission image (Figure 10; A) served for an overview of retinal layers. By FISH cpCx47.6 transcripts were detected in large cells in the proximal INL, possessing large nuclei (Figure 10; B). By indirect immunofluorescence GABAergic cells were detected (Figure 10; C).
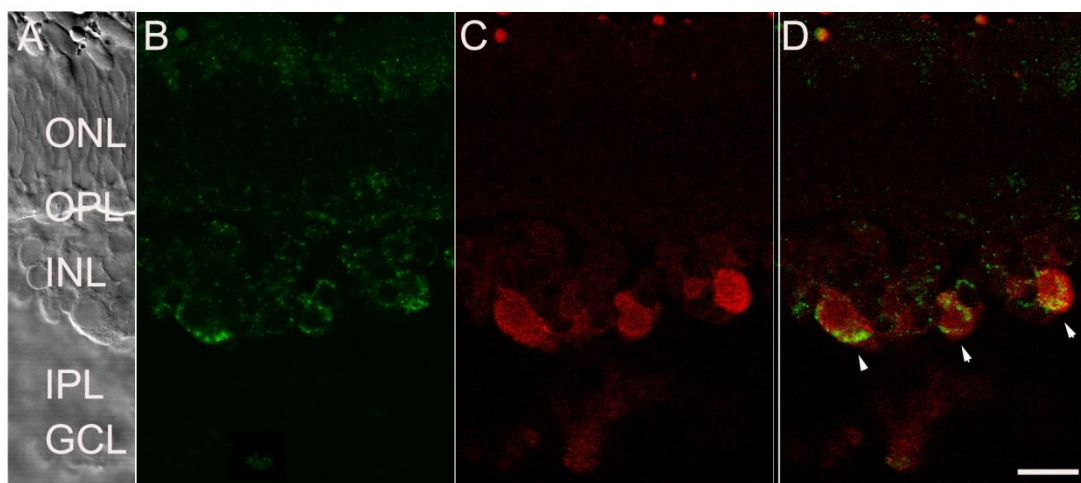
Figure 10: Co-localization of cpCx47.6 expressing cells and GABA immunoreactivity. A) Overview of the retinal layers. B) Detected cpCx47.6 mRNA expressing cells in the proximal INL. C) Immunoreactivity of GABAergic amacrine cells in the proximal INL. D) Merge of positive cell detected by FISH and Immunofluorescence. Co-localization in the case of three cells (white arrows) provided evidence for cpCx47.6 mRNA expression in GABAergic amacrine cells. GCL: ganglion cell layer; INL: inner nuclear layer; IPL: inner plexiform layer; ONL: outer nuclear layer; OPL: outer plexiform layer. Scale: 20 µm.

Positive cells were labeled in the middle and proximal INL and in the GCL. Stained cells were large and round with large nuclei like the cells detected by FISH. Merging of FISH signal and GABA immunoreactivity (Figure 10; D; white arrowheads) showed a co-localization of cpCx47.6-expressing cells and GABAergic amacrine cells. The results indicated a cpCx47.6 expression by GABAergic amacrine cells. Because not all GABA positive cells matched with FISH staining, cpCx47.6 may, like cpCx43.4, be expressed by a subtype of GABAergic ACs.

3.2.2 Comparison of cpCx43.4 and cpCx47.6 expression patterns with glycine immunoreactivity

Supporting that both connexins are expressed by GABAergic ACs, an Immuno-FISH was performed with a glycine antibody. Because of the previous results, no co-localization was expected.

Figure 11 shows the results of cpCx43.4 Immuno-FISH with glycine antibody. In contrast to GABA the glycine antibody detected smaller cells in the proximal INL. No cells were stained in the GCL (Figure 11; C). The overlay of FISH and glycine immunoreactivity showed no co-localization, as expected (Figure 11; D).

Figure 11: No co-localization of cpCx43.4 mRNA expression and glycine immunoreactivity. A) Overview of the retinal layers. B) cpCx43.4 positive cells in the proximal INL and in the GCL. C) Immunoreactivity of a glycinergic amacrine cell in the proximal INL. D) Merge of cells detected by FISH and Immunofluorescence. No co-localization of cpCx43.4 transcripts and glycinergic amacrine cells. GCL: ganglion cell layer; INL: inner nuclear layer; IPL: inner plexiform layer; ONL: outer nuclear layer; OPL: outer plexiform layer. Scale: 20 µm.

The same glycine immunoreactivity patterns were presented by cpCx47.6 Immuno-FISH (Figure 12). Smaller cell bodies were labeled in the proximal INL. The overlay of FISH and immunostaining showed no matches. The glycine Immuno-FISH of both connexins evidenced an expression of both connexins by GABAergic ACs and not by glycinergic ones.
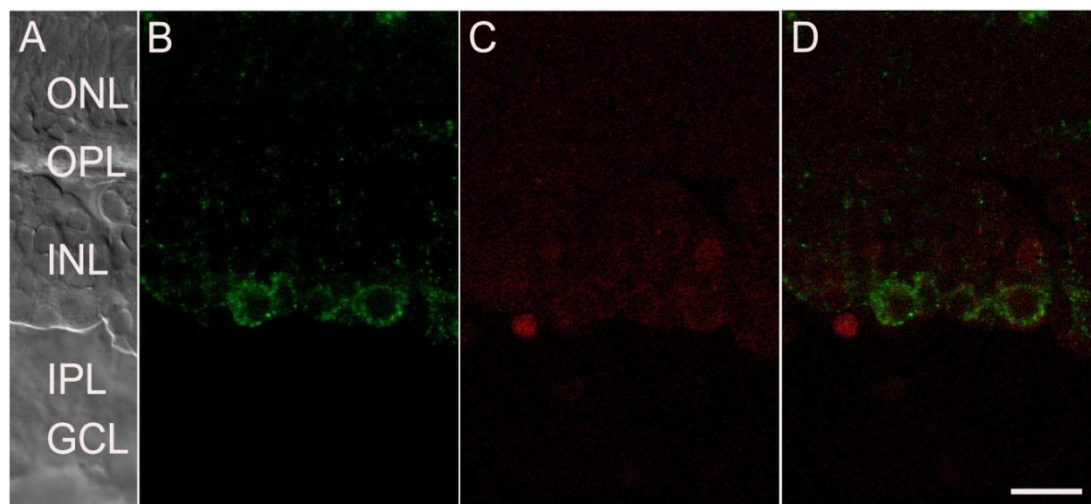
Figure 12: No co-localization of cpCx47.6 mRNA expression and glycine immunoreactivity. A) Overview of the retinal layers. B) Stained cpCx47.6 mRNA expressing cells in the proximal INL. C) Immunoreactivity of a glycinergic amacrine cell in the proximal INL. D) Overlay of cells labeled by FISH and Immunofluorescence. No matches of cpCx47.6 mRNA expression and glycinergic amacrine cells. GCL: ganglion cell layer; INL: inner nuclear layer; IPL: inner plexiform layer; ONL: outer nuclear layer; OPL: outer plexiform layer. Scale: 20 µm.

3.2.3 Comparison of cpCx43.4 and cpCx47.6 expression patterns with TH immunoreactivity

In order to find out, which type of GABAergic amacrine cells express both connexins, an antibody detecting tyrosine hydroxylase (TH) was selected. This antibody immunodetects dopaminergic amacrine cells. Previous work on monkey, cat and mouse (Wässle and Chun, 1988; Haverkamp and Wässle, 2000; Andrade da Costa and Hoko, 2003) had already proved the existence of GABAergic ACs contraining TH.

By Immuno-FISH, no co-localization of cpCx43.4 mRNA expression (Figure 13) or even cpCx47.6 mRNA expression (Figure 14) and TH immunoreactivity was found. Co-localization was not found because the antibody did not detect any immunoreactive proteins (Figure 13 & Figure 14; C). Because the existence of dopaminergic cells had already been proved especially for carp retina (Teranishi and Negishi, 1986, 1988), the antibody has probably lost its function.
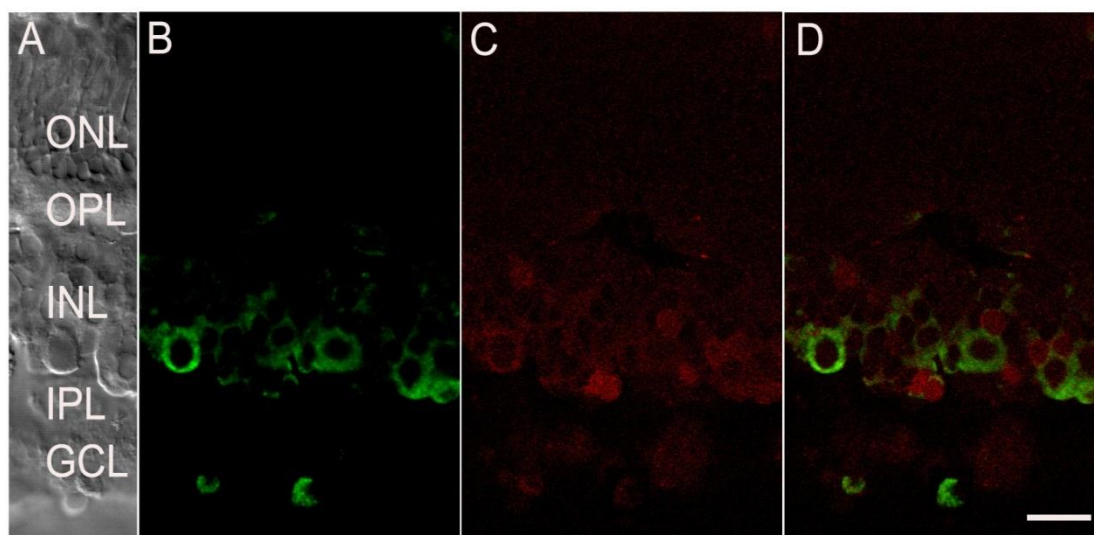
Figure 13: No co-localization of cpCx43.4 expression and TH immunoreactivity. A) Overview of the retinal layers. B) Detected cpCx43.4 mRNA expressing cells in the proximal INL and GCL. C) No Immunoreactivity of TH. D) Merge of FISH signal and Immunofluorescence. No matches of cpCx43.4 mRNA expression and TH immunoreaction. GCL: ganglion cell layer; INL: inner nuclear layer; IPL: inner plexiform layer; ONL: outer nuclear layer; OPL: outer plexiform layer. Scale: 20 µm.
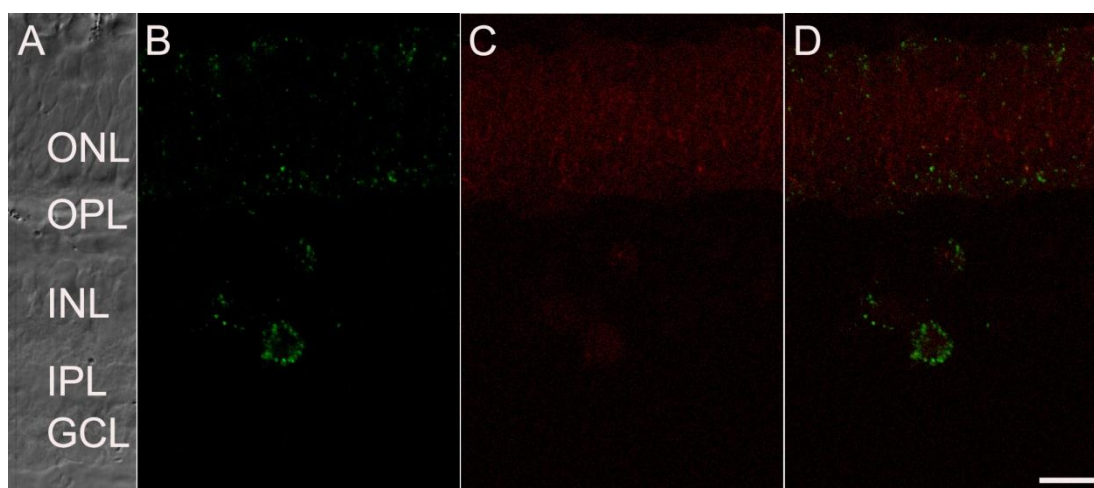
Figure 14: No co-localization of cpCx47.6 expression and TH immunoreactivity. A) Overview of the retinal layers. B) Labeled cpCx47.7 transcripts in cells located in the proximal INL. C) No Immunoreactivity of TH. D) Overlay of cells detected by FISH and Immunofluorescence. No co-localization of cpCx47.6 mRNA expression and TH immunoreaction. GCL: ganglion cell layer; INL: inner nuclear layer; IPL: inner plexiform layer; ONL: outer nuclear layer; OPL: outer plexiform layer. Scale: 20 µm.

3.2.4 Comparison of cpCx43.4 and cpCx47.6 expression patterns with ChAT immunoreactivity

Because the expression of cpCx43.4 and cpCx47.6 could also occur in GABAergic amacrine cells using acetylcholine as second neurotransmitter, the co-localization of FISH staining and ChAT antibody immunoreaction was analyzed. These cell types

were already described (Haverkamp and Wässle, 2000; Kang et al., 2004) so that an expression of the connexins by these cells were likely.

The signals of cpCx43.4 FISH did not merge the signals of antibody-reactivity which ruled out the expression of this connexin in cholinergic amacrine cells (Figure 15, D). Generally, immunoreactive proteins in the proximal INL were detected by ChAT antibody. Stained cells bodies were large and round, indicating a labeling of cholinergic amacrine cells. ChAT positive cell bodies were rare with a great distance which made a presentation together with cpCx43.4 FISH staining impossible. Consequently, no immunoreaction of ChAT antibody is shown for cpCx43.4 Immuno-FISH (Figure 15; C).
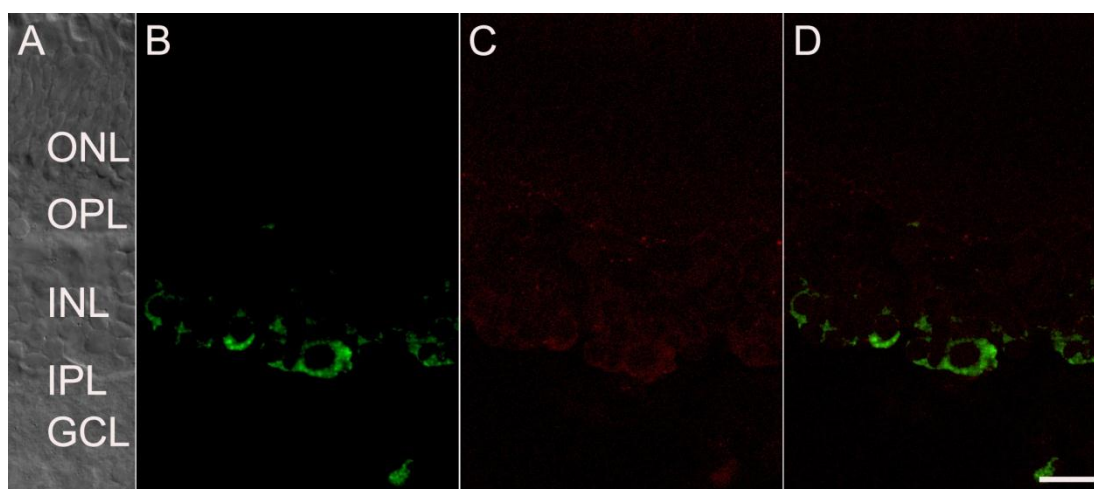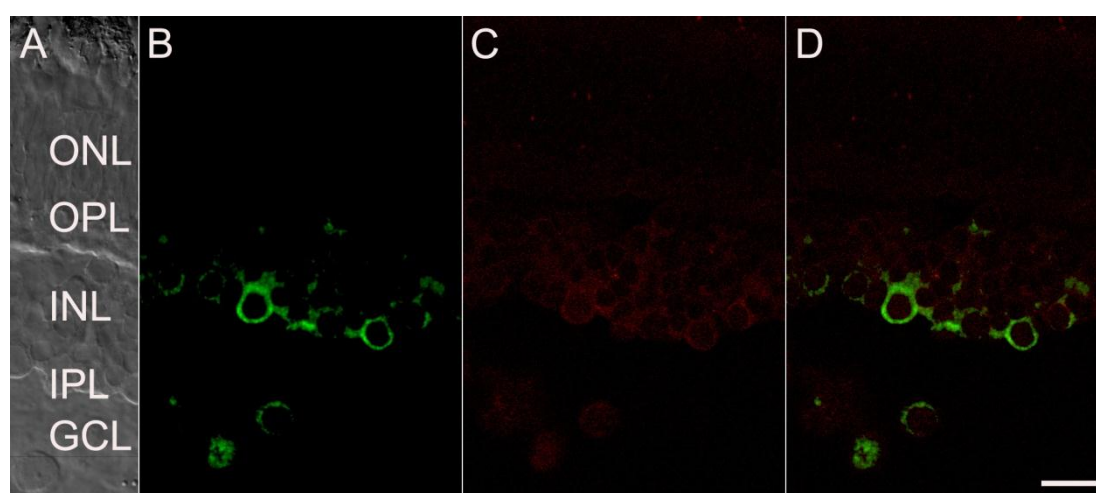

Figure 15: No co-localization of Cx43.4 mRNA expression and ChAT immunoreactivity. A) Overview of the retinal layers. B) Detected cpCx43.4 mRNA expressing cells in the proximal INL and GCL. C) No immunoreactivity of ChAT. D) Overlay of cells detected by FISH and Immunofluorescence. No matches of cpCx43.4 mRNA expression and ChAT immunoreaction. GCL: ganglion cell layer; INL: inner nuclear layer; IPL: inner plexiform layer; ONL: outer nuclear layer; OPL: outer plexiform layer. Scale: 20 µm.

In the cpCx47.6 Immuno-FISH, signals of cpCx47.6 transcripts and ChAT were merging (Figure 16, D; white arrows). Because ChAT positive cells were rare, not all cpCx47.6 expressing cells were cholinergic (not shown). Therefore the Immuno-FISH of cpCx47.6 with ChAT antibody indicated that some of the GABAergic amacrine cells expressing cpCx47.6 also contain acetylcholine.
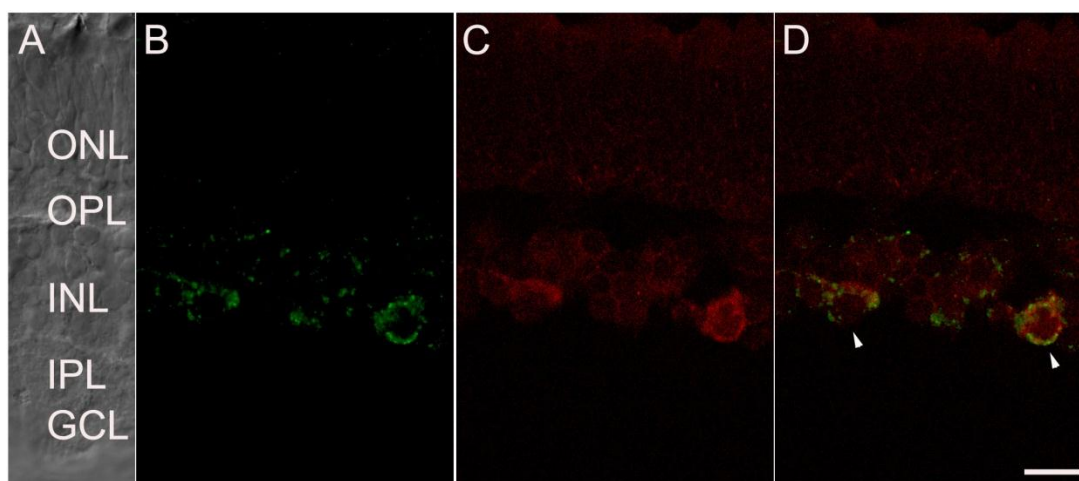
Figure 16: Co-localization of cpCx47.6 mRNA expression and ChAT immunoreactivity.
A) Overview of the retinal layers. B) Labeled cpCx47.6 transcripts in cells located in the proximal INL. C) Immunodetection of ChAT positive cells in the proximal INL. D) Merge of FISH signal and immunofluorescence. Co-localization in the case of two cells indicated cpCx47.6 mRNA expression in cholinergic amacrine cells (white arrowheads). GCL: ganglion cell layer; INL: inner nuclear layer; IPL: inner plexiform layer; ONL: outer nuclear layer; OPL: outer plexiform layer. Scale: 20 µm.

## 3.2.5 Comparison of cpCx43.4 and cpCx47.6 expression patterns with bNOS immunoreactivity

For further characterization of GABAergic ACs expressing cpCx43.4 and cpCx47.6, a brain nitric oxide synthase (bNOS) antibody was selected. In mammalian retina, NO was found in ACs which were located in INL as well as in GCL (Pang et al., 2010) and make chemical synapses onto ACs and GCs. These chemical synapses are expected to be GABAergic and nitric oxidergic (Kim et al., 1999). For this reason, it was presumptive that the subtype of GABAergic ACs, expressing the connexins cpCx43.4 and cpCx47.6 may also be nitric oxidergic.

Figure 17 shows the results of the cpCx43.4 Immuno-FISH with bNOS antobody. Two to three putative ACs were shown, detected by the bNOS antibody (Figure 17; C). One large cell body was stained in the proximal INL and a smaller one in the GCL. Perchance, another displaced AC was stained by the antibody, but because of the high background staining, an accurate conclusion was not possible. The overlay of FISH and immunodetection of bNOS showed two to three matches of both signals (Figure 17; D; white arrowheads). The displaced AC, which was faintly stained by bNOS, matched with a putative cpCx43.4 positive cell, leading to the assumption that this cell was bNOS and cpCx43.4 positive. The co-localization of cpCx43.4 expression and bNOS immunoreactivity indicates that cpCx43.4 is expressed in a

subtype of GABAergic ACs which also express nitric oxide as second neurotransmitter.
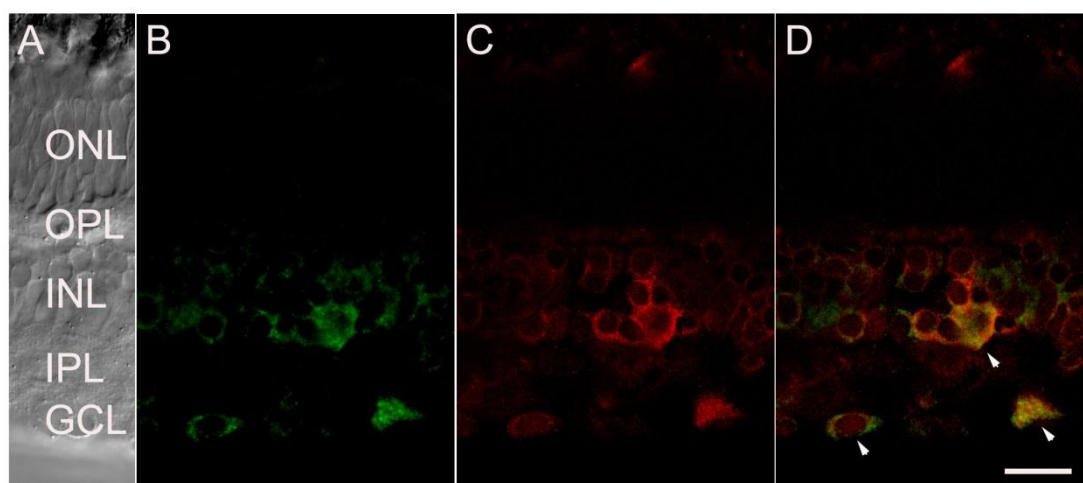
Figure 17: Co-localization of cpCx43.4 mRNA expression and bNOS immunoreactivity.
A) Overview of the retinal layers. B) Detected cpCx43.4 mRNA expressing cells in the proximal INL and GCL. C) Immunodetection of bNOS. Positive amacrine cells in the proximal INL and GCL were stained. D) Merge of cells detected by FISH and Immunofluorescence. Matches in the case of three cells (white arrows) indicated a cpCx43.4 mRNA expression in bNOS positive amacrine cells. GCL: ganglion cell layer; INL: inner nuclear layer; IPL: inner plexiform layer; ONL: outer nuclear layer; OPL: outer plexiform layer. Scale: 20 µm.

bNOS positive cells also matched with cpCx47.6 mRNA expression (Figure 18). Two cells were found, presenting the co-localization of cpCx47.6 FISH signal and bNOS immunoreactive proteins (Figure 18; D; white arrowheads).
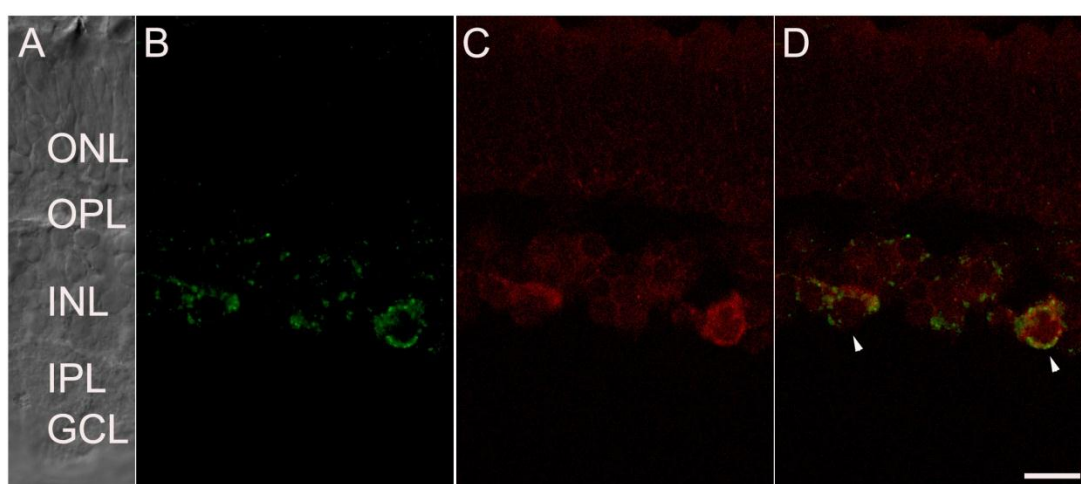
Figure 18: Co-localization of cpCx47.6 mRNA expression and bNOS immunoreactivity.
A) Overview of the retinal layers. B) cpCx47.6 transcripts were labeled in cells located the proximal INL. C) Detected bNOS positive cells in the proximal INL. D) Overlay of cells detected by FISH and Immunofluorescence. Co-localization in the case of two cells indicated cpCx47.6 mRNA expression in NO containing amacrine cells (white arrows). GCL: ganglion cell layer; INL: inner nuclear layer; IPL: inner plexiform layer; ONL: outer nuclear layer; OPL: outer plexiform layer. Scale: 20 µm.

By this Immuno-FISH, a second GABAergic amacrine cell type was found beside ChAT which expressed cpCx47.6. This cell type also released the retrograde messenger NO.

To sum up, by means of Immuno-FISH, an expression of cpCx43.4 in GABAergic amacrine cells was found, which were not only located in the INL, but also in GCL. In addition, a subtype of these GABAergic amacrine cells also transmitting nitric oxide as second neuromodulator. As well, cpCx47.6 expression was identified in GABAergic amacrine cells. These cells were exclusively located in the proximal INL. A co-localisation of cpCx47.6 mRNA expression with cholinergic ACs and NO transmitting ACs, led to two possible assumptions. By the first, cpCx47.6 is located in GABAergic ACs, containing both neurotransmitter or secondly, the connexin is expressed in two different subtypes of GABAergic amacrine cells.

3.3 Expression of cpCx43.4 & cpCx47.6 in N2A cells

In order to analyze the connexins on protein level, cpCx43.4 and cpCx47.6 coding sequences were cloned into expression vectors for a later expression in N2A cells. The pIRES2-EGFP vector was selected in which an IRES sequence between the connexin of interest and the EGFP allows a separate translation of both proteins out of one mRNA. Because of the co-expressed EGFP, transfected cells were identified by a green fluorescence. In this study the expression of connexins was used for identifying possible cross-reactions with antibodies. For cpCx43.4 and cpCx47.6, cross-reactions with a Cx45 antibody were tested possessing an epitope of the cytoplasmic loop of mouse connexin Cx45. Because the antibody was prepared by the Department of Neurobiology, three different sera of this antibody were available. Beside the expression of the two connexins using pIRES2-EGFP, cells were transfected with the connexin comprising pEGFP-N1, by which a fusion protein of the connexin linked to EGFP was built. These vector constructs have already existed.

3.3.1 Cross-reaction of expressed cpCx43.4 with the mmCx45 antibody

Because cpCx43.4 is a homologue of mmCx45, cross-reactions of mmCx45 antibody and cpCx43.4 are likely. By a comparison of the peptide sequence of the antibody and the cytoplasmic loop of cpCx43.4, a sequence similarity of 44% was calculated (Figure 19). At the end of the cytoplasmic loop of cpCx43.4, eight

sequent amino acids matched with the peptide sequence. Taken together, cross-reactions are likely.

```
anti-mmCx45   -------------------------------EMELESEKE---------NKEQSQPKP--    18
Cx43.4        HKIARMNDDEYKPSNRKRMPMITRGANRDYEEAEDNGEEDPMMMEEIMPEKEKAPEKPAA    60
                                            * * :.*::          :**::  **

anti-mmCx45   KHDGRRRIR------                                                27
Cx43.4        KHDGRRRIKRDGLMK                                                75
              ********:
```

Figure 19: Alignment of the cytoplasmic loop of cpCx43.4 and the mmCx45 antibody. The alignment of the amino acid sequences of connexin and antibody resulted in 44% sequence similarity. Eight amino acids in a row matched, so that a detection of cpCx43.4 by anti-mmCx45 is conceivable. "*" = identical in all sequences in the alignment; "." = semi-conserved substitutions are observed; ":" = conserved substitutions have been observed.

First, cross-reaction of cpCx43.4 with mmCx45 antibody was analyzed by connexin expression using pIRES2-EGFP. 48h after transfection, cells were yielded and homogenised. Crude subcellular fractions were prepared in order to localize the connexin in membrane fraction (+). As a negative controls, crude subcellular fractions of transfected N2A cells without connexin (-; pIRES2-EGFP vector) were prepared, either. Samples of mouse cytoplasmic loop (CL) and a membrane fraction of mouse heart (mHz) served as positive controls. The proteins of the different fractions were separated by SDS-PAGE (8-10%) and blotted on a nitrocellulose membrane. The immunodetection was performed by using the ECL detection system in combination with a HRP conjugated secondary antibody. After immunodetection, the antibodies were stripped, allowing multiple detections of proteins on one blot. Figure 20 summarizes all western blots. As a prerequisite for the comparison of immunoreactivity, an equal amount of protein in similar fractions was observed via ponceau staining (Figure 20; A). The detection of proteins by EGFP antibody showed a high immunoreactivity in fractions without connexin expression at the expected molecular weight of ~30 kDa (Figure 20; B; white marks). The immunoreactivity ebbed from TH to P2, indicating a cytosolic allocation of EGFP. A small protein band was even detected in the CL sample (Figure 20; B; black arrowheads) at a molecular weight of ~32 kDa. The connexin positive fractions showed a faint immunodetection, only visible in TH. This indicated a low transfection rate of N2A cells and consequently a low EGFP expression. In culture dishes, a high rate of dead cells was observed after transfection with cpCx43.4-pIRES2-EGFP. A repeated transfection revealed similar results. Because little expression of EGFP implied a low but significant expression of cpCx43.4, cross-reactions of the connexin and mmCx45 antibody were analyzed. Western blots were incubated with the three

different sera of the prepared antibody. All sera detected proteins in the positive controls. A protein band of ~32 kDa was stained in the CL sample, whereas a ~45 kDa protein was labeled in the heart sample. These proteins were likely to be the mmCx45 in mouse heart membrane fraction with a molecular weight of ~45 kDa and the cytoplasmic loop in CL with a molecular weight of ~32 kDa.
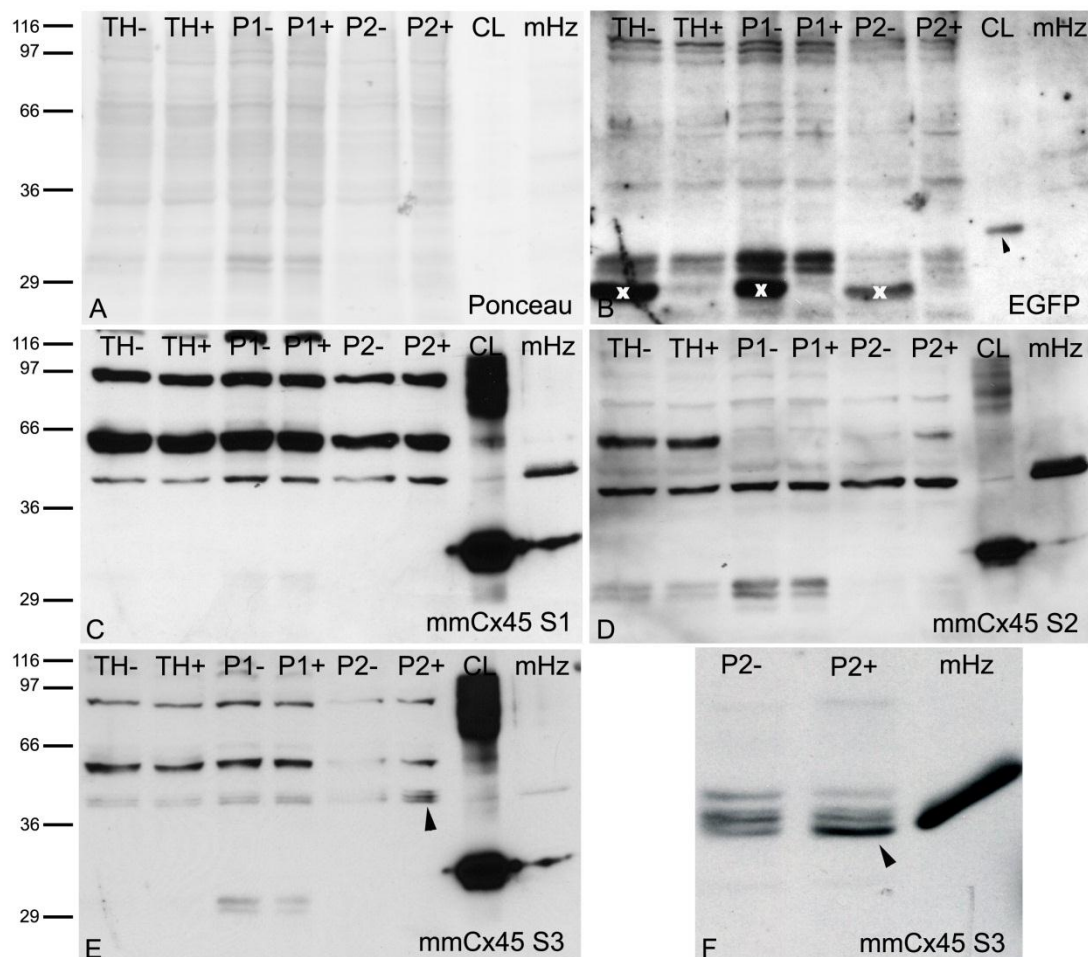
Figure 20: Detection of cpCx43.4 protein on western blot by mmCx45 S3 antibody. Crude subcellular fractions of pIRES2-EGFP transfected N2A cells with (+) and without (-, negative control) expressed cpCx43.4 are shown. The cytoplasmic loop of mouse Cx45 (CL) and a membrane sample of mouse heart (mHz) served as positive controls. A) Ponceau staining of proteins indicated equal amount of protein. B) EGFP detection showed high transfection success for pIRES2-EGFP (white marks) than for cpCx43.4 positive fractions. The black arrowhead marks a non-specific protein band at ~32 kDa. C) No detection of cpCx43.4 protein by serum 1. D) No detection of cpCx43.4 protein by serum 2. E) Detection of cpCx43.4 in membrane sample (P2+) by serum 3. In contrast to P2-, in P2+ three small lines at the expected size of ~ 45kDa were detected by the antibody (black arrow). F) Higher electrophoretic separation of proteins showed a higher detection of proteins in the lowermost line of the three detected ones in E), which is nearly under the detected mmCx45 in the membrane sample of mouse heart (black arrow). Fractions: TH (total homogenate), P1 (crude membrane fraction), P2 (membrane fraction). On the left side molecular weights are shown in kDa.

By serum 1, many proteins were stained in crude fractions. Proteins with a molecular weight of ~45, 50 and 97 kDa were labeled in every fraction (Figure 20; C). The equal staining of connexin positive and negative fractions showed no cross-reaction of cpCx43.4 and serum 1. Serum 2 detected many proteins, either, but without differences of cpCx43.4 fractions and fractions without connexin (Figure 20; D), indicating no labeling of cpCx43.4 by serum 2. By using the third serum, differences between the immunodetected proteins of cpCx43.4 positive and negative fractions occurred (Figure 20; E, F). As expected for a membrane protein, there was an enrichment of immunoreactive proteins in the cpCx43.4 P2 fraction (black arrow) which was absent in the fraction without connexin. Three protein bands were stained at an expected molecular weight of ~45 kDa. A greater separation of proteins showed a higher immunoreaction in the lower band closely under the detected band of the positive control (mHz). A protein was detected with a molecular weight a bit smaller than 45 kDa. This indicated a cross-reaction of cpCx43.4 and the serum 3 of the mmCx45 antibody.

Furthermore, detection of cpCx43.4 by mmCx45 S3 antibody was examined by immunocytochemical analysis. To avoid cell death, possibly caused by ion linkage of functional hemichannels, after transfection with cpCx43.4, the calcium concentration of the medium was increased from 1.36 mM to 5 mM. Because a higher extracellular calcium concentration leads to a lower channel conductance (Kamermans and Fahrenfort, 2004), in this study a concentration of 5 mM was used in order to close putative hemichannels.

Figure 21 shows the effect of enhanced extracellular calcium on cells transfected with cpCx43.4. Cells were transfected with and without enhanced calcium. Figure 21 A and B show cells treated with 1.36 mM calcium. In contrast to the transmission image (Figure 21; A), only two cells were visualized by EGFP fluorescence (Figure 21; B). In culture, before fixation, a high number of dead cells were observed, swimming on the surface of the medium. A high number of non-transfected cells and the increased cell death indicated an increased cell death only of transfected cells. At high extracellular calcium (5 mM), cell death was not existent (Figure 21; C and D). Normal and transfected cells were seen. This phenomenon could imply that cpCx43.4 is capable of the formation of functional hemichannels.
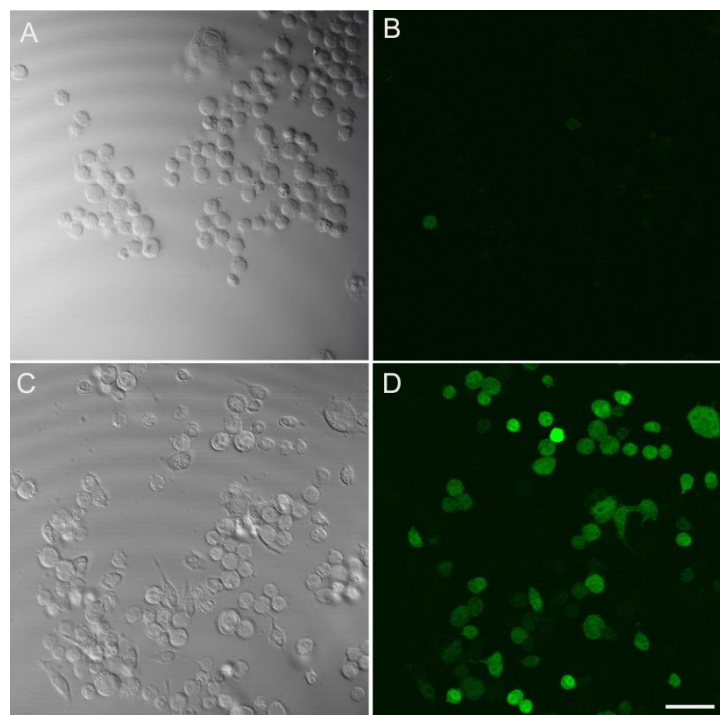
Figure 21: Overview of cpCx43.4 protein expression in N2A cells with and without enhanced calcium concentration. N2A cells transfected with cpCx43.4-pIRES2-EGFP. A and B) No or rather little transfected cells because of enhanced cell death of the transfected ones by a normal calcium concentration of 1.36 mM (DMEM). In contrast to the transmission picture (A),which showed all cells, no or even two EGFP expressing cells (green) were detected by fluorescence (B). C and D) High number of transfected cells with enhanced calcium concentration (5mM). The transmission picture (C) showed a few more cells than the fluorescence picture (D). Scale: 50 µm.

After reducing the cell death of transfected cells, immunocytochemical analysis was performed using the mmCx45 S3 antibody to visualize cross-reactions with cpCx43.4 proteins. N2A cells transfected with cpCx43.4 were incubated with mmCx45 S3 antibody, the preimmune serum 3 and were incubated with the secondary antibody alone, in order to test the specificity and to exclude possible non-specific detections (Figure 22, A – I). By serum 3, proteins were detected which were located near the nucleus (Figure 22; A; white arrowheads). Because connexins are generated in the rough endoplasmic reticulum (ER) which is located near the nucleus, the detected proteins could be processed cpCx43.4. A small line of proteins was detected, where the membranes of the two shown cells contacted, leading to the assumption that gap junction plaques formed by cpCx43.4 were labeled by the mmCx45 S3 antibody (Figure 22; C; white arrowhead). EGFP staining was localized in the whole cytoplasm. No staining of proteins was achieved by the preimmune serum 3 and the secondary antibody validating the specificity of mmCx45 S3 antibody. Cells transfected with the pIRES2-EGFP vector did not show any immunoreactive proteins labeled by mmCx45 S3 antibody (Figure 22; J-L).
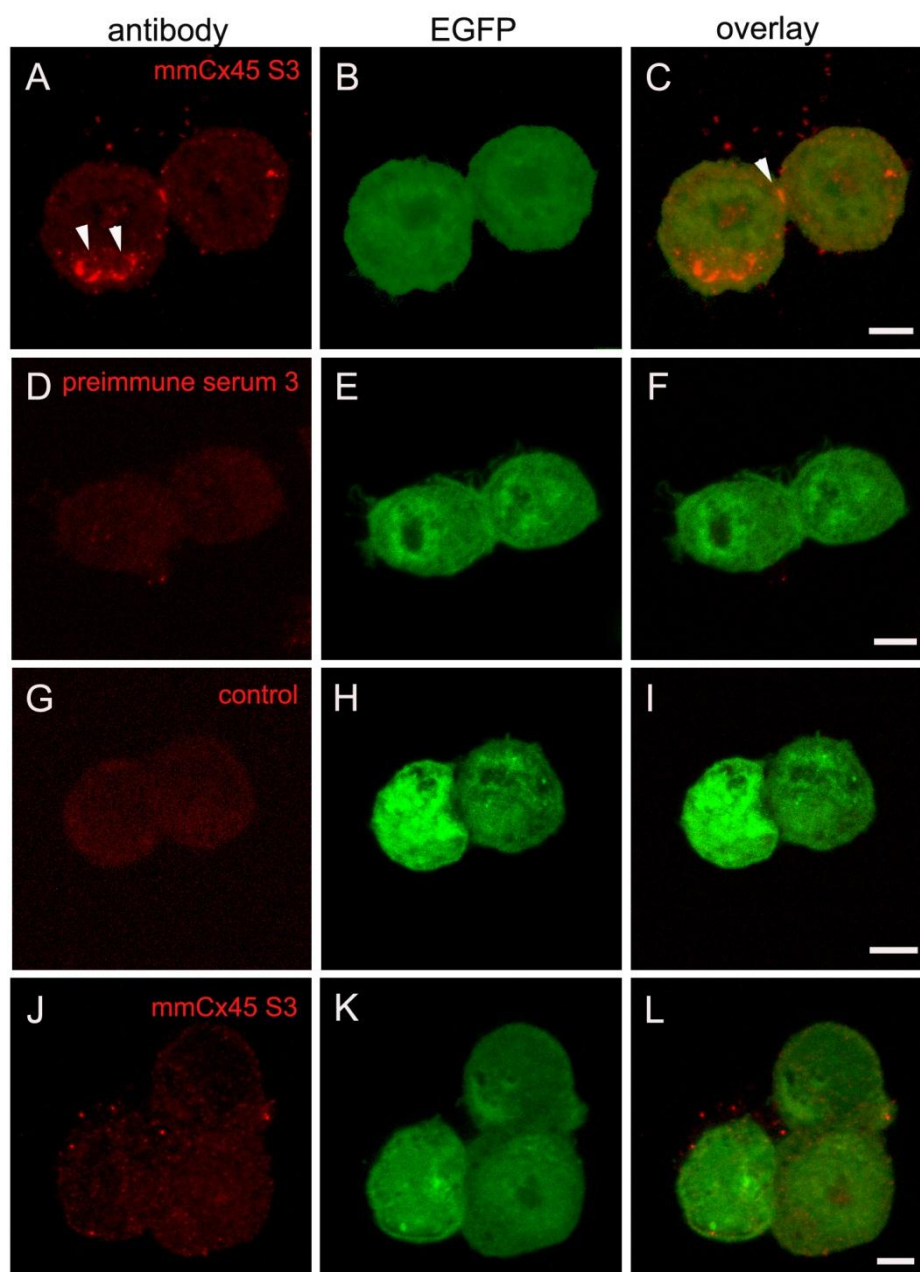
Figure 22: Detection of cpCx43.4 protein in transfected N2A cells. Transfected N2A cells are shown, incubated with different antibodies (A, D, G, J) to analyze the specificity of mmCx45 S3 antibody. Images B, E, H and K show the EGFP fluorescence, indicating the transfection success. The last column shows the overlay of the EGFP fluorescence and the immunostaining. A - I show cpCx43.4-pIRES2-EGFP transfected cells. A - C) By mmCx45 S3 antibody stained proteins. Aggregations of proteins were detected near the nuclei of the left cell (A; white arrows). The antibody labeled proteins where the membranes of the two cells contact (C; white arrow). D - F) No detection of proteins by the preimmune serum 3, excluding unspecific bindings of mmCx45 S3 antibody. G - I) Incubation of cells with just the second antibody to exclude its unspecific bindings. J - L) Cells were transfected with pIRES2-EGFP vector. There were no immunoreactive proteins stained by mmCx45 S3 antibody. Scale: 5 µm.

Because of greater localization of cpCx43.4, N2A cells were transfected with cpCx43.4-EGFP-N1 in order to express a Cx43.4-EGFP fusion protein. Consequently, the location of the connexin merges with the fluorescence of EGFP.

A co-localization of EGFP fluorescence and the immunostaining of anti-mmCx45 S3 points out the cross-reaction of cpCx43.4 with mmCx45 antibody.

The transfection was performed under condition of normal or enhanced calcium (Figure 23). At low calcium concentration (1.36 mM), a low number of transfected cells was visible (Figure 23; A and B). Before fixation in culture dishes, an increased cell death was observed. No cell death was visible at high calcium concentration (5 mM, Figure 23; C and D) and a high rate of transfected cells was achieved. These results reflected the effects obtained by cpCx43.4 expression using pIRES2-EGFP, that a higher Ca^{2+}-concentration enhanced cell viability.
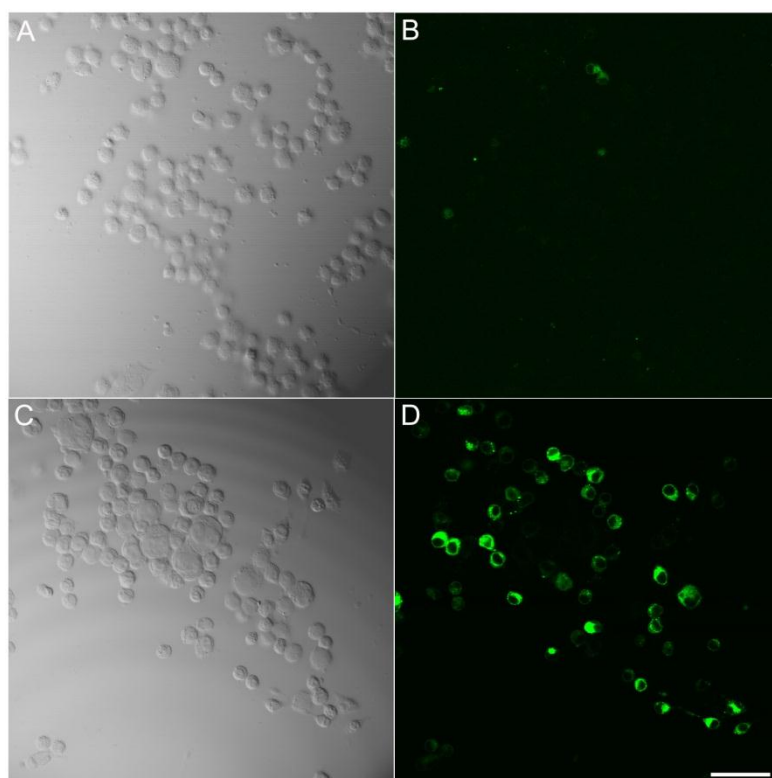
Figure 23: Overview of cpCx43.4-EGFP protein expression in transfected N2A cells with and without enhanced calcium concentration. N2A cells transfected with cpCx43.4-EGFP-N1. A and B) No or rather little transfected cells at normal calcium concentration of 1.36 mM (DMEM). In contrast to the transmission image (A),which showed all cells, no or even two EGFP expressing cells (green) were detected by EGFP fluorescence (B). C and D) High number of transfected cells with enhanced calcium concentration (5mM). The transmission picture (C) showed a few more cells than the fluorescence image (D).

N2A cells transfected with cpCx43.4-EGFP-N1 were finally incubated with mmCx45 S3 antibody, the preimmune serum 3 and incubated without a first antibody to exclude non-specific reactions (Figure 24, A - I). By mmCx45 S3 antibody proteins were detected which were located near the nuclei. In contrast to single expression of cpCx43.4, the signal was very weak. Also a small line of proteins was stained, where the membranes of adjacent cells contacted. The same pattern was visible at

EGFP fluorescence (Figure 24; A and B; white arrowheads). For this resultrs, it was assumable that putative gap junction plaques formed by cpCx43.4 were labeled by the antibody. EGFP fluorescence showed a punctual allocation of cpCx43.4-EGFP. Even here, the typical aggregation of the expressed connexins in the ER was not found. A decreased expression rate of connexins caused by an increased calcium concentration is a possible explanation. Nevertheless, the overlay of EGFP fluorescence and mmCx45 S3 antibody signal showed a co-localization not of not all, but of the most of labeled proteins. No staining of proteins was achieved by the preimmune serum 3 and the secondary antibody which approved the specificity of mmCx45 S3 antibody. Cells transfected with pEGFP-N1 vector showed even no signal of mmCx45 S3 antibody (Figure 24; J - L). A different allocation of the EGFP was visible. In contrast to the punctual allocation of the EGFP fusion protein, the single expressed protein showed a diffuse arrangement in the whole cytoplasm.
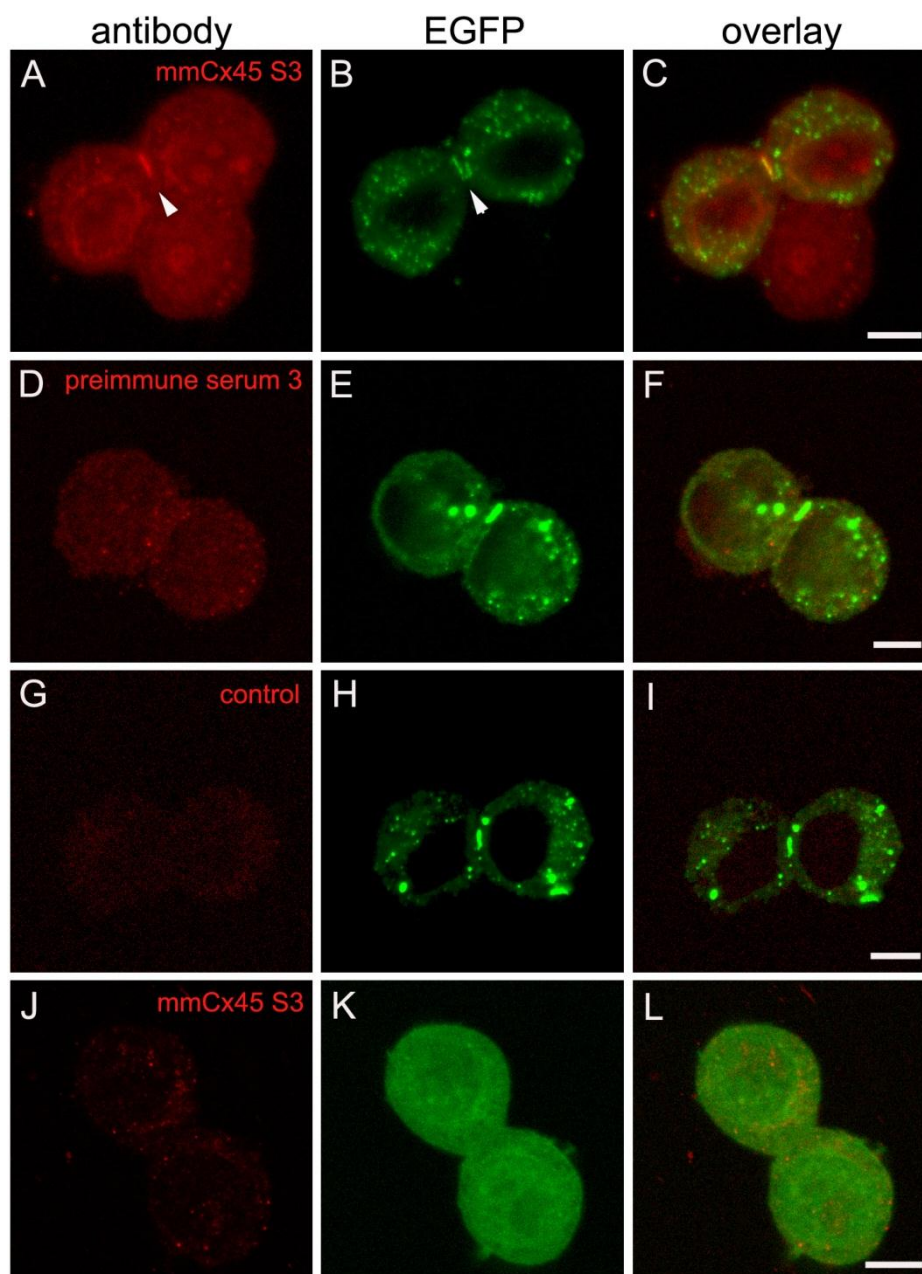
Figure 24: Detection of cpCx43.4-EGFP fusion protein in transfected N2A cells.
Transfected N2A cells are shown, incubated with different antibodies (A, D, G, J) to evidence the specificity of mmCx45 S3 antibody. Images B, E, H and K show the EGFP fluorescence, indicating the transfection success and the location of the cpCx43.4 fusion protein. The last column shows the merge of the EGFP signal and the immunodetection. A - I) cpCx43.4-pEGFP-N1 transfected cells. A - C) By mmCx45 S3 antibody detected proteins. Proteins around the nuclei were detected. The antibody stained putative gap junctions (white arrow). The EGFP fluorescence showed a similar pattern (white arrow). D - F) With preimmune serum 3 incubated cells showed no immunoreactivity, excluding unspecific bindings of mmCx45 S3. G - I) Incubation of cells with the second antibody alone to exclude its unspecific bindings. J - L) Cells transfected with pEGFP-N1 vector. There were no detection of proteins by mmCx45 S3 antibody. The EGFP signal was spread over the whole cytoplasm. Scale: 5 µm.

In summary, a cross-reaction of the mmCx45 S3 antibody with cpCx43.4 was shown.

On western blot, a specific protein band was detected at a molecular weight of ~45

kDa. By immunocytochemical analysis putative gap junction plaques between contacted membranes of adjacent cells were labeled by expression of cpCx43.4 as single as well as fusion protein linked to EGFP. The merge of EGFP signal as fusion protein and the mmCx45 S3 antibody staining in the case of the detected putative gap junction plaques, leading to the assumption that cpCx43.4 was detected by mmCx45 S3 antibody.

3.3.2 Cross-reaction of expressed cpCx47.6 with the mmCx45 antibody

Because cpCx47.6 is like cpCx43.4 a homologue of mmCx45, cross-reactions of mmCx45 antibody with cpCx47.6 are likely, either. By a comparison of the peptide sequence of the antibody and the cytoplasmic loop of cpCx47.6, a sequence similarity of 37% was calculated (Figure 25). At the end of the cytoplasmic loop of cpCx47.6, eight sequent amino acids matched with the epitope. The alignment indicated possible cross-reactions.

```
anti-mmCx45  --------------------------------EMELE--------------SEKENKEQS   14
cpCx47.6     HKIARTSEEERCKNQIYQKRNRHSGWRNGHHLQEVLEEDDAEPMIYEEDTLDEQEIKPET   60
                                             :  **                 .*:* * ::

anti-mmCx45  -----QPKPKHDGRRRIR------                                       27
cpCx47.6     DKGKIQDQMKHDGRRRIMQEGLMR                                       84
                  * : ********
```

Figure 25: Alignment of cpCx47.6 cytoplasmic loop and the mmCx45 antibody sequence. The alignment of the amino acid sequences of connexin and antibody resulted in 37% sequence similarity. Eight amino acids in a row matched, so that a detection of cpCx47.6 by anti-mmCx45 is supposable. "*" = identical in all sequences in the alignment; "." = semi-conserved substitutions are observed; ":" = conserved substitutions have been observed.

Cross-reactions of cpCx47.6 with mmCx45 antibody were first analyzed by connexin expression using pIRES2-EGFP. Western blots were prepared as described in 3.3.1. The same positive controls and antibodies were used, as before.

Figure 26 presents all performed western blot analyses. The ponceau staining (Figure 26; A) showed an equal amount of proteins in all fractions, allowing a comparison of immunoreactivity. Because of high immunoreaction, small volumes of positive controls were used. Immunodetection of proteins using EGFP antibody showed a high immunoreactivity in all fractions at the expected molecular weight of ~30 kDa (Figure 26; B; white marks). The signal faded from TH to P2, indicating a cytosolic allocation of EGFP. The expression of EGFP reflected the transfection success and consequently the expression of cpCx47.6. Even a faintly stained

protein band was labeled in CL sample at a molecular weight of ~32 kDa (Figure 26; B; black arrowhead). Cross-reactions of the connexin and mmCx45 antibody were analyzed by using three different sera of the prepared antibody. All sera detected proteins in the positive controls. A protein of ~32 kDa was detected in the CL sample, whereas a ~45 kDa protein was stained in the heart sample. These proteins were likely to be the mmCx45 in mouse heart membrane fraction with a molecular weight of ~45 kDa and the cytoplasmic loop in CL sample with a molecular weight of ~32 kDa. Serum 1 stained many proteins in crude fractions. Proteins with a molecular weight of ~45, 50 and 97 kDa were labeled in every fraction (Figure 26; C). The equal staining of connexin positive and connexin negative fractions excluded cross-reaction of cpCx47.6 and serum 1. By serum 2, many proteins were detected without differences of cpCx47.6 fractions and fractions without connexin (Figure 26; D) and consequently indicated no staining of cpCx47.6 by serum 2. Especially by using the third serum, differences of immunoreactive protein bands of cpCx47.6 positive and negative fractions arose (Figure 26; E, F). An enrichment of immunodetected proteins in the cpCx47.6 P2 fraction occurred, missing in the fraction without connexin. Three protein bands were localized at an expected molecular weight of ~45 kDa (black arrow). At higher resolution, a high immunoreaction in the middle band at the level of the positive control (mHz) was suggested with a molecular weight of ~45 kDa. No stained proteins in P2- at the same level indicated a labeling of cpCx47.6 protein by the third serum of mmCx45 antibody.
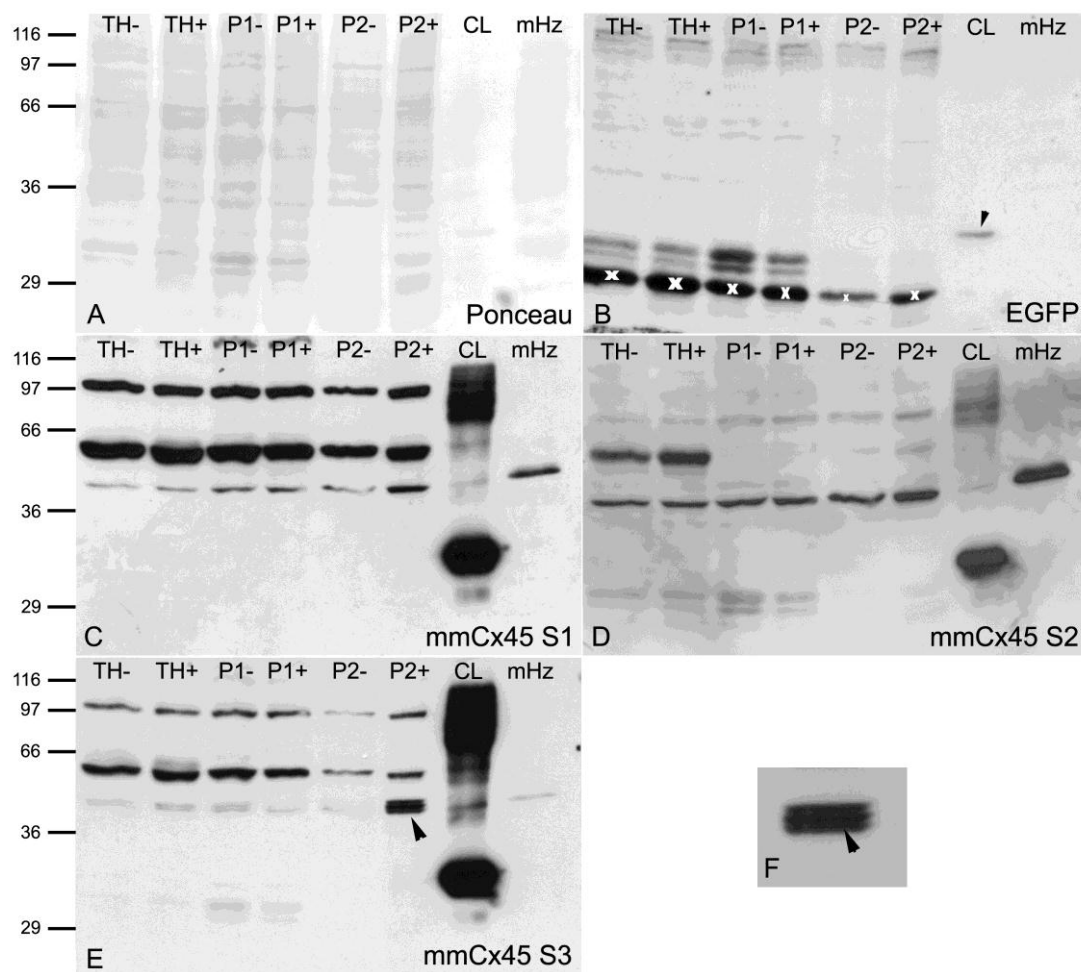
Figure 26: Detection of cpCx47.6 protein on western blots. Crude subcellular fractions of N2A cells transfected with pIRES2-EGFP with (+) and without (-, negative control) expressed cpCx47.6. The cytoplasmic loop of mouse Cx45 (CL) and a membrane sample of mouse heart (mHz) served as positive controls. A) Ponceau staining of proteins to analyze the equal amount of proteins. B) EGFP detection showed high transfection success for transfection with and without Cx47.6 protein (white marks). A ~32 kDa protein was stained in CL (black arrow). C) No labeling of cpCx47.6 protein by serum 1. D) No detection of cpCx47.6 protein by serum 2. E) Detection of cpCx47.6 in membrane sample (P2+) by serum 3 (black arrow). In contrast to P2-, in P2+ three small lines at the expected size of ~ 45kDa were visualized by the antibody. F) Higher electrophoretic separation of proteins showed the highest immunoreaction of proteins in the middle line of the three detected ones in E) (black arrow). Fractions: TH (total homogenate), P1 (crude membrane fraction), P2 (membrane fraction). On the left side molecular weights are shown in kilo Dalton.

In order to approve mmCx45 S3 antibody cross-reactivity with cpCx47.6, immunocytochemical analysis was performed. Because of the existence of two different vector constructs, cpCx47.6 was either expressed as a single protein using pIRES2-EGFP or as a fusion protein linked to EGFP (Figure 27) using pEGFP-N1. Both transfections showed a high transfection rate. Because EGFP is a cytosolic protein, single expression led to an allocation in the cytoplasm (Figure 27; B). As fusion protein linked to cpCx47.6, the EGFP signal was mainly located in the rough ER where connexin processing takes place (Figure 27; D).
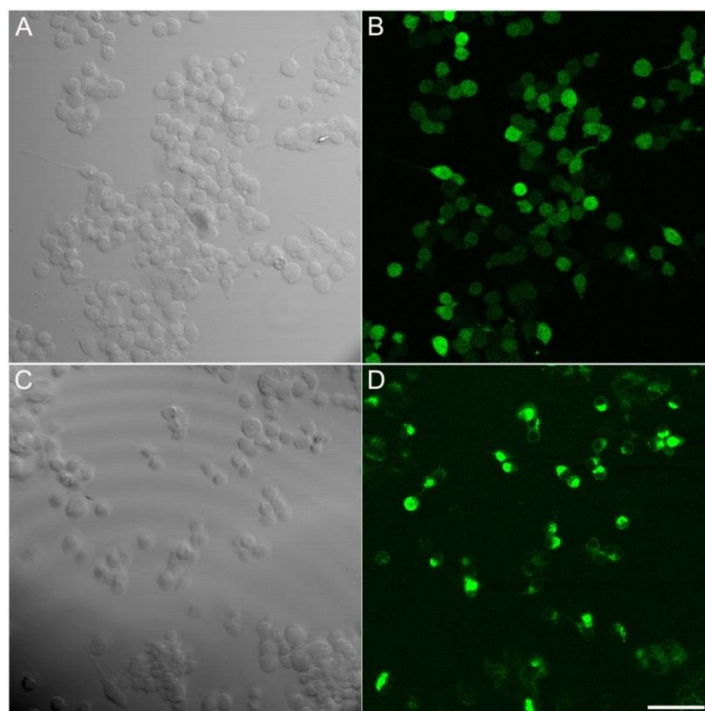
Figure 27: Overview of cpCx47.6 and cpCx47.6-EGFP fusion protein expression in transfected N2A cells. A and B) cpCx47.6-pIRES2-EGFP transfected cells. A) Transmission image shows all cells in culture. B) Transfected cells are shown by EGFP fluorescence. C and D) Cells transfected with cpCx47.6-pEGFP-N1. A) Transmission image presents all cells in culture. B) Transfected cells are visualized by EGFP signal. Scale: 50 µm.

cpCx47.6-pIRES2-EGFP transfected N2A cells were incubated with mmCx45 S3 antibody, the preimmune serum 3 and incubated with the secondary antibody without the first to exclude non-specific signals (Figure 28, A - I). Serum 3 detected proteins, located near the nuclei. The immunodetected proteins were suggested to be expressed cpCx47.6, for the reason that connexins are processed in the rough endoplasmic reticulum (ER) (Figure 28; A; white arrowhead). A high immunoreaction was visible at putative gap junction plaques formed by cpCx47.6 (Figure 28; C; white arrowheads). EGFP signal was localized in the whole cytoplasm. No immunoreactive proteins were detected by the preimmune serum 3 and the secondary antibody, approving the specificity of anti-mmCx45 S3. Using pIRES2-EGFP, transfected cells without connexin possessed even no immunodetected proteins after incubation with mmCx45 S3 antibody (Figure 28; J - L).
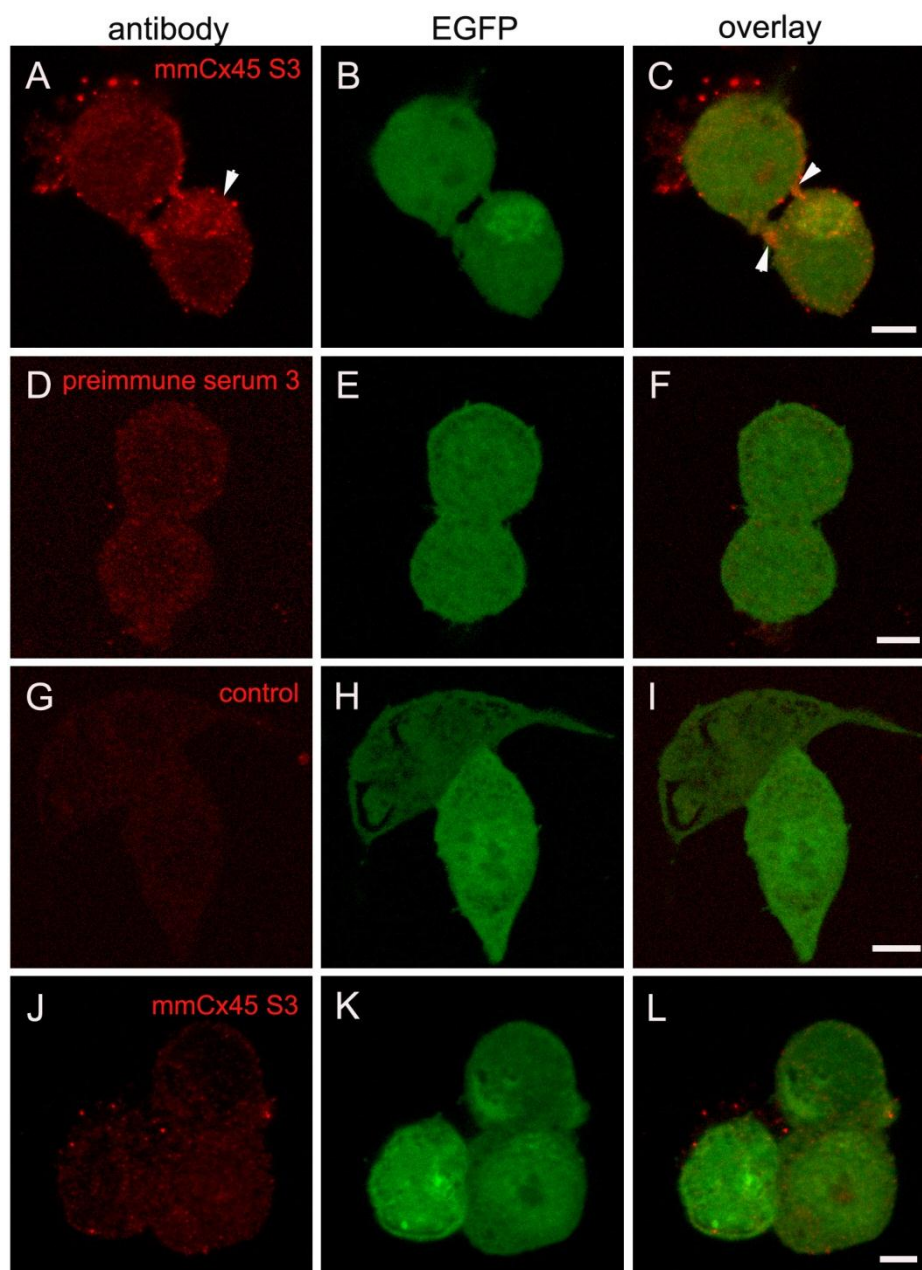
Figure 28: Detection of cpCx47.6 protein in transfected N2A cells. Transfected N2A cells are shown which were incubated with different antibodies (A, D, G, J) to evidence the specificity of mmCx45 S3. Images B, E, H and K show the EGFP fluorescence to analyze the transfection success. The last column shows the merge of the EGFP siganl and the immunostaining. A - I) cpCx47.6-pIRES2-EGFP transfected cells. A - C) Detection of proteins by the mmCx45 S3 antibody. Aggregations of proteins were stained near the nuclei of the lower cell (A; white arrow). The antibody labeled proteins where the membranes of adjacent cells contact (C; white arrows). D - F) No detection of proteins by the preimmune serum 3, excluding unspecific bindings of mmCx45 S3. G - I) Incubation of cells with the second antibody alone to analyze its unspecific bindings. J - L) With pIRES2-EGFP transfected cells. There was no detection of proteins by the mmCx45 S3 antibody. Scale: 5 μm.

N2A cells transfected with cpCx47.6-pEGFP-N1 were finally incubated with mmCx45 S3 antibody, the preimmune serum 3 and incubated with the secondary antibody alone, as before (Figure 29, A - I). mmCx45 S3 antibody labeled proteins,

located near or around the nuclei. In contrast to single expression of cpCx43.4 protein, the signal was very weak. A small line of proteins was detected at two contacted membranes of adjacent cells (Figure 29; A; white arrowhead). This line was even observable by EGFP fluorescence (Figure 29; B; white arrowhead), gave rise to the assumption that gap junction plaques formed by cpCx47.6 were stained. There was a punctual allocation of cpCx47.6-EGFP shown by the EGFP signal. Like cpCx43.4 fusion protein, the typical aggregation of the expressed connexins in the ER was not found. A decreased expression rate of connexins, caused by an increased calcium concentration, could be a possible explanation. Taken together, the overlay of EGFP fluorescence and mmCx45 S3 antibody staining showed a co-localization of most labeled proteins. By the preimmune serum 3 and the secondary antibody no immuoreactive proteins were found, pointing out the specificity of mmCx45 S3 antibody. Transfection with EGFP-N1 vector showed even no labeled proteins by mmCx45 S3 antibody (Figure 29; J - L). A different allocation of the EGFP was visible. In contrast to the punctual allocation of EGFP fusion protein, by single expression of single EGFP, a diffuse arrangement was found in the cytoplasm.
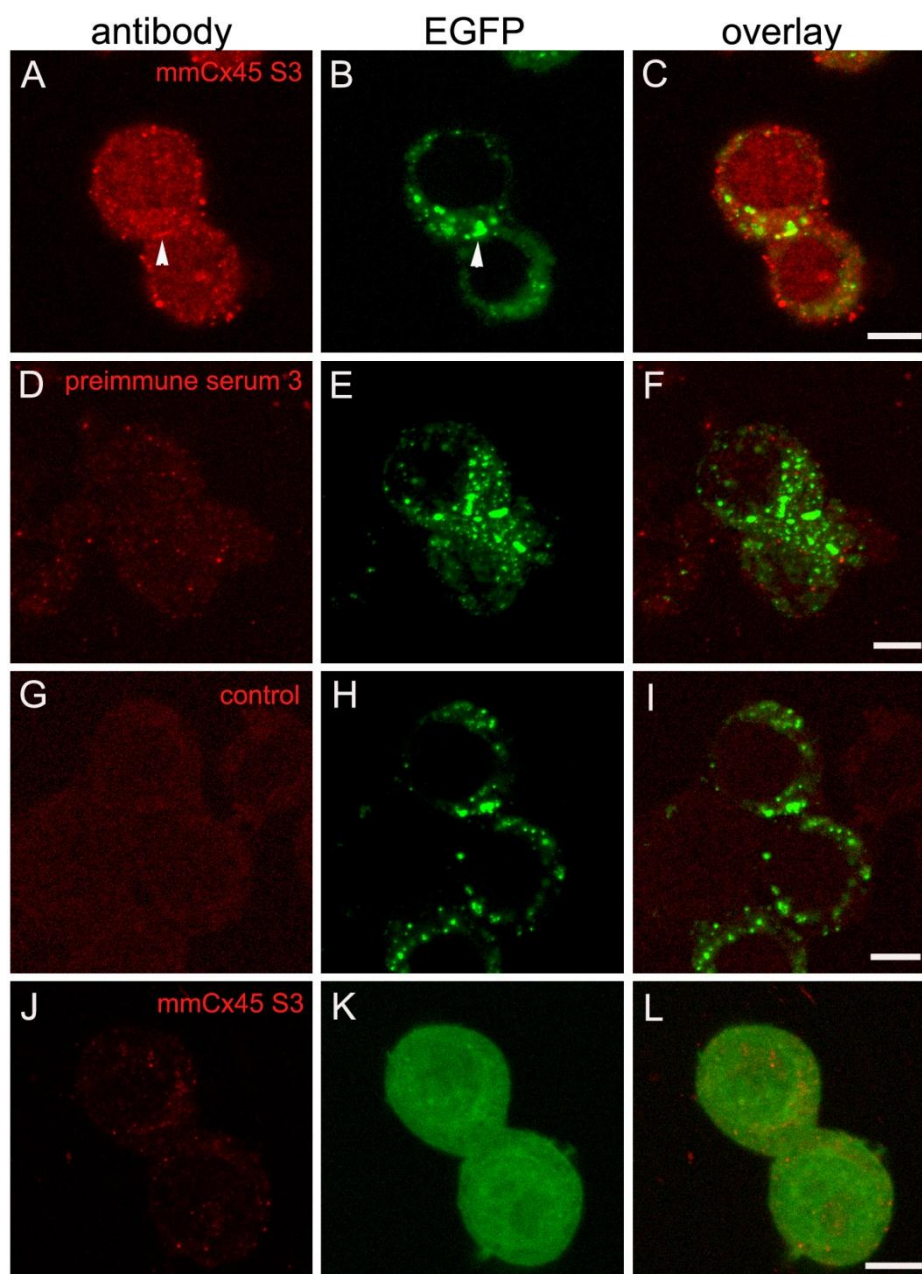
Figure 29: Detection of cpCx47.6-EGFP fusion protein in transfected N2A cells.
Transfected N2A cells are shown which were incubated with different antibodies (A, D, G, J)
to examine the specificity of the mmCx45 S3 antibody. Images B, E, H and K show the
EGFP signal to visualize the transfection success and the location of the cpCx47.6 fusion
protein. The last column shows the overlay of the EGFP fluorescence and the
immunodetection. A - I) cpCx47.6-pEGFP-N1 transfected cells. A - C) Detection of proteins
by the mmCx45 S3 antibody. Proteins around the nuclei were stained. The antibody
detected putative gap junctions (A; white arrow). The EGFP signal showed a similar pattern
(B; white arrow). D - F) No immunodetection by the preimmune serum 3 which excludes
non-specific staining of mmCx45 S3 antibody. G - I) Incubation of cells with the second
antibody alone to exclude unspecific bindings. J - L) Transfected cells using pEGFP-N1.
There were no labeled proteins by the mmCx45 S3 antibody. The EGFP signal was spread
over the whole cytoplasm. Scale: 5 µm.

To sum up, a cross-reaction of mmCx45 S3 antibody with cpCx47.6 was presented by means of western blot and immunocytochemical analysis. On western blot, a specific protein band was stained at a molecular weight of ~45 kDa, indicating the detection of cpCx47.6. After expression of cpCx47.6 as single protein and fusion protein with EGFP, putative gap junction plaques between contacted membranes of adjacent cells were detected by indirect immunofluorescence. The co-localization of EGFP fluorescence as fusion protein and the immunodetection of mmCx45 S3 antibody in the case of the labeled gap junction plaques gave rise to the assumption that cpCx47.6 was detected by mmCx45 S3 antibody.

3.4 Proof of cpCx53.8 antibody-specificity

In addition to the analysis of cpCx43.4 and cpCx47.6, a second project arose out of the expression of connexins in N2A cells. To analyze the specificity of the cpCx53.8 antibody, expression studies of cpCx53.8 and two related connexins (zfCx52.7 and zfCx52.9) were performed in N2A cells.

Because of the high genetic affinity of the connexins with a molecular weight around 50 kDa, cross-reactions of cpCx53.8 antibody with zfCx52.7 and zfCx52.9 were analyzed. An alignment of protein sequences compared the two amino acid sequences of the cytoplasmic terminal of the zebrafish connexins with the C-terminal of the cpCx53.8 connexin (Figure 30). The marked blue sequence presents the epitope of the cpCx53.8 antibody. The alignment showed no significant sequence similarities so that a cross-reaction of the antibody with the zebrafish connexins was not assumed.

```
Cx53.8    FHLGVKKIKETIYG--SKYSGDDESICRSKKNSMVQQVCILTNSSPQK--HMHLTHTSLV    56
Cx52.7    SHLGVRKIKQTLSG--LQFVEED-SLCKP-KHSTIQQLCVMTEYSPHK--NPQLKT----    50
Cx52.9    LHLAYKKLKKGLRDHCPALRDGPADSSAPNRNSVGQQARKATMPMALSGYTALLEKQGNG    60
            **. :*:*: : .          . . . ::*  **   *   . .      *

Cx53.8    VVPDGQMAPMPLYMPMAGP----PSSQEVPNSNP--NGSEQPPRQNRLPSQPEFQSLQQL   110
Cx52.7    FIPQGQMDKHLFGSSSNDI----LRHNSLAASTLPVSCITQQPRQMRQPSQGMIHELHSQ   106
Cx52.9    PTYPSIIHPLSAFVPIQGPSAPDMENRDALRSPLEHNSSNNTSSGSRSPLVQERGPAASP   120
            . :       . .        ..  *   .  : .  * *           .

Cx53.8    GATERRPTLDNRP---HSCSSEESGPKGSGPPRNFSQQPRASLRASNIEIPAALR-KQSR   166
Cx52.7    GSLRLLEDQENQHPDSSNCSERDIRPFSSGHPG----------SEGHTEIPACLRNALHR   156
Cx52.9    SDYHTLPQTDSLPLIATLPLTDPLPQMDLFPLR----------DASSCPAVLHKQRRVSP   170
            .  .      :.        .               .         : 

Cx53.8    VSQCKDFSEESD-SQESGNYPTARKASFMSRGLSESPSESPTSKSGSDTETNRIAQGESP   225
Cx52.7    PSRLADLADDAMESSESDFCPPNRKASFMARMPSESMSGSPSCPSTRSSES-ELGSLNDL   215
Cx52.9    PWNCSTVMESTGSDSGDSSSGGLSQGRRTRCGRSVSRSDLRLTPDSQPHCAAESPSLSPQ   230
            .  . :.: .. ..      :.       * * *     .      : . . .

Cx53.8    AMTPPPATGRRMSMS MILELSSIMKK                                   251
Cx52.7    PMNPPPGGGRRMSMASRWK-------                                   234
Cx52.9    RQRPAIGSSRRADLQI----------                                   246
            *. . .** .:
```

Figure 30: Alignment of the amino acid sequence of the cytoplasmic terminals of cpCx53.8, zfCx52.7 and zfCx52.9. The alignment of the amino acid sequences of the three connexins showed no high sequence similarities. "*" = identical in all sequences in the alignment; "." = semi-conserved substitutions are observed; ":" = conserved substitutions have been observed; ":" = epitope of cpCx53.8 antibody.

Cross-reactions of zebrafish connexins and cpCx53.8 antibody were first analyzed on western blot. As a preparation, N2A cells were transfected with zfCx52.7-pIRES2-mRFP, zfCx52.9-pIRES2-EGFP and for a positive control with cpCx53.8-pIRES2-EGFP. 48h after transfection, cells were harvested and homogenised. Crude subcellular fractions were prepared in order to localize the connexin in membrane fraction (+). As a negative control, crude subcellular fractions of transfected N2A cells without connexin (-) were prepared, either. The proteins of different fractions were first separated by SDS-PAGE (8-10%) and blotted on a nitrocellulose membrane. Using the ECL detection system in combination with a HRP conjugated secondary antibody, an immunodetection was performed. After immunodetection, the western blot was stripped, facilitating multiple immunodetections by different antibodies.

In Figure 31 the ponceau staining is presented. The staining showed an equal amount of proteins in all fractions which allowed a comparison of immunoreactivity.
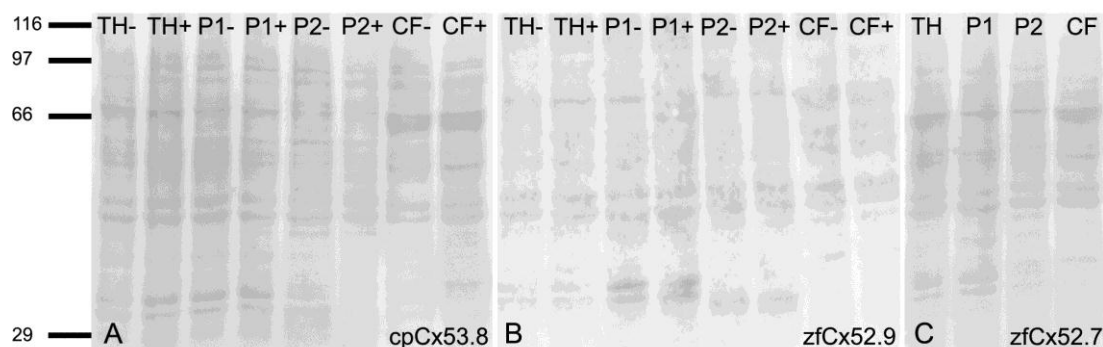
Figure 31: Ponceau staining of subcellular fractions from transfected N2A cells. Crude subcellular fractions of transfected N2A cells with (+) and without (-, negative control) expressed fish connexin on western blot are shown. Each blot showed an equal amount of proteins. A) cpCx53.8-pIRES2-EGFP transfected cells. B) Cells transfected with zfCx52.9-pIRES2-EGFP. C) With zfCx52.7-pIRES2-mRFP transfected cells. Fractions: TH (total homogenate), P1 (crude membrane fraction), P2 (membrane fraction), CF (cytosolic fraction). On the left side molecular weights are shown in kDa.

Next, EGFP or even RFP were detected on different blots, indicating the successes of transfection (Figure 32). On cpCx53.8 blot, high immunoreactive proteins were detected in cytosolic fractions with and without cpCx53.8 at the expected molecular weight of EGFP (~30 kDa) (Figure 32; A; white arrowheads). The staining decreased from TH fractions to membrane fractions caused by the cytosolic location of EGFP. The zfCx52.9 blot showed a similar result for connexin positive fractions. In negative fractions there was a weak immunodetection at the expected molecular weight of EGFP (Figure 32; B; white arrowheads). Nevertheless, little EGFP expression was visualized in the cytosolic fraction without connexin, indicating the success of transfection using pIRES2-EGFP.
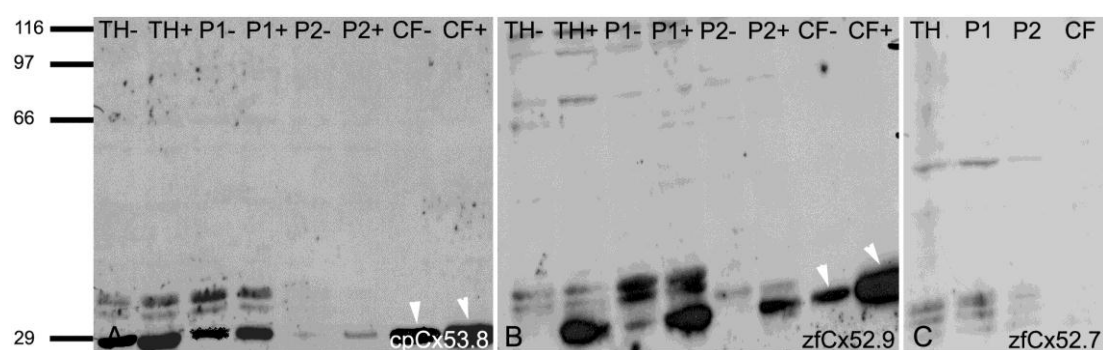
Figure 32: Detection of EGFP or RFP as a success of transfection. Crude subcellular fractions of transfected N2A cells with (+) and without (-, negative control) expressed fish connexin are shown. A) Cells transfected with cpCx53.8-pIRES2-EGFP. Detection of a ~30 kDa protein in every fraction by EGFP antibody. Highest immunoreaction in CF (white arrows). B) zfCx52.9-pIRES2-EGFP transfected cells. Detection of a ~30 kDa protein in nearly every fraction by anti-EGFP. C) Cells transfected with zfCx52.7-pIRES2-mRFP. Staining of proteins at ~30 kDa by DsRed antibody. Fractions: TH (total homogenate), P1 (crude membrane fraction), P2 (membrane fraction), CF (cytosolic fraction). On the left side molecular weights are shown in kDa.

On zfCx52.7 blot proteins were detected at a molecular weight of ~30 kDa, matching with the molecular weight of RFP (Figure 32; C). The immunoreactivity of the detected proteins ebbed from TH to CF. No pIRES2-mRFP vector was available for negative control.

On cpCx53.8 blot (Figure 33, A), a highly specific detection pattern of immunoreactive proteins was visualized by cpCx53.8 antibody as expected. The antibody labeled a single protein band only in cpCx53.8 positive fractions at the weight of ~54 kDa. Because connexins are membrane proteins, no signal was found in the cytosolic fraction and there was an enrichment of immunoreactive proteins from TH to P2. On zfCx52.9 blot (Figure 33; B), a high immunoreaction was observed. In contrast to cpCx53.8 blot, an antibody with a higher BSA concentration was used, causing enormous non-specific protein detection. In order to visualize putative weak cross-reactions of the antibody with zfCx52.9 protein, the blot was exposited longer which enlarged the immunoreactivity. Comparing the zfCx52.9 positive to the negative fractions, no different signalling was observed, excluding a cross-reaction of the antibody with zfCx52.9. On zfCx52.7 blot (Figure 33; C) a faint signal was detected even after long exposition. Proteins at a weight of ~66 kDa were stained which appeared to be non-specific. Because no immunodetection was visible at the molecular weight of ~53 kDa for zfCx52.7 protein, consequently cross-reactions of cpCx53.8 antibody with zfCx52.7 protein were unlikely.
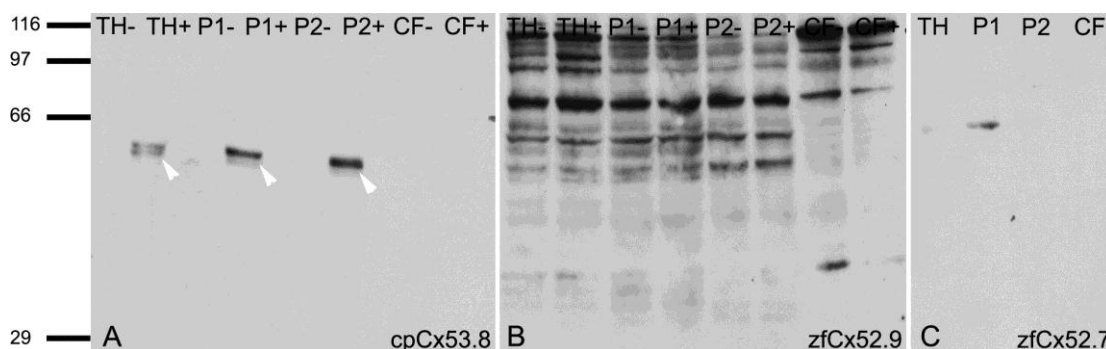
Figure 33: Cross-reactivity of the cpCx53.8 antibody with zfCx52.7 and zfCx52.9. Crude subcellular fractions of transfected N2A cells with (+) and without (-, negative control) expressed fish connexin are shown. To analyze the cross-reactivity blots were incubated with the cpCx53.8 antibody. A) Cells transfected with cpCx53.8-pIRES2-EGFP. In samples containing cpCx53.8 (except for CF) proteins of a weight of ~54 kDa were detected. B) With zfCx52.9-pIRES2-EGFP transfected cells. No detection of specific proteins at ~53 kDa in connexin fractions. C) Cells transfected with zfCx52.7-pIRES2-mRFP. No detection of proteins at the expected weight of ~53 kDa. Fractions: TH (total homogenate), P1 (crude membrane fraction), P2 (membrane fraction), CF (cytosolic fraction). On the left side molecular weights are shown in kDa.

Finally, the zebrafish connexins were detected by their own specific antibodies (Figure 34) to analyze their expression. The detection was carried out by alkaline

phosphatase reaction. On zfCx52.9 blot (Figure 34; A) the zfCx52.9 antibody stained proteins in all connexin positive fractions at a molecular weight of ~53 kDa. The detected proteins will probably be the zfCx52.9 proteins. On zfCx52.7 blot (Figure 34; B), a faint signal was labeled as before. Nevertheless, the signal in the membrane fraction at the expected molecular weight of ~53 kDa (black arrow) indicated that zfCx52.7 was correctly expressed by the N2A cells.
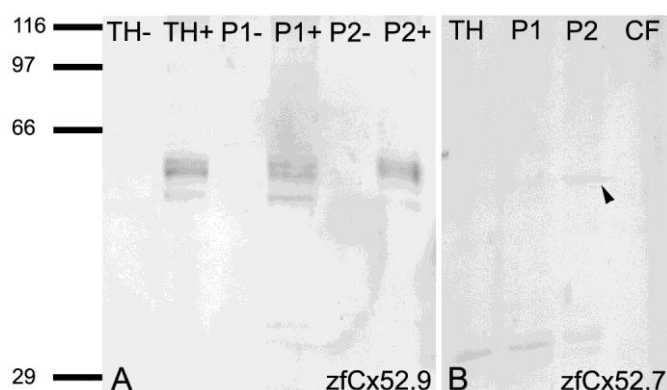
Figure 34: Detection of zfCx52.7 and zfCx52.9 proteins. Crude subcellular fractions of transfected N2A cells with (+) and without (-, negative control) expressed fish connexin are shown. To proof expression of the different fish connexins in N2A cells blots were incubated with a specific antibody against the expressed connexin. A) Cells transfected with zfCx52.9-pIRES-EGFP. Detection of proteins at an expected molecular weight of ~53 kDa by zfCx52.9 antibody. B) zfCx52.7 transfected cells. Detection of proteins at the expected weight of ~53 kDa by zfCx52.7 antibody as faint bands (black arrow). Fractions: TH (total homogenate), P1 (crude membrane fraction), P2 (membrane fraction), CF (cytosolic fraction). On the left side molecular weights are shown in kDa.

Cross-reactions of cpCx53.8 antibody with zfCx52.7 and zfCx52.9 were also analyzed by immunocytochemistry. As positive control, N2A cells were transfected with cpCx53.8 in pIRS2-EGFP (Figure 35, A – I). Cells were incubated with anti-cpCx53.8 (Figure 35; A – C) and the secondary antibody alone (Figure 35; D - F) to exclude possible non-specific detections. Furthermore, cells were transfected with pIRES2-EGFP vector and incubated with anti-cpCx53.8, approving the specificity of the antibody (Figure 35; G – I). Immunoreactive proteins were detected in the cell membrane indicating an integration of processed connexins into it (white arrowheads upper cells). Besides, there was massive staining of intracellular compartments in close proximity of the nucleus (white arrowheads lower cell). This signal could putatively arise from generated cpCx53.8 protein, because connexins as membrane proteins were generated and processed in the rough ER. No immunoreaction was found without cpCx53.8 antibody so that non-specific signals of the secondary antibody were excluded (Figure 35; D). By anti-cpCx53.8, proteins were detected in cell membrane of N2A cells which were transfected with pIRES2-

EGFP vector. Immunodetection was also found in untransfected cells (Figure 35; G; white arrowheads). These non-specific signals in cell membrane had to be regarded in further analysis. In all cells, EGFP signal was located in cytosol as well as in the nucleus.
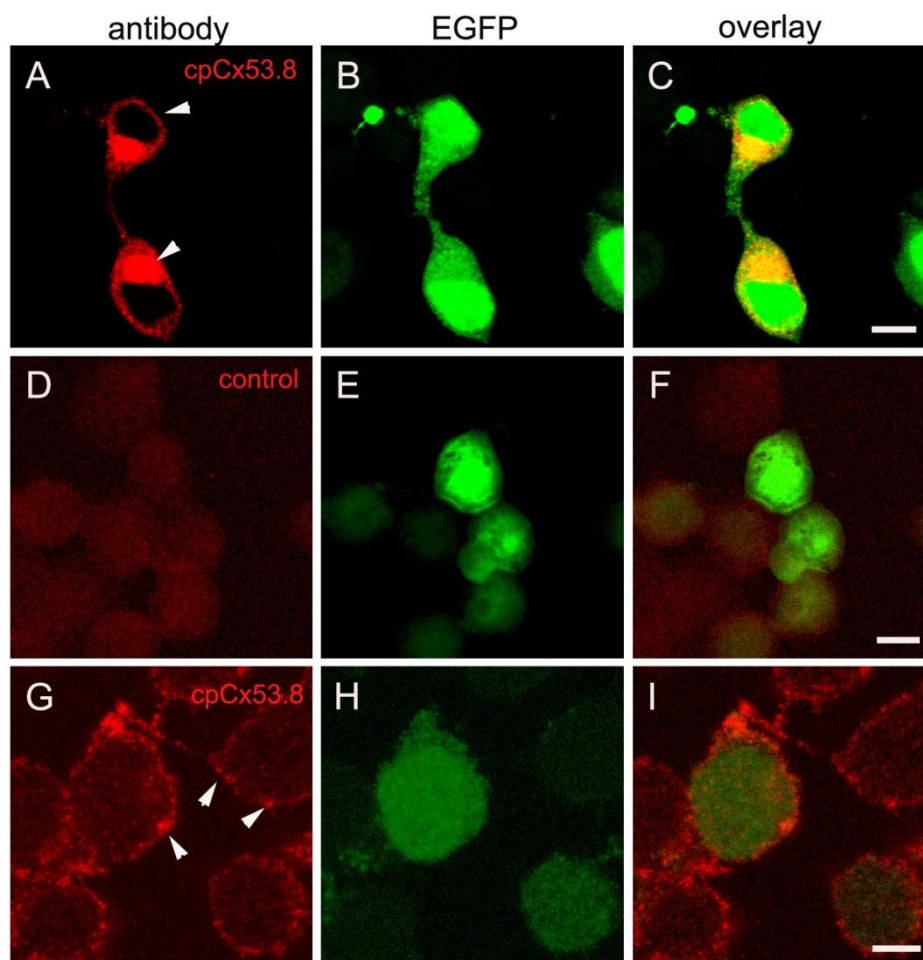
Figure 35: Detection of cpCx53.8 protein in transfected N2A cells. Transfected N2A cells are shown which were incubated with different antibodies (A, D, G) to prove the specificity of cpCx53.8 antibody. Pictures B, E and H show the EGFP fluorescence to prove the transfection success. The last column shows the overlay of the EGFP fluorescence and the immunostaining. A - F) cpCx53.8-pIRES2-EGFP transfected cells. A - C) Detection of proteins by anti-cpCx53.8 in cell membrane (white arrow upper cell). Aggregates of proteins were detected near the nuclei of the cell cells (white arrow lower cell). D - F) Incubation of cells with the second antibody alone to exclude its unspecific bindings. G - I) With pIRES2-EGFP transfected cells without expression of cpCx53.8. Non-specific detection of proteins in the cell membrane by anti-cpCx53.8 (white arrows). Scale: 5 µm.

To prove cross-reactions of cpCx53.8 antibody with zfCx52.7, N2A cells were transfected with zfCx52.7 in pIRES2-mRFP (Figure 36). In contrast to further transfections, a red fluorescent protein was expressed and consequently a green secondary antibody had to be selected. As positive control, cells were incubated with zfCx52.7 antibody (Figure 36; A – C). As negative control, cells were incubated

with secondary antibody alone (Figure 36; G – I). The second negative control, using pIRES2-mRFP for transfection, was missing because no vector was available. Transfected cells were finally incubated with cpCx53.8 (Figure 36; D – F) for proving cross-reactivity. By zfCx52.7 immunodetection, a weak signal was found in cell membrane indicating that the integration of this protein was rare. Besides, a high amount of immunoreactive proteins near the nuclei of the cells was detected (Figure 36; A; white arrowheads). The connexin characteristical punctate immunoreactive pattern indicated a correct expression of zfCx52.7. By anti-Cx53.8, proteins in the cell membrane were stained (Figure 36; D; white arrowheads).
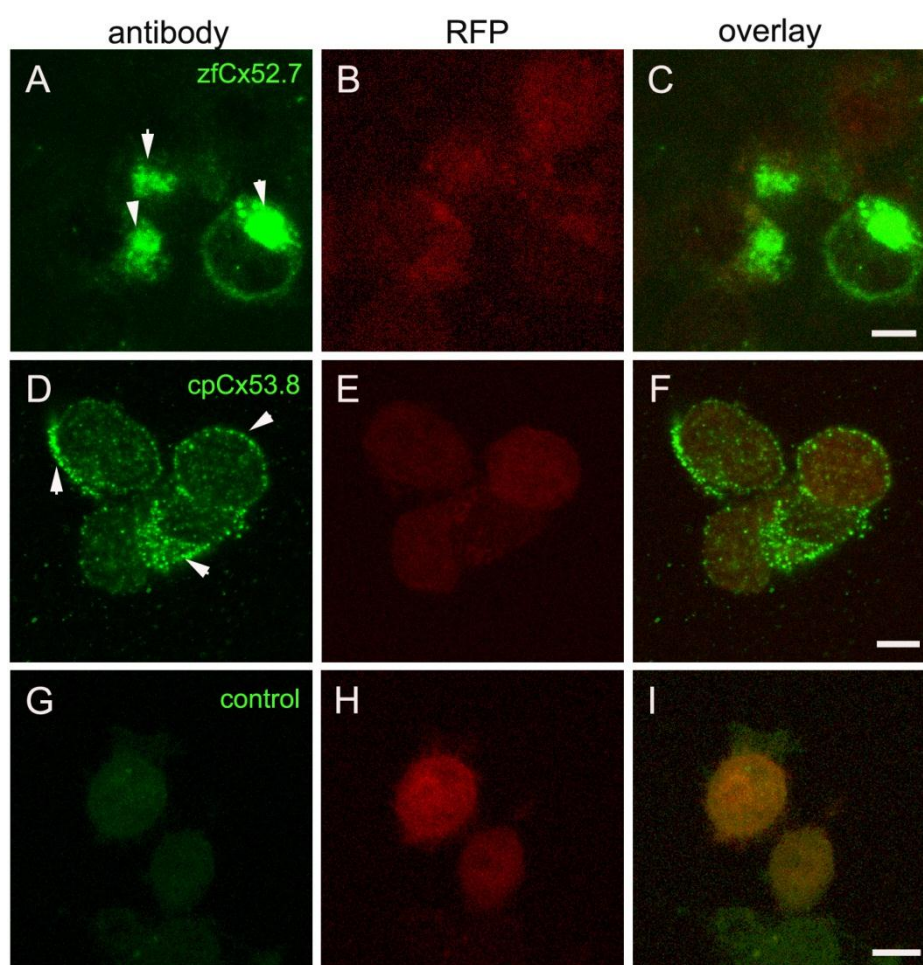
Figure 36: No cross-reactivity of zfCx52.7 protein and cpCx53.8 antibody. Transfected N2A cells are shown which were incubated with different antibodies (A, D, G) to analyze the specificity of anti-cpCx53.8. Pictures B, E and H show the RFP fluorescence, visualizing the transfection success. The last column shows the overlay of the RFP fluorescence and the immunostaining. A - I) Transfected cells using zfCx52.7-pIRES2-RFP. A - C) Detection of proteins by anti-zfCx52.7. Aggregations of proteins were detected near the nuclei of the cells (white arrows). The antibody detected also proteins which were located in the cell membrane. D - F) No specific detection of proteins by anti-cpCx53.8 (white arrows). G - I) Incubation of cells with the second antibody alone, to exclude its unspecific bindings. Scale: 5 µm.

In comparison to Figure 35 G, the same non-specific detection pattern was found in this approach, excluding a detection of zfCx52.7 by cpCx53.8 antibody. The negative control showed no labeled proteins (Figure 36; G). The RFP signal was significantly weaker than the EGFP signal.

For analyzing cross-reactions of cpCx53.8 antibody with zfCx52.9, N2A cells were transfected with zfCx52.9 in pIRES2-EGFP (Figure 37; A – I). Cells were incubated with zfCx52.9 antibody for positive control (Figure 37; A), with anti-cpCx53.8 to prove cross-reactions (Figure 37; D) and with the secondary antibody alone, for negative control (Figure 37; G and H). Another negative control was performed by transfection with pIRES2-EGFP vector and incubation with zfCx52.9 antibody (Figure 37; J). For positive controls, only a green fluorescing secondary antibody was available, causing that a differentiation between EGFP fluorescence and antibody was not possible. Nevertheless, putative gap junction plaques were detected which indicated the expression of zfCx52.9 protein (Figure 37; A; white arrow). By cpCx53.8 antibody, a few immunoreactive proteins were detected in the cell membrane. In comparison to the non-specific signal made by this antibody (Figure 35; G) even this staining was assumed to be non-specific and a detection of zfCx52.9 by cpCx53.8 antibody was excluded. All negative controls (Figure 37G; H, J) showed no immunoreactive proteins. In transfected cells without zfCx52.9, no gap junction plaques were detected by zfCx52.9 (Figure 37; J – L).
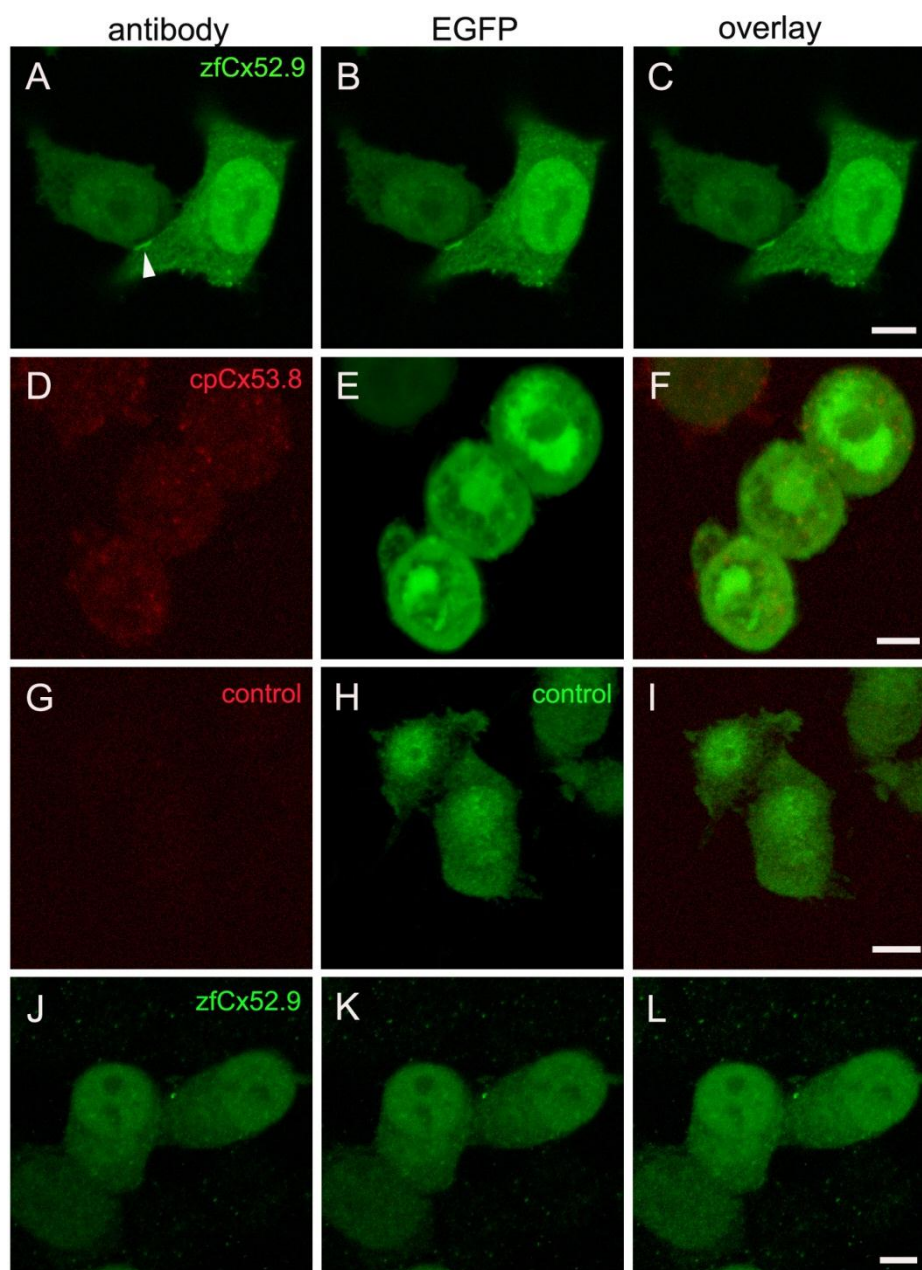
Figure 37: No cross-reactivity of zfCx52.9 protein and cpCx53.8 antibody. Transfected N2A cells are shown which were incubated with different antibodies (A, D, G, J) to prove the specificity of cpCx53.8 antibody. Pictures B, E, H and K show the EGFP fluorescence as indicator for the transfection success and the detected proteins by the antibody, because of a missing red secondary antibody. The last column presents the overlay of the EGFP fluorescence and the immunostaining. A - I) zfCx52.9-pIRES2-EGFP transfected cells. A - C) Detection of proteins by anti-zfCx52.9. The antibody detected proteins where the membranes of the two cells contact (A; white arrow). D - F) No detection of proteins by anti-cpCx53.8. G - I) Incubation of cells with just the second antibody to exclude its unspecific bindings. J - L) Cells transfected with pIRES2-EGFP vector. There was no detection of proteins by anti-zfCx52.9. In contrast to the connexin expressing cells there was less green fluorescence. Scale: 5 μm.

In summary, no cross-reactivity between cpCx53.8 antibody and the zebrafish connexins Cx52.7 and Cx52.9 was detected by protein biochemical and immunocytochemical methods. On western blot no specific protein band was

visualized, evidencing any detection of the zebrafish connexins. Only cpCx53.8 protein was specifically recognized by the antibody. In line with the immunocytochemical data, no specific protein was identified in zfCX52.7 and zfCx52.9 transfected cells by cpCx53.8 antibody, indicating no cross-reaction with the zebrafish connexins even in an over-expression system. Only the non-specific detection of intrinsic membrane proteins by the antibody was observed.

4. Discussion

This study showed evidence for cpCx43.4 and cpCx47.6 expression in GABAergic amacrine cells releasing nitric oxide as second neurotransmitter. Whereas cpCx47.6 is exclusively located in amacrine cells in the INL, cpCx43.4 expression was also identified in cells, located in the GCL of carp retina, putative displaced amacrine cells. In addition, there was evidence for a co-expression of acetylcholine in cpCx47.6 expressing cells.

By heterologous expression of cpCx43.4 and cpCx47.6 in N2A cells, a cross-reaction of the mouse Cx45 S3 antibody with both connexins was found. Adhesive structures resembling gap junction plaques were identified, indicating the correct integration and function of membrane proteins. The enhanced cell death by expression of cpCx43.4 is a hint of a formation to functional hemichannels.

By the second project, a cross-reaction between cpCx53.8 antibody and the connexins zfCx52.7 and zfCx52.9 was excluded. Neither on western blot nor by indirect immunofluorescence of transfected cells, a detection of zebrafish connexins was identified.

4.1 Expression of cpCx43.4 and cpCx47.6 in GABAergic amacrine cells

At the beginning of this work it was already known that cpCx43.4 and cpCx47.6 are expressed in cells INL and GCL in the carp retina. Localization of cpCx43.4 in putative amacrine cells was only analyzed by ISH at this time (Diploma thesis of Deutz, 2010 and Master thesis of Greb, 2010). The localization of cpCx47.6 was first analyzed by Beermann (Diploma thesis 2006) by means of ISH and FISH, who localized cpCx47.6 expression exclusively in amacrine cells in the INL. The expression in glycine, calbindin, caldendrin and calretinin positive cells was excluded by Immuno-FISH. Several reproductions of ISH indicated the expression of cpCx47.6 in the GCL (Diploma thesis of Deutz, 2010 and Master thesis of Greb, 2010). Because of different results, in this thesis a new vector construct with a specific sequence was used for producing RNA probes to approve and broaden the existing conclusions. As an improvement of previous efforts, the chosen sequence was 225 bp long so that alkaline hydrolysis was not necessary. To produce RNA probes for localization of cpCx43.4, an already existing and tested vector construct was used (Beermann, 2008). Alkaline hydrolysis of RNA probes was not necessary,

either. The alkaline hydrolysis could have led to the arbitrarily fragmentation of RNA probes, causing that small molecules occurred, which generate non-specific signalling. This could be the reason for the fail of reproduction of cpCx47.6 expression exclusively in cells in the INL, whereas the putatively non-specific labeling in the GCL was reproduced. Although the most variable region of both connexins was chosen, a similarity of 50% was calculated by the alignment. Because the sequences of even the most different region of cpCx43.4 and cpCx47.6 are very similar, cross-reactions of the RNA probes could not be excluded, but may be avoided by stringency washes and high temperature during hybridization of RNA probes.

First results made by ISH showed an expression of both connexins in the INL, as well as in GCL. Positive cells in INL were localized at the proximal region of the layer which indicated an expression of both connexins in amacrine cells. The signal was found in large cells with large nuclei. In some cases, the FISH indicated nuclear staining, leading to the assumption that transcripts were detected in the endoplasmic reticulum near the nucleus in which connexins are translated and integrated into the cell membrane. Signals were also found in the GCL for both connexins. cpCx43.4 expression in GCL was found in smaller and oval cells with large nuclei. In GCL, an equal amount of cells was detected as in INL. The expression pattern for cpCx47.6 differed from cpCx43.4 using ISH. The detection of cpCx47.6 transcripts was very infrequent in GCL. Large cells with large nuclei were detected in INL. Because of the rare events in the GCL, possible non-specific signals of alkaline phosphatase were suggested which were common at the border of tissue. At the pigment epithelium non-specific signalling occurred either. By means of FISH, no signals of cpCx47.6 expression were detected in the GCL anymore. This phenomenon traced back to the fact that non-specific signalling arises from endogenous alkaline phosphatase. The developmental time for AP signal was 4 times longer for cpCx47.6 than for cpCx43.4 probes making non-specific signalling by endogenous alkaline phosphatase visible. To inactivate the endogenous AP activity, a higher acid concentration of 0.2 M HCl should be used (Kiyama and Emson, 1991) if long signal development is needed. For cpCx47.6 detection by means of FISH, large and round cells in the proximal INL were detected, possessing large nuclei. Because of mRNA detection, no staining in the cell nucleus was found, but outside of it. A punctual detection near the nucleus was visible, indicating the detection of mRNA in the rough ER in which connexins were processed as described before. For cpCx43.4 FISH, the detection pattern was

similar to that from ISH. Large cells in the proximal INL were stained, whereas detected cells in GCL were oval and smaller. All positive cells showed relatively large nuclei. As well as in cpCx47.6 FISH, the ER was stained. To prove, whether the observed aggregations near the nuclei are located in the ER, an ER staining could be performed in combination with FISH. The proximal localization of INL detection patterns of both connexins was a hint for protein expression in amacrine cells. Because of a high fluorescent background, a shorter signal development should be chosen next time, reducing background and therefore heighten the specific signal of detected mRNA probes. Previous work examining the location of the homologous connexin mmCx45 reported that this connexin is expressed by two types of amacrine cells in the INL, A17 and the SWF (small wide-field; Pérez de Sevilla Müller et al., 2007) which consolidates this assumption. The cpCx43.4 mRNA positive cells in the GCL could either be ganglion cells or even displaced amacrine cells which are already described for a high number of organisms. The homologous connexin mmCx45 was proved to engage in coupling of bistratisfying ganglion cells (Schubert et al., 2005b) as well as an expression was found in displaced amacrine cells in the GCL (Pérez de Sevilla Müller et al., 2007). The latter even showed the existence of ten different displaced amacrine cells in the mouse retina. Further studies found out that in other species displaced amacrine cells were not uncommon. Thus, in the goldfish one (Marc et al., 1990), in the mouse ten (Gustincich et al., 1997) in the rat six (Perry and Walker, 1980), in the guinea pig eleven (Kao and Sterling, 2006) and in the cat retina four (Wässle et al., 1987) different displaced amacrine cell types were described.

For a functional analysis of cpCx43.4 and cpCx47.6 positive cells, FISH was combined with indirect immunofluorescence, so-called Immuno-FISH. The co-localization of FISH signal and antibody staining indicated an mRNA expression of the respective connexin in a cell type characterized by the expression of a particular protein (neurotransmitter) detected by indirect immunofluorescence. Because all amacrine cells in the vertebrate retina possess either the inhibitory neurotransmitter γ-aminobutyric acid (GABA) or glycine (Marc et al., 1994), antibodies against GABA and glycine were selected for a first characterization of cpCx43.4 and cpCx47.6 positive cells. Because GABA immunostaining had been performed ineffectively, but cpCx47.6 Immuno-FISH with glycine showed no matches (Diploma thesis Beermann, 2006), cpCx47.6 was supposed to be expressed in GABAergic amacrine cells.

By cpCx47.6 Immuno-FISH with GABA antibody, co-localizations of cpCx47.6 transcripts and GABA signal were found, leading to the assumption that this connexin is expressed by GABAergic amacrine cells because of its location in the proximal INL. In line with these results, Immuno-FISH with glycine antibody showed no co-localization, reproducing the results of Beermann (2006). For cpCx43.4, a co-localization with GABA immunoreactivity was found in INL as well as in GCL. No co-localization with glycine immunoreactivity was recognized. This indicated an expression of cpCx43.4 in GABAergic amacrine cells. This classically inhibitory neurotransmitter was detected in different types of amacrine cells as A10, A 13, A17 and A19 (Pourcho and Goebel, 1983; Marc et al., 1995). Expression of the heterologous connexin mmCx45 was proved in at least three different types of GABAergic amacrine cells (Pérez de Sevilla Müller et al., 2007; Dedek et al., 2009). By Pérez de Sevilla Müller et al. (2007) two different GABAergic ACs were characterized. One was located exclusively in the INL, whereas the second type was found in the INL and in the GCL. These amacrine cell types were identical to the S1 and S2 indoleamine-accumulating amacrine cells in the rabbit and similar to the A17 amacrine cells in cat retina. The A17 amacrine cell was also detected in the GCL as displaced one which expressed the mmCx45 (Pérez de Sevilla Müller et al., 2007). Dedek et al. (2009) described an interplexiform GABAergic AC stratifying in strata 4 and 5 in the IPL. This so-called IPA-S4/S5 cell was characterized as medium-field cell (Dedek et al., 2009). Because of their expression in similar loci, it is suggestible that cpCx43.4 and cpCx47.6 are expressed by resembling A17 amacrine cells in carp.

For further characterization of GABAergic amacrine cells expressing cpCx43.4 or cpCx47.6, different antibodies were chosen. Because co-localization of GABA and tyrosine hydroxylase (TH) were already reported for monkey, cat and mouse (Wässle and Chun, 1988; Haverkamp and Wässle, 2000; Andrade da Costa and Hoko, 2003) an antibody against TH was selected to prove putative co-localizations by Immuno-FISH. The antibody detected any immunoreactive proteins and consequently no matches of either cpCx43.4 or cpCx47.6 FISH staining with TH positive cells was identified. This could be based on a fail of TH antibody, because it is contrary to the results of Teranishi and Negishi (1986 & 1988), who showed TH positive GABAergic amacrine cells in carp retina. In order to improve Immuno-FISH with TH antibody, a different buffer system like TBS should be tested to achieve TH staining or a higher concentration of the antibody should be used. Because TH antibody was produced for labelling dopaminergic cells in rat and mouse, it is even

conceivable that this antibody does not detect proteins on carp retina. Beneficially, a different TH antibody should be used which is already tested on similar species as zebrafish or goldfish (Yazulla and Studholme, 2002; Yazulla and Zucker, 1988).

ChAT (choline acetyltransferase) antibody was used for Immuno-FISH because GABAergic amacrine cells using acetylcholine as neurotransmitter were reported for mouse retina (Haverkamp and Wässle, 2000; Kang et al., 2004; May et al., 2008). May et al. (2008) proved that all ChAT positive amacrine cells were even GABAergic, making up 17% of it. In this study ChAT antibody labeled a few cell bodies in the proximal INL. For cpCx43.4 mRNA expression, no matches with antibody staining were observed. But in combination with cpCx47.6 FISH, a co-localization of ChAT immunoreactive proteins with cpCx47.6 mRNA expression was found. This results gave rise to the suggestion that cpCx47.6 is expressed in a subtype of amacrine cells using GABA together with ChAT as neurotransmitter. The fact that not all cpCx47.6 positive cells contained ChAT, led to the assumption that another subtype of cpCx47.6 positive GABAergic amacrine cells existed. This study is the first providing evidence for the expression of cpCx47.6 in GABAergic and cholinergic amacrine cells. These subtypes of amacrine cells play an important role in direction selectivity (Amthor et al., 2002; Yoshida et al., 2001). In zebrafish large and round cholinergic amacrine cells were identified in the proximal INL which ramify in the strata 1, 2, 4 and 5 and even a weak staining of small cells in the GCL (putative displaced amacrine cells) was reported (Yazulla and Studholme, 2002). Because of the restricted time, the cholinergic GABAergic amacrine cells expressing cpCx47.6 were not characterized on branching. In contrast to the latter study, no displaced cholinergic amacrine cells were identified in the carp retina. Further research on this special cell type will be necessary in order to get an more detailed characterization of cpCx47.6 and its function. As side effect another subtype or types of GABAergic amacrine cells expressing cpCx47.6 could be identified.

Another approach to analyze the cell physiology of cpCx43.4 and cpCx47.6 expressing cells used a bNOS antibody, cross-reacting with brain-derived nitric oxide synthase. Co-localization of bNOS with GABA was already described in the retinas of several species, including cat, rabbit, rat, monkey and turtle (Müller et al., 1988; Vaney and Young, 1988; Oh et al., 1998; Haverkamp et al., 2000; Andrade da Costa and Hoko, 2003). FISH staining of cpCx43.4 and cpCx47.6 co-localizes with bNOS positive immunosignals. Even the cells in the GCL stained by cpCx43.4 FISH, matched with bNOS immunofluorescence. These results provided evidence for a

cpCx43.4 expression in GABAergic NO releasing amacrine cells, located in the INL and GCL and a cpCx47.6 expression in GABAergic NO releasing amacrine cells which were exclusively located in the INL. In literature, this type of amacrine cell is not only described for INL but as displaced amacrine cell in the GCL of different species (Kim et al.; 1999; May et al., 2008). Kim et al. (1999), who analyzed the immunoreaction of bNOS in rat, mouse, guinea pig, rabbit and cat retinae showed that all positive cells in INL possess large and round cell bodies with large nuclei. These morphological properties were shown by the identified bNOS positive cells in the carp retina in this study. In contrast, displaced NO positive amacrine cells in the GCL were smaller but own large nuclei in relation to their cytoplasm. Based on the structure of the nuclei and staining intensity, NO transmitting amacrine cells were generally classified into two major types in other reports (Oh et al., 1998; Kim et al., 2000). The type I cells showed large, extensively stained somata in the INL and were ramifying in stratum 3 in the IPL, while type II cells possessed small and weakly stained cell bodies in the INL and GCL which were ramifying in strata 1 and 5. In this study the cells stained by bNOS were suggested as type I in INL and the type II for displaced amacrine cells in GCL. Because no information about branches of cpCx43.4 and cpCx47.6 expressing amacrine cells were available, a detailed characterization cannot worked out. Amacrine cells are supposed to be the major source of nitric oxide for all cells in the INL and GCL in the mammalian retina (Kim et al., 1999). NO is a membrane passing gas, allowing that one cell could modulate several adjacent cells. It is already reported that NO release of amacrine cells activates cGMP synthesis in ON-bipolar cells and ganglion cells which results in activating of cGMP gated channels (Shiells and Falk, 1992; Ahmad et al., 1994; Gotzes et al., 1998). Different retinal processes are targeted by NO, suggesting that it is a powerful transmitter in mammalian eyes (cf. Pang et al., 2010). In context of connexins, NO also modulates the coupling of gap junctions. By now both the increase (Hoffmann et al., 2003) and decrease (Miyachi et al., 1990) of coupling of different gap junctions upon NO stimulation are described so that a positive or a negative influence of NO on cpCx43.4 and cpCx47.6 could not be estimated. The first coupling of NO releasing amacrine cells with ganglion cells was described by Pang et al. (2010). To date, a detailed characterization of NO positive GABAergic amacrine cells expressing either cpCx43.4 or cpCx47.6 in the case of branching and connectivity cannot be made. But in this study, the expression of cpCx43.4 and cpCx47.6 in NO positive GABAergic amacrine cells was proved for the first time. Whereas cpCx47.6 positive cells were exclusively located in the INL, the cpCx43.4 expressing cells were located in the INL and GCL. Because of their high similarity, it

was not surprising that both connexins were expressed in related or even the same cell type. Both connexins are expressed by a subtype of amacrine cells which is supposed to play an important role in the regulation and modulation of retinal processes, for example by modulating the phototransduction cascade caused by an increase of cone glutamate release (Savchenko et al., 1997) or an decrease of the coupling between cone bipolar and AII cells (Mills and Massey, 1995) and therefore further research on characterization and function of these connexins should be investigated.

The following table summarizes the results of the cell characterization by means of Immuno-FISH:

Table 6: Summarization of Immuno-FISH. (+) Co-localization of immunoreactive proteins and connexin expression. (-) No match of FISH signal and antibody staining. (x) Fail of Immunodetection

antibody connexin	GABA	glycine	TH	ChAT	bNOS
cpCx43.4	+	-	x	-	+
cpCx47.6	+	-	x	+	+

In this study an expression of cpCx43.4 and cpCx47.6 was identified in GABAergic amacrine cells releasing nitric oxide as second neurotransmitter. Whereas cpCx43.4 expression was found in amacrine cells located in the proximal INL and in putative displaced amacrine cells in the GCL, cpCx47.6 was exclusively expressed by amacrine cells in the proximal INL. For cpCx47.6 another subtype of GABAergic amacrine cells was identified using acetylcholine as second neurotransmitter.

4.2 Detection of cpCx43.4 and cpCx47.6 proteins by mmCx45 antibody

The genetic background of mmCx45, cpCx43.4 and cpCx47.6 and the therefore resulting sequence similarities led to the assumption that the Cx45 antibody, specific against mouse cytoplasmic loop, detects the homologous carp connexins. Previous work showed any detection of cpCx43.4 and cpCx47.6 fusion protein with EGFP by the serum 2 of this antibody (Diploma thesis Deutz, 2010). Previous studies in the Department of Neurobiology turned out that serum 2 is the most specific serum for histological and on western blot analysis on mouse. Because of sequence differences between carp and mouse connexins, the immunoreaction of all sera

should be tested in this study. Alignments calculated a sequence similarity of 44% for cpCx43.4 and 37% for cpCx47.6 and the peptide sequence of the antibody. The epitope matched with eight sequent amino acids of both connexins gave rise to the assumption that mmCx45 antibodies cross-react with cpCx43.4 and cpCx47.6 proteins.

In this study, the pIRES2-EGFP vector was selected for protein expression allowing a separate translation of EGFP and the respective connexin from one mRNA. Owning an IRES sequence, the connexin will be expressed without a disturbing tag and a correct protein folding will be ensured. Protein expression was performed in mouse neuroblastoma 2A (N2A) cells. First, the immunoreaction of the mmCx45 antibodies were tested on western blots which were prepared with crude subcellular fractions of transfected N2A cells. In order to detect cross-reactions with cpCx43.4 or cpCx47.6, crude fraction of N2A cells transfected with pIRES2-EGFP vector were prepared. Secondly, cross-reactions with both connexins were analyzed by immunocytochemical analysis of single protein and fusion protein linked to EGFP.

For analyzing cpCx43.4, first transfections of N2A cells were complicated. After transfection, an enhanced cell death was observed in cells transfected with cpCx43.4. Repeated transfections showed similar results. Nevertheless, crude fraction were prepared and analyzed on western blot. To visualize the success of transfection, EGFP was detected. In contrast to fractions without cpCx43.4, there was a weak detection of immunoreactive proteins at ~30 kDa indicating a low transfection rate. EGFP immunoreactive proteins were also found in the sample of the cytoplasmic loop for positive control of mmCx45 antibody. The blot was first incubated with the three sera of mmCx45 antibody, producing a massive staining of immunoreactive proteins. This led to the assumption that a complete stripping of mmCx45 antibodies failed, explaining the faint protein band in CL sample at ~32 kDa. Even the molecular weight was in line with the cytoplasmic loop of mouse connexin. By testing mmCx45 antibodies, only the third serum detected a specific protein band in the cpCx43.4 positive membrane fraction at ~45 kDa. At higher resolution the molecular weight of the detected protein band was found to be a tad smaller than the detected protein band in the mouse heart in which mmCx45 should be detected. These results indicated the cross-reaction of cpCx43.4 with mmCx45 antibody.

For further support, transfections were performed for immunocytochemical analysis. This method allows a direct detection of expressed protein in cells by antibodies and

additionally for analyzing their allocation in cells. Because of enhanced cell death after transfection with cpCx43.4, there was the assumption that the death could be caused by functional hemichannels of this connexin. For this reason, the calcium concentration of the culture medium was increased up to 5 mM. Calcium is a known modulator for gap junctions. There is evidence that increased extracellular calcium causes an uncoupling of gap junctions (Rose and Loewenstein, 1975) or even the closure of hemichannels (Pfahnl and Dahl, 1999). Expression experiments using cpCx43.4 in pIRES2-EGFP and cpCx43.4 in EGFP-N1 were performed in N2A cells to analyze cpCx43.4 as a single expressed and as fusion protein linked with EGFP. The latter has the advantage of possible protein localization by EGFP signal. Transfected cells were cultured in medium with normal calcium concentration (1.36 mM) and increased calcium concentration (5 mM) for the reason that differences can be compared. The transfection success with and without enhanced calcium was distinct. Growing at normal extracellular calcium, an enhanced cell death was recognized. In this study dead cells were identified by microscopic analysis. Dead cells were observed, swimming on the surface and being globular. Another indication for enhanced cell death was the color of the DMEM medium which was unchanged, an indication of an absent metabolism. Further analysis on cell death or viability could be measured by a trypan blue test, staining dead cells or a neutral red uptake (NRU) test, labeling viable cells, but was not performed in this study because of restricted time. Fluorescence images indicated cell death of only transfected cells, because untransfected cells were still alive, but none or just a few transfected cells survived. In contrast, cells cultured in enhanced extracellular calcium showed a high transfection rate and no cell death was observed. These results supported strong evidence that cpCx43.4 form functional hemichannels which are open at physiological conditions. The general function of these hemichannels are still unknown, but they are proposed to play a role in ephaptic communication, a special form of communication between anatomically and electrically proximate neurons through modulation of the extracellular potential (Kamermans and Fahrenfort, 2004). There is evidence that the extracellular potential in the synaptic terminal of photoreceptors is modulated by current, flowing through connexin hemichannels at the tips of the horizontal cell dendrites, which mediates negative feedback from horizontal cells to cones (Kamermans et al., 2001). Further studies reported that ATP, released via gap junction hemichannels from the pigment epithelium, regulates neural retinal progenitor proliferation (Pearson et al., 2005). In combination with the results achieved by Immuno-FISH, that cpCx43.4 is expressed in GABAergic, nitric oxide releasing amacrine cells, a highly sensitive modulation and regulation of

amacrine cells and adjacent cells by functional hemichannels and NO as a retrograde neurotransmitter could be suggested. Previous studies on NO indicated that even hemichannels were modulated by this neurotransmitter. For Pannexin 1, an enhanced hemichannel opening was recognized after NO stimulation (Zhang et al., 2008). The increased opening caused by NO is suggested to be forced by S-nitrosylation of cysteines, and not by the well-known NO/cGMP pathway (Zhang et al., 2008). NO is also suggested to be a donor for Cx43 permeabilization and S-nitrosylation by Retamal et al. (2006). Even for Cx46, a change in electrophysiological properties and permeability of hemichannels was reported, caused by NO (Retamal et al., 2009).

In order to analyze cross-reaction of mmCx45 S3 antibody with cpCx43.4 proteins, cells treated with enhanced calcium were incubated with anti-mmCx45 S3 or the respective preimmune serum 3, proving the specificity of the antibody. Incubation with the secondary antibody alone and mmCx45 S3 antibody incubation of cells transfected with the vector served as negative control. Both, negative controls and the preimmune serum, showed no immunodetection of proteins. The mmCx45 S3 antibody recognized proteins in the with cpCx43.4 transfected N2A cells. Either as single or fusion protein, putative gap junction plaques were detected between two contacted membranes of adjacent cells. As fusion protein these detected immunoreactive lines were also visible by EGFP fluorescence. These results indicated that a functional connexin was generated by N2A cells. Because connexins were processed in the rough ER, the immunoreactive proteins detected near the nucleus were suggested to be processed connexins. No aggregates of fusion protein were found near the nucleus by the antibody and EGFP signal. These results indicated a low protein expression possibly caused by enhanced calcium. Taken together, serum 3 of mmCx45 antibody detected cpCx43.4 protein. The expression of a functional connexin was shown by labeled aggregates near the nucleus and putative gap junction plaques. As expected, the EGFP allocation as single protein or in fusion with cpCx43.4 presented a different pattern. Whereas the EGFP fusion protein bound to cpCx43.4 is punctual located in the cytoplasm, the single EGFP protein was found in the cell nucleus and an overall fluorescence was observed. Several studies have shown that the ~27 kDa protein EGFP can diffuse bidirectional through the nuclear pore complex (NPC; Wei et al., 2003; Seibel et al., 2007) avoiding a diffusion linked to cpCx43.4. The punctual allocation of fusion protein linked to a connexin could be explained by the location in vesicular structures by which connexins were transported to the membrane.

For analysing cross-reactions of cpCx47.6 with mmCx45 antibodies, crude subcellular fractions were first studied on western blot. No enhanced cell death appeared after transfection with cpCx47.6 so that cells were cultured in normal medium. Results of detected EGFP on blots reflected the successful transfection of N2A cell. Immunoreactive proteins at ~30 kDa were visualized on connexin positive and negative fractions as equal bands. This result indicated an equal transfection rate. Like cpCx43.4, even cpCx47.6 was exclusively detected by the serum 3 of the three sera of mmCx45 antibody. Whereas no differences were visible in cpCx47.6 positive and negative fractions after incubation of S1 or S2, a strong difference was found between membrane fractions after incubation with S3. In cpCx47.6 positive membrane fraction, three highly immunoreactive protein bands of a molecular weight of ~45 kDa were detected. At higher resolution the middle band of the three were suggested to be the most immunoreactive one and putative cpCx47.6, leading to the assumption that the mmCx45 S3 antibody detected the expressed cpCx47.6 protein.

To underline the specific reaction of mmCx45 S3 antibody with cpCx47.6, immunodetection was performed in over-expressing N2A cells. Transfected cells were incubated with either mmCx45 S3 antibody or the respective preimmune serum 3 to analyze the specificity of the antibody. Incubation with the secondary antibody alone and anti-mmCx45 S3 incubation of cells transfected with the empty vector served as negative controls. Both negative controls and the preimmune serum showed no staining of immunoreactive proteins excluding unspecific staining. By mmCx45 S3 antibody, immunoreactive proteins were identified. High immunoreaction was predominantly found at positions, where two membranes of adjacent cells contacted, indicating putative gap junction plaques and therefore an expression of functional connexin protein. Even a higher immunoreaction was found near the nuclei of transfected cells, in the ER, where connexins were processed. The co-localization of EGFP fluorescence as fusion protein and antibody staining supported the assumption of cpCx47.6 protein detection by mmCx45 S3 antibody. Even here, the correct expression of functional cpCx47.6 protein was indicated by labeled putative gab junction plaques.

In summary, by western blot analysis and immunocytochemistry it was presented that mmCx45 S3 antibody detected both carp connexins, cpCx43.4 and cpCx47.6. On western blot, specific proteins bands in membrane fractions were identified at a molecular weight of ~45 kDa, indicating the cross-reaction of S3 antibody with

cpCx43.4 or cpCx47.6. By immunocytochemistry, putative gap junction plaques were detected by mmCx45 S3 antibody which supports the assumption of cross-reactivity with both connexins. Additionally, these results provided evidence of the correct expression and generation of cpCx43.4 and cpCx47.6 in N2A cells.

4.3 No cross-reaction of cpCx53.8 antibody and zebrafish connexins

Within a second project, the specificity of an antibody against cpCx53.8 was analyzed in the case of identifying two zebrafish connexins, zfCx52.7 and zfCx52.9. Because of the genetic background of the fish connexins possessing a molecular weight around ~50 kDa, it is likely that specific antibodies cross-react with other similar connexins. To exclude cross-reactions of cpCx53.8 antibody with zebrafish connexins, western blots and immunocytochemical analyses were performed with transfected N2A cells. Vector-DNA constructs for heterologous expression of the zebrafish connexins in N2A cells already existed and gave the main impulse for this project. First sequence alignments indicated that cross-reaction were unlikely. Nevertheless expression experiments were performed to approve the antibodies specificity in vivo.

First, crude subcellular fractions of transfected N2A cells were analyzed on western blots. Cells were transfected with zfCx52.7-pIRES2-mRFP and zfCx52.9-pIRES2-EGFP for detection of possible cross-reactions. Transfection with cpCx53.8 using pIRES2-EGFP served as positive and transfection with pIRES2-EGFP vector as negative control. No pIRES2-mRFP vector was available as negative control. Ponceau staining of all blots showed an equal amount of proteins in all fractions allowing a comparison of immunoreactivity. By EGFP or DsRed antibody, the transfection success was visualized. High immunoreactive protein bands were detected at an molecular weight of ~30 kDa (expected for EGFP and RFP) in nearly all fractions. Only the negative control on zfCx52.9 blot showed a low expression of EGFP which indicated a low transfection rate for pIRES2-EGFP vector. To show the specific immunodetection of the antibody, cpCx53.8 blot was incubated with cpCx53.8 antibody. The detection pattern showed highly immunoreactive protein bands at a molecular weight of ~54 kDa. An enrichment of immunoreactive proteins in the membrane fraction was found, as expected for a membrane protein. In connexin negative fractions no proteins were stained. In contrast to cpCx53.8 blot, no differences between connexin positive and negative fraction were identified,

neither on zfCx52.7 nor on zfCx52.9 blot, excluding a detection of both zebrafish connexins by cpCx53.8 antibody. Because an antibody diluted in BSA was selected for zfCx52.9 blot, a high number of unspecific protein bands were visualized. BSA is often used to stabilize peptides, but even generates unspecific labelling of proteins. At least the proteins of the zebrafish connexins were detected by their specific antibodies. This analysis had to be the last, caused by an antibody conjugated with alkaline phosphatase. With these antibodies only weak signalling was achieved after several stripping of blots. On zfCx52.7 blot, only a faint protein band was labeled at the expected molecular weight of ~53 kDa. For zfCx52.9, a new blot with the same samples was prepared because there was no signal at all. Using the new blot, a strong signal of protein bands was found at the molecular weight of ~53 kDa in connexin positive fractions. These results indicated that either the zebrafish antibodies or the AP conjugated secondary antibody cannot stand the stripping of blots. For this reason, the zfCx52.7 blot should also be repeated to reach a higher immunoreaction. Because of restricted time, it was not performed in this study.

Immunocytochemical analysis of cross-reactions of cpCx53.8 with zfCx52.7 and zfCx52.9 supported previous results. First, for positive control, cpCx53.8 antibody was tested on cpCx53.8 expressing cells. Antibody detected a high amount of immunoreactive protein aggregations near the cell nucleus suggested to be processed cpCx53.8 proteins. By negative controls with empty vector, a detection of membrane proteins was found in N2A cells. These immunoreactive proteins had to be considered by interpreting cross-reactions of the antibody. To analyze cross-reactions of antibody and zfCx52.7, expression of this connexin was first analyzed by their specific antibody. Using zfCx52.7 antibody, a massive staining of proteins was observed near the nucleus of the cell body which indicates the generation of connexins in the rough ER. By cpCx53.8 antibody, a few membrane proteins were detected similar to the negative control of cpCx53.8 antibody. Taken together, zfCx52.7 was not recognized by cpCx53.8 antibody.

Analyzing zfCx52.9 expression, only a green secondary antibody for detection of zfCx52.9 was available causing that differences of EGFP and the connexin expression cannot be made upon the colour of fluorescence. But a special characteristic of connexin detection was visible. A putative gap junction plaque was detected, evidencing the expression of zfCx52.9 in N2A cells. By cpCx53.8 antibody, for which a red antibody was available, no specific detection of connexins was recognized. A few membrane proteins were detected, typical for this antibody. This

results led to the assumption that cpCx53.8 antibody did not cross-react with zfCx52.9 protein.

To sum up, a detection of zfCx52.7 and zfCx52.9 by cpCx53.8 antibody was excluded. Neither on western blot nor by immunocytochemical analysis of expressed connexin, a cross-reaction of both zebrafish connexins with cpCx53.8 antibody was identified. Only a cross-reaction of cpCx53.8 antibody with intrinsic membrane proteins of N2A cells was recognized.

4.4 Perspectives

Recent findings of this study resulted in a number of new and interesting questions and raised starting points for further investigation.

The readout of cpCx47.6 ISH showed a strong background signal. In order to obtain less background caused by unspecific binding of alkaline phosphatase in GCL, a higher HCl concentration should be used and even the developmental time should be reduced, if possible.

To verify the specificity of signals, an immunostaining of mmCx45 S3 antibody combined with FISH should be performed. Here, a co-localization could be suggested, but is not proven, especially in the case of cpCx43.4 which is rarely expressed in the carp retina.

To cover the results of Immuno-FISH, a repetition with co-localized antibodies like GABA, ChAT and bNOS should be done. Because most sections were tangential, a repetition is necessary. TH production in cpCx43.4 and cpCx47.6 positive cells should be analyzed with another TH antibody, because no apparently functional antibody for carp retina was used in this study. By repetition of FISH, even a shorter signal development should be used in order to reduce high background fluorescence and therefore heighten the specific signalling of RNA probes.

For further characterization of GABAergic amacrine cells expressing either cpCx43.4 or cpCx47.6, any other neuropeptides could be proved in order to co-localize. Studies on co-localization of enkephalin and glucagon immunoreactivity reported their localization in GABAergic amacrine cells in the turtle retina (Zhang and Eldred, 2003). Further investigation in the tiger salamander retina found enkephalin and glucagon immunoreactive amacrine cells and other identified amacrine cells that express the neuropeptides Substance P and somatostatin (Yang

and Yazulla, 2004). In the goldfish retina neuropeptide Y, substance P and neurotensin immunoreactive amacrine cells were detected (Li et al., 1986; Osborne et al., 1985). As another possible neuropeptide, serotonin could be analyzed because it was already proved in one type of amacrine cell in zebrafish (Yazulla and Studholme, 2004). Even, Teranishi *et al.* (1987) reported two subtypes of 5HT positive amacrine cells in the carp retina.

A second possibility for characterizing GABAergic amacrine cells in the case of cpCx47.6 could be a double Immuno-FISH with bNOS and ChAT antibody to visualize feasible co-localisations of these two antibodies with cpCx47.6.

In order to characterize the properties and function of cpCx43.4 and cpCx47.6 on protein level, the produced vector construct could be used for electrophysiological experiments to characterize channel properties and their function.

By means of dye-coupling, the existence of functional gap junctions between transfected cells could be analyzed, using microinjection of fluorescent probes.

In the case of cpCx43.4, further research should be investigated on the existence of functional hemichannels. This could be performed by adding fluorescent probes to the culture medium of transfected N2A cells. By using different calcium concentrations, the gating of the hemichannels could be analyzed. Other known substances or factors like ATP or pH could additionally be used in different concentrations to modulate hemichannels in order to characterize putative modulating factors for channel gating. In addition, hemichannels could be analyzed by patch-clamp.

For the second project, to test the specificity of cpCx53.8 antibody, a repetition of the zfCx52.7 blot is necessary for a correct analysis of zfCx52.7 expression by alkaline phosphatase. Perhaps it could be useful to test a different secondary antibody conjugated with HRP which was not available in this study to get stronger results even after stripping of blots.

Another repetition could be performed to identify zfCx52.9 expression in N2A cells. Because only a green secondary antibody was available, the improvement of connexin expression was handicapped by the green fluorescent protein which was co-expressed in these cells. A repetition with a secondary antibody against chicken conjugated with a red fluorescent protein could support recent results.

In addition to the tested zebrafish connexins, a long series of connexins with a molecular weight similar to 50 kDa, especial mmCx50, zfCx55.5 or cpCX49.5, could

be analyzed on cross-reactions with cpCx53.8 antibody. New vector constructs could be cloned for a detailed analysis by western blot or immunocytochemistry.

5. Literature

Ahmad, I., Leinders-Zufall, T., Kocsis, J.D., Shepherd, G.M., Zufall, F. and Barnstable, C.J., (1994) Retinal ganglion cells express a cGMP-gated cation conductance activatable by nitric oxide donors. Neuron 12: 155 ± 165.

Amthor, F. R., Keyser, K. T. and Dmitrieva, N. A. (2002) Effects of the destruction of starburst-cholinergic amacrine cells by the toxin AF64A on rabbit retinal directional selectivity. Vis Neurosci.19: 495–509.

Andrade da Costa, B. L. and Hoko, J. N. (2003) Co-existence of GAD-65 and GAD- 67 with tyrosine hydroxylase and nitric oxide synthase in amacrine and interplexiform cells of the primate, Cebus apella. Vis Neurosci. 20: 153–163.

Beermann, S. (2006) Identifizierung und Lokalisation von cpCx43.4 und cpCx47.6-mRNA in der Karpfenretina mittels RACE-PCR und in situ Hybridisierung. Diploma thesis.

Bevans, C.G. and Harris, A.L. (1998) Direct high affinity modulation of connexin channel activity by cyclic nucleotides. J Biol Chem. 274 (6): 3720-3725.

Beyer, E.C., Paul, D.L. and Goodenough, D.A. (1987) Connexin43: a protein from rat heart homologous to a gap junction protein from liver. J Cell Biol. 105: 2621-2629.

Bloomfield, S.A. and Völgyi, B. (2009) Review: The diverse functional roles and regulation of neuronal gap junctions in the retina. Nature. 495-506.

Bruzzone, R., White, T.W. and Paul, D.L. (1996) Connections with connexins: the molecular basis of direct intercellular signalling. Eur J Biochem. 238: 1–27.

Cao, F., Eckert. R., Elfgang, C., Nitsche, J.M.., Snyder, S.A., Hulser, D.F., Willecke, K. and Nicholson, B.J (1998) A quantitative analysis of connexin-specific permeability differences of gap junctions expressed in HeLa transfectants and Xenopus oocytes. J Cell Sci. 111: 31-43.

Connaughton, V., Graham, D. and Nelson, R. (2004) Identification and Morphological Classification of Horizontal, Bipolar, and Amacrine Cells within the Zebrafish Retina. JCN 477: 371-385.

Cook, J. and Becker, D. (1995) Gap junctions in the vertebrate retina. Microsc.Res. Tech. 31: 408-419.

Dahl, G., Levine, E., Rabadan Diehl, C. and Werner, R. (1991) Cell/cell channel formation involves disulfide exchange. Eur J Biochem. 197: 141-144.

Dang, L., Pulukuri, S., Mears, A., Swaroop, A., Reese, B. and Sitaramayya, A. (2004) Connexin 36 in photoreceptor cells: studies on transgenic rod-less and cone-less mouse retinas. Mol Vis.11: 323-327.

Dedek, K., Schultz, K., Pieper, M., Dirks, P., Maxeiner, S., Willecke, K., Weiler, R. and Janssen-Bienhold, U. (2006) Localisation of heterotypic gap junctions composed of connexin45 and connexin36 in rod pathway of the mouse retina. Eur J Neurosc. 24: 1675-1686.

Dedek, K., Breuninger, T., Pérez de Sevilla Müller, L., Maxeiner, S., Schultz, K., Janssen-Bienhold, U., Willecke, K., Euler, T. and Weiler, R. (2009) A novel type of interplexiform amacrine cell in the mouse retina. European Journal of Neuroscience. 30: 217–228.

Demb J. and Pugh E. (2002) Connexin 36 forms synapses essential for night vision. Neuron. 36: 551-553.

Dermietzel, R., Kremer, M., Paputsoglu G., Stang, A., Skerrett, I., Gomes, D., Srinivas, M., Janssen-Bienhold, U., Weiler, R., Nicholson, B., Bruzzone, R. and Spray, D. (2000) Molecular and Functional Diversity of Neuronal Connexins in the Retina. J Neurosci. 20: 8331- 8343.

Deutz, K. (2010) Lokalisation und Charakterisierung von cpCx43.4 und cpCx47.6 mRNA in der Karpfenretina. Diploma thesis.

Eastman, S., Chen, T, Falk, M., Mendelson, T. and Iovine, K. (2005) Phylogenetic analysis of three complete gap junction gene families reveals lineage-specific duplications and highly supported gene classes. Genomics 87: 265 – 274.

Elfgang, C., Eckert, R., Lichtenberg-Frate, H., Butterweck, A., Traub, O., Klein, R., Hulser, D. and Willecke K. (1995) Specific permeability and selective formation of gap junction channels in connexin-transfected HeLa cells. J Cell Biol. 129: 805-817.

Evans, W. and Martin, P. (2002) Review: Gap junctions: structure and function. Mol Membr Biol. 19: 121-136.

Falk, M., Buehler, L., Kumar, N. and Gilula, N. (1997) Cell-free synthesis an assembly of connexins into functional gap junction membrane channels. EMBO J. 16: 2703–2716.

Fallon, R. F. and Goodenough, D. A. (1981) Five hour half-life of mouse liver gap-junction protein. J Cell Biol 90: 521-526.

Feigenspan, A., Teubner, B., Willecke, K. and Weiler, R. (2001) Expression of neuronal connexin36 in AII amacrine cells of the mammalian retina. J Neurosci. 21: 230–239.

Feigenspan, A., Janssen-Bienhold, U., Hormuzdi, S., Monyer, H., Degen, J., Söhl, G., Willecke, K. and Weiler, R. (2004) Expression of connexin36 in cone pedicles and OFFcone bipolar cells of the mouse retina. J Neurosci. 24: 3325–3334.

Gaietta, G., Deernick, T., Adams, S., Bouver, J., Tour, O., Laird, D., Sosinsky, G., Tsien, R. and Ellisman, M. (2002) Multicolor and electron microscopic imaging of connexin trafficking. Science. 296: 503–507.

Gilula, N. (1987) Topology of gap junction protein and channel function. Ciba Found Symp. 125: 128-139.

Goodenough, D. A. and Paul, D. L. (2003) Beyond the gap: functions of unpaired connexon channels. Nature Rev Mol Cell Biol. 4 285-295.

Goodenough, D. A. and Paul, D. L. (2010) Gap Junctions. Cold Spring Harb Sym.

Gotzes, S., de Vente, J. and Müller, F. (1998) Nitric oxide modulates cGMP levels in neurons of the inner and outer retina in opposite ways. Vision Neurosci. 15: 945 ± 955.

Greb, H. (2010) Molekularbiologische, biochemische und immuncytochemische Charakterisierung von Connexinen in der Karpfenretina. Master thesis.

Güldenagel, M., Söhl, G., Plum, A., Traub, O., Teubner, B., Weiler, R. and Willecke, K. (2000) Expression Patterns of Connexin Genes in Mouse Retina. J Comp Neurol. 425: 193-201.

Gustincich, S., Feigenspan, A., Wu, D. K., Koopman, L. J. and Raviola, E. (1997) Control of dopamine release in the retina: a transgenic approach to neural networks. Neuron. 18: 723–736.

Harris, A. L., Spray, D. C. and Benett, M. V. (1981) Kinetic properties of a voltage-dependent junctional conductance. J Gen Physiol. 11 (1): 95-117.

Haverkamp, S. and Wässle, H. (2000) Immunocytochemical analysis of the mouse retina. J Comp Neurol. 424: 1–23.

Hoffmann, A., Gloe, T., Pohl, U.and Zahler, S. (2003) Nitric oxide enhances de novo formation of endothelial gap junctions. Cardiovasc Res. 1; 60 (2):421-30.

Hombach, S., Janssen-Bienhold, U., Söhl, G., Schubert, T., Büssow, H., Ott, T., Weiler, R. and Willecke, K. (2004) Functional expression of connexin57 in horizontal cells of the mouse retina. Eur J Neurosci. 19: 2633-2640.

Hsieh, C. L., Kumar, N. M., Gilula, N. B. and Francke, U. (1991) Distribution of gene for gap junction membrane channel proteins of human and mouse chromosomes. Somat Cell Moll Genet. 17 (2): 191-200.

Janssen-Bienhold, U., Schultz, K., Gellhaus, A., Schmidt, P., Ammermüller, J. and Weiler, R. (2001) Identification and localization of connexin26 within the photoreceptor-horizontal cell synaptic complex. Vis Neurocsi. 18: 169-178.

Jansen-Bienhold, U., Dirks, P., Ommen, G., Hilgen, G. and Weiler, R. (2007) Connexins expressed in horizontal cells of the fish retina. Göttingen, Meeting of the German Neuroscience Society.

Kamermans, M., Kraaij, D. A. and Spekreijse, H. (2001) The dynamic characteristics of the feedback signal from horizontal cells to cones in the goldfish retina. J Physiol. 534. 2: 489-500.

Kamermans, M. and Fahrenfort, I. (2004) Ephaptic interactions within a chemical synapse: hemichannel-mediated ephaptic inhibition in the retina. Current Opinion in Neurobiology. 14: 531–541.

Kang, T. H., Ryu, Y. H., Kim, I. B., Oh, G. T. and Chun, M. H. (2004) Comparative study of cholinergic cells in retinas of various mouse strains. Cell Tissue Res. 317: 109–115.

Kao, Y.-H., Sterling, P. (2006) Displaced GAD65 amacrine cells of the guinea pig retina are morphologically diverse. Vis Neurosci. 23:931–939.

Kim, I. B, Lee, E. J., Kim, K. Y., Ju, W. K., Oh, S. J., Joo, C. K. and Chun, M. H. (1999) Immunocytochemical localization of nitric oxide synthase in the mammalian retina. Neurosci Lett. 267:193–196.

Kim, I. B., Oh, S. J. and Chun, M.H. (2000) Neuronal nitric oxide synthase immunoreactive neurons in the mammalian retina. Microsc Res Tech. 50: 112–123.

Kiyama, H. and Emson, P.C. (1991) An In Situ Hybridization Histochemistry Method for the Use of Alkaline Phosphatase-labeled Oligonucleotide Probes in Small Intestine. The Journal of Histochemistry and Cytochemistry. 39: 10. pp. 1377-1384.

Krüger, O., Plum, A., Kim, J. S., Winterhager, E., Maxeiner, S., Hallas, G., Kirchhoff, S., Traub, O., Lamers, W. H. and Willecke, K. (2000) Defective vascular development in connexin 45-deficient mice. Development. 127: 4179– 4193.

Kumar, N. and Gilula, N. (1992) Review: Molecular biology and genetics of gap junction channels. Semin Cell Biol. 3: 3-16.

Kumar, N. and Gilula, N. (1996) Review: The gap junction communication channel. Cell. 84: 381-388.

Lampe, P. D. and Lau, A.F. (2000) Regulation of gap junctions by phosphorylation of connexins. Arch Biochem Biophys. 384: 205-215.

Lampe, P. D. and Lau, A.F. (2004) The effects of connexin phosphorylation on gap junctional communication. Int J Biochem Cell Biol. 36: 1171-1186.

Löwenstein, W. (1981) Junctional intercellular communication: the cell-to-cell membrane channel. Physiol Rev. 61: 829-913.

Li, H.-B., Marshak, D., Dowling, J. and Lam, D.-K. (1986) Colocalization of immunoreactive substance P and neurotensin in amacrin cells of the goldfish retina. Brain Res. 366: 307-313.

Marc, R. E., Liu, W. L., Kalloniatis, M., Raiguel, S. F. and van Haesendonck, E. (1990) Patterns of glutamate immunoreactivity in the goldfish retina. J Neurosci. 10 (12): 4006-34.

Marc, R. (1994) Visualizing amino acids in the retina. Great Basin Visual Science Symposium, University of Utah. 1: 58-68.

Marc, R. and Cameron, D. (2001) A molecular phenotype atlas of the zebrafish retina. J Neurocyt. 30: 593-654.

Makowski, L., Caspar, D., Phillips, W. and Goodenough, D. (1977) Gap junction structures. II. Analysis of the X-ray diffraction data. J Cell Biol. 74: 629-645.

Maxeiner, S., Dedek, K., Janssen-Bienhold, U., Ammermuller, J., Brune, H., Kirsch, T., Pieper, M., Degen, J., Kruger, O., Willecke, K. and Weiler R. (2005) Deletion of Connexin45 in Mouse Retinal Neurons Disrupts the Rod/Cone Signaling Pathway between AII Amacrine and ON Cone Bipolar Cells and Leads to Impaired Visual Transmission. J Neurosci. 25: 566-576.

May, C. A., Nakamura, K., Fujiyama, F. and Yanagawa, Y. (2008) Quantification and characterization of GABA-ergic amacrine cells in the retina of GAD67-GFP knock-in mice. Acta Ophthalmol. 86 (4): 395-400.

Mills, S. L. and Massey, S. C. (1995) Differential properties of two gap junctional pathways made by AII amacrine cells. Nature. 377: 734–737.

Mills, S., O.Brien, J. J., Li, W., O´Brien, J. and Massey, S. (2001) Rod pathways in the mammalian retina use connexin 36. J Comp Neurol 436: 336-350.

Miyachi, E., Murakami, M. and Nakaki T. (1990) Arginine blocks gap junctions between retinal horizontal cells. NeuroReport. 1: 107–110.

Müller, F., Wässle, H. and Brecha, N. (1988) NADPH-diaphorase positive amacrine cells show GABA-like immunoreactivity in cat retina. Eur J Neurosci. 1: 153–159.

Mullins, K., Faloona, F., Scharf, S., Saiki, R., Horn, G. and Erlich, H. (1986) Specific enzymatic amplification of DNA in vitro: the polymerase chain reaction. Cold Spring Harb Symp. 51: 263-273.

O´Brien, J. J., Li, W., Pan, F., Keung, J., O´Brien, J. and Massey S. C. (2006) Coupling between A-type horizontal cells is mediated by connexin 50 gap junctions in the rabbit retina. J Neurosci. 26: 11624-11636.

Oh, S. J., Kim, I. B., Lee, M. Y., Chun, M. H. and Chung, J. W. (1998) nNOS-like immunoreactive neurons express GABA-like immunoreactivity in rabbit and rat retinae. Exp Brain Res. 120: 109–113.

Osborne, N., Patel, S., Terenghi, G., Allen, J., Polak, J. and Bloom, S. (1985) Neuropeptide Y (NPY)- like immunoreactive amacrine cells in the retina of frog and goldfish. Cell Tissue Res. 241: 651-656.

Pang, J. J., Gao, F. and Wu, S. M. (2010) Light responses and morphology of bNOS-immunoreactive neurons in the mouse retina. J Comp Neurol. 1; 518 (13): 2456-74.

Pearson, R. A., Dale, N., Llaudet, E. and Mobbs, P. (2005) ATP released via gap junction hemichannels from the pigment epithelium regulates neural retinal progenitor proliferation. Neuron. 2; 46 (5): 731-44.

Pérez de Sevilla Müller, L., Maxeiner, S., Willecke, K. and Weiler, R. (2007) Amacrine Cells Expressing Connexin 45 In The Mouse Retina. 31. Göttinger Neurobiologie Kongress.

Perkins, G., Goodenough, D. and Sosinsky, G. (1997) Three-dimensional structure of the gap junction connexon. Biophys J. 72: 533-544.

Perry, V. H. and Walker, M. (1980) Amacrine cells, displaced amacrine cells and interplexiform cells in the retina of the rat. Proc R Soc Lond B Biol Sci 208: 415–431.

Pfahnl, A. and Dahl, G. (1999) Gating of cx46 gap junction hemichannels by calcium and voltage. Pflugers Arch. 437 (3): 345-53.

Pfeffer, S. and Rothmann, J. (1987) Review: Biosynthetic protein transport and sorting by the endoplasmic reticulum and golgi. Annu Rev Biochem. 56: 829–852.

Pottek, M., Schultz, K. and Weiler, R. (1997) Effects of nitric oxide on the horizontal cell network and dopamine release in the carp retina. Vision Res 37 (9): 1091-1102.

Pourcho, R. and Goebel, D. (1987) Visualization of endogenous glycine in cat retina: an immunocytochemical study with Fab fragments. J Neurosci. 7: 1189 –1197.

Rapley, R. and Manning, D. L. (1998) Methods in molecular biology TM: RNA Isolation and Characterization Protocols. Hum Press Inc 86.

Retamal, M. A., Yin, S., Altenberg, G. A. and Reuss, L. (2009) Modulation of Cx46 hemichannels by nitric oxide. Am J Physiol Cell Physiol. 296: 1356-1363.

Retamal, M. A., Cortes, C. J., Reuss, L., Bennett, M. V. and Saez, J.C. (2006) S-nitrosylation and permeation through connexin 43 hemichannels in astrocytes: induction by oxidant stress and reversal by reducing agents. Proc Natl Acad Sci U S A. 103: 4475–4480.

Revel, J. and Karnovsky, M. (1967) Hexagonal array of subuntis in intercellular junctions of the mouse heart and liver. J Cell Biol. 33: C7-C12.

Risek, B., Guthrie, S., Kumar, N. and Gilula, N. B. (1990) Modulation of gap junction transcript and protein expression during pregnancy in the rat. J Cell Biol 110: 269-282.

Rose, B. and Loewenstein, W. R. (1975) Permeability of cell junction depends on local cytoplasmic calcium activity. Nature. 254 (5497): 250-2.

Rose, B., Simpson, I. and Loewenstein, W. R. (1977) Calcium ion produces graded changes in permeability of membrane channels in cell junction. Nature. 267: 625- 627.

Savchenko, A., Barnes, S. and Kramer, R. H. (1997) Cyclic-nucleotidegated channels mediate synaptic feedback by nitric oxide. Nature. 390: 694–698.

Schubert, T., Degen, J., Willecke, K., Hormuzdi, S., Monyer, H., and Weiler, R. (2005 a) Connexin36 mediates gap junctional coupling of alpha-ganglion cells in mouse retina. J Comp Neurol. 485: 191-201.

Schubert, T., Maxeiner, S., Krüger, O., Willecke, K. and Weiler, R. (2005 b) Connexin45 mediates gap junctional coupling of bistrafified ganglion cells in the mouse retina. J Comp Neurol. 490: 29-39.

Seibel, N. M., Eljouni, J., Nalaskowski, M. M. and Hampe, W. (2007) Nuclear localization of enhanced green fluorescent protein homomultimers. Anal Biochem. 368 (1): 95-9.

Shiells, R. A. and Falk, G. (1992) Retinal on-bipolar cells contain a nitric oxide-sensitive guanylate cyclase. NeuroReport. 3: 845 ± 848.

Simpson, I., Rose, B. and Loewenstein W. (1977) Size limitation of molecules permeating the junctional membrane channels. Science. 195: 294–296.

Söhl, G., Degen, J., Teubner, B. and Willecke, K. (1998) The murine gap junction gene connexin36 is highly experssed in mouse retina und regulated during brain development. FEBS Lett. 428: 27-31.

Söhl, G. and Willecke, K. (2003) Review: An Update on Connexin Genes and their Nomenklatur in Mouse and Man. Cell Commun and Adh. 10: 173-180.

Söhl, G., Maxeiner, S. and Willecke K. (2005) Review: Expression and functions of neuronal gap junctions. Nat Rev Neurosci. 6: 191-200.

Spray, D. C., Harris, A. L. and Bennett, M. V. (1981) Gap junctional conductance is a simple and sensitive function of intracellular pH. Science. 211: 712-715.

Steinberg, T. H., Civitelli, R., Geist, S. T., Robertson, A. J., Hick, E., Veenstra, R. D., Wang, H. Z., Warlow, P. M., Westphale, E. M. and Laing, J. G. (1994) Connexin43 and connexin45 form gap junctions with different molecular permeabilities in osteoblastic cells. EMBO J. 13: 744-750.

Teranishi, T. and Negishi, K. (1986) Dendritic morphology of dopaminergic cells revealed by intracellular injection of Lucifer yellow in fixed carp retina. Brain Res. 2; 370 (1): 196-9.

Teranishi, T., Negishi, K., Hidaka, S. and Naka, K. I. (1987) Dendritic morphology of indoleamine cells revealed by intracellular injection of lucifer yellow in fixed carp retina. Neuroscience. 22 (1): 323-9.

Teranishi, T. and Negishi, K. (1988) Regional difference in the dendritic morphology of dopamine cells in carp retina. Brain Res. 1; 467 (1): 9-17.

Towbin, H., Staehelin, T. and Gordon, J. (1979) Electrophoretic transfer of proteins from polyacrylamide gels to nitrocellulose sheets: procedure and some applications. Proc Natl Acad Sci. 76: 4350-4353.

Tsukamoto, Y., Morigiwa, K., Ueda, M. and Sterling, P. (2001) Microcircuits for night vision in mouse retina. J Neurocsi. 21 (21): 8616-8623.

Vaney, D. I. and Young, H. M. (1988) GABA-like immunoreactivity in NADPH-diaphorase amacrine cells of the rabbit retina. Brain Res 474: 380–385.

Volpi, E. V. and Bridger, J. M. (2008) FISH glossary: an overview of the fluorescence in situ hybridization technique. Biotechniques. 45 (4): 385-6, 388, 390.

Wässle, H., Chun, M. H. and Müller, F. (1987a) Amacrine cells in the ganglion cell layer of the cat retina. J Comp Neurol. 265: 391–408.

Wässle, H., Voigt, T. and Patel, B. (1987b) Morphological and immunocytochemical identification of indoleamine-accumulating neurons in the cat retina. J Neurosci. 7: 1574–1585.

Wässle, H. and Chun, M. H. (1988) Dopaminergic and indoleamine-accumulating amacrine cells express GABA-like immunoreactivity in the cat retina. J Neurosci. 8: 3383– 3394.

Wei, X., Henke, V. G., Strußbing, C., Brown, E. B. and Clapham, D. E. (2003) Real-time imaging of nuclear permeation by egfp in single intact cells. Biophys J. 84: 1317-1327.

Weiler, R., Pottek, M., He, S. and Vaney, D. (2000) Modulation of coupling between retinal horizontal cells by retinoic acid and endogenous dopamine. Brain Res Rev. 32: 121-129.

Yang, C. and Yazulla, S. (2004) Neuropeptide-Like immunoreactive cells in the retina of the larval tiger salamander: Attention to the symmetry of dendritic projections. J Com Neuro. 248: 105-118.

Yazulla, S. and Studholme, K. M. (2002) Neurochemical anatomy of the zebrafish retina as determined by immunocytochemistry. Journal of Neurocytology. 30: 551–592.

Yazulla, S. and Zucker, C. L. (1988) Synaptic organization of dopaminergic interplexiform cells in the goldfish retina. Visual Neuroscience. 1: 13–30.

Yoshida, K., Watanabe, D., Ishikane, H., Tachibana, M., Pastan, I. and Nakanishi, S. (2001) A key role of starburst amacrine cells in originating retinal directional selectivity and optokinetic eye movement. Neuron. 30 (3): 771-80.

Zhang, D. and Eldred, W. (2003) Colocalization of enkephalin-, glucagon-, and corticotropin-releasing factor-like immunoreactivity in GABAergic amacrine cells in turtle retina. Brain Res. 596: 46-57.

Zhang, L., Deng, T., Sun, Y., Liu, K., Yang, Y. and Zheng X. (2008) Role for Nitric Oxide in Permeability of Hippocampal Neuronal Hemichannels During Oxygen Glucose Deprivation. Jour of Neuros Res. 86: 2281–2291.

6. Appendix

6.1 Used materials and equipment

Table 7: Laboratory equipment

Materials	Company, place
Glass ware	Roth, Karlsruhe
Nitrocellulose membrane	Schleicher & Schüll, Dassel
Non-sterile plastic ware	Brandt, Gießen
Object slide, cover glass	Menzel-Gläser, Marienfeld
Pipette tips, reaction tubes	Peqlab, Eppendorf
Röntgenfilm Kodak X-O-MAT	Kodak, Stuttgart
Sterile injection	Neolab, Heidelberg
Sterile plastic cellculture ware	Falkon, Nunc, Sarstedt
Technical equipment, type	**Company**
Axiophot2 and Axia Cam MRc	Carl Zeiss AG, Jena
BioPhotometer	Eppendorf, Hamburg
Blotting chamber	Bio-Rad Laboratories, München
Centrifuge 5147R	Eppendorf, Hamburg
Centrifuge Minispin	Peqlab, Erlangen
Centrifuge, Type J2-21	Beckmann Coulter, Krefeld
Confocal Laserscannning Microscope TCS-SL	Leika Microsystems AG, Wetzlar
Electrophoresis chamber (SDS-PAGE)	Bio-Rad Laboratories, München
Electrophoresis chamber Compact XS/S	Biometra, Göttingen
Electrophoresis chamber Midi-Wide	Biometra, Göttingen
Incubator	Heraeus Instruments, Osterode
Cryostat-Microtome, Kryocut 5030	Bright Instrument Company Ltd.
Mastercycler® pro	Eppendorf, Hamburg
Oven	Appligene, Illkirch
pH-meter	WTW, Weilheim
Precision weighing machine, Sartorius 1106	Sartorius, Göttingen
Shaker	Edmund Buhler, Hechingen
Sterile working bench	Holten Laminair
Ultrasonic bath TransonicT460	Branson, Dietzenbach
UV-Transilluminator	Biometra, Göttingen
Vortex Reax 2000	Heidolph Instruments, Nürnberg

Table 8: Enzymes and kits

| Description	Company
Attractene Transfection Reagent	Qiagen, Hilden
DIG RNA-Labeling Mix	Roche, Mannheim
DNaseI, RNase free (10 U/µL)	Roche, Mannheim
DNaseI Amplification Grade (1 U/µL)	Invitrogen, Karlsruhe
DNA standard	Peqlab, Erlangen
dNTP Mix (10 mM)	Qiagen, Hilden
ECL-Westernblot Detection Kit	Amersham Bioscience, Freiburg
EcoRI (10 U/µL)	Roche, Mannheim
HindIII (10 U/µL)	Roche, Mannheim
HotStar Taq Polymerase Kit (2,5 U/µL)	Qiagen, Hilden
NucleoSpin®RNA II	Macherey-Nagel, Düren
Oligo(dT) Primer (500 µg/µL)	Promega, Mannheim
peqGOLD Plasmid Miniprep Kit I	Peqlab, Erlangen
pGEM-T-Easy Vector System	Promega, Mannheim
Protein standards: HMW, LMW	Sigma, St. Louis USA
PureYield^{TM} Plasmid Midiprep System	Peqlab, Erlangen
QIAEX II Gel Extraction Kit	Qiagen, Hilden
QIAquick PCR Purification Kit	Qiagen, Hilden
Rapid DNA Ligation Kit (5 U/µL)	Roche, Mannheim
RNasin Plus® RNase Inhibitor (40 U/µL)	Promega, Mannheim
Superscript^{TM} III Reverse Transcriptase (200 U/µL)	Invitrogen, Karlsruhe
T3 RNA Polymerase (20 U/µL)	Roche, Mannheim
T7 RNA Polymerase (20 U/µL)	Roche, Mannheim
TissueTek® Compound 4583	Sakura Finetechnical Co.Ltd
TSA™ Plus Fluorescence Systems	PerkinElmer, Bosten, USA
XhoI (10 U/µL)	Roche, Mannheim

Table 9: Primer

Name	Sequence (5' –> 3')	Annealing	Usage
Carp ß-actin for	GAG GTA TCC TGA CCC TGA AGT A	60 °C	cDNA purity
Carp ß-actin rev	CCA TCT CCT GCT CAA AGT CAA G	60 °C	cDNA purity
Cx43.4 XhoI F	ACTACTCGAGACCATGAGCTGGAGCTTTCT	56 °C	Cloning of cpCx43.4 into pIRES2-EGFP
Cx43.4 EcoRI R	ACGCTTAAGTCAAGCAAGGATCCCTTTTTC	56 °C	Cloning of cpCx43.4 into pIRES2-EGFP
Cx47.6 F ISH	ACTCTTCGCAAACGTCGAAGCCAT	59 °C	Cloning of cpCx47.6 into pBluescriptII KS+
Cx47.6 R ISH	TATTGTCCCTGCCCTCTCAGTGCT	59 °C	Cloning of cpCx47.6 into pBluescriptII KS+
Cx47.6 XhoI F	ACTACTCGAGACCATGAGTTGGAGCTTTCT	57 °C	Cloning of cpCx47.6 into pIRES2-EGFP
Cx47.6 EcoRI R	ACGCTTAAGTTAAATCCACACAGAAGT	57 °C	Cloning of cpCx47.6 into pIRES2-EGFP

Table 10: Antibodies

Name	Host	Dilution	Company	Usage
primary antibodies				
anti-mmCx45 S1	rabbit	1 : 1000	Pineda, Berlin	ECL
anti-mmCx45 S2	rabbit	1 : 1000	Pineda, Berlin	ECL
anti-mmCx45 S3	rabbit	1 : 1000	Pineda, Berlin	ECL, IF
preimmune serum 3 (Cx45)	rabbit	1 : 5000	Pineda, Berlin	ECL, IF
anti-zfCx52.7	chicken	1 : 250	Kamermans, M.; Netherlands Institute for Neuroscience	ECL, IF
anti-zfCx52.9	chicken	1 : 250	Kamermans, M.; Netherlands Institute for Neuroscience	ECL, IF

anti-cpCx53.8 S1 (3% BSA, 50% gycerine)	rabbit	1 : 750	Pineda, Berlin	ECL, IF
anti-EGFP	rabbit	1 : 10000	BD Bioscience Clontech, Heidelberg	ECL
anti-DsRed	rabbit	1 : 5000	BD Bioscience Clontech, Heidelberg	ECL
secondary antibodies				
anti-rabbit Alexa 568	goat	1 : 600	Invitrogen, Karlsruhe	IF
anti-rabbit Alexa 488	goat	1 : 600	Invitrogen, Karlsruhe	IF
anti-rabbit HRP conjugated	goat	1 : 3000	Biorad, Munich	ECL
anti-chicken AP	goat	1 : 250	Biorad, Munich	AP reaction
anti-DIG AP	-	1 : 500	Roche	ISH
anti-DIG POD	-	1 : 500	Roche	FISH

6.2 Used plasmids
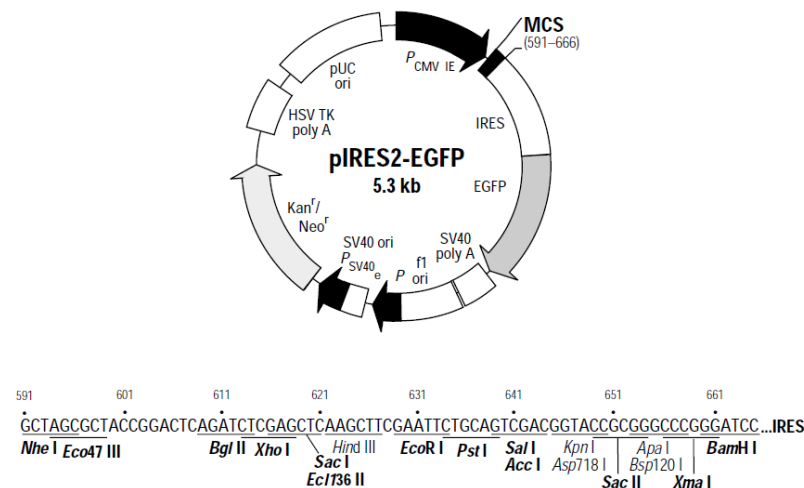
**Figure 38: pIRES2-EGFP plasmid.** pIRES2-EGFP (5300 bp) is an eukaryotic expression vector. It has a kanamycin resistance as well as an IRES (internal ribosome entry side) sequence to allow an separate expression of an integrated protein in the MCS (multiple cloning side) and the EGFP (enhanced green fluorescent protein) out of one mRNA (Mental Health Research Institute, University of Michigan).
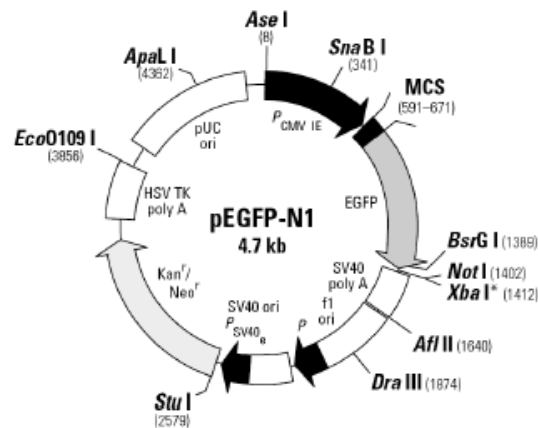
Figure 39: pEGFP-N1 plasmid. This plasmid (4700 bp) is a eukaryotic expression vector and was used to get a fusion protein out of the integrated connexin and EGFP. The vector has a kanamycin resistance (Clontech).
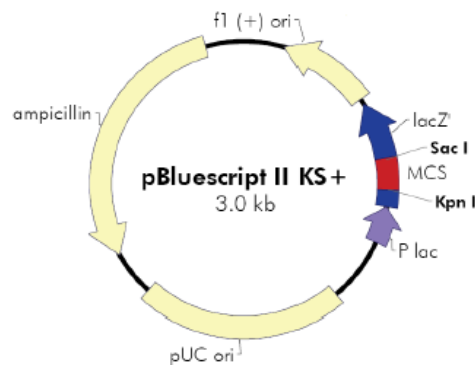
Figure 40: pBluescript II KS+ plasmid. This plasmid (3000 bp) is a cloning vector and was used to create mRNA probes. It has an ampicillin resistance and a lacZ gene for blue/with selection. The MCS (multiple cloning side) is flanked by two phage promoters (T3 and T7) for RNA transcription (Stratagene, Heidelberg).
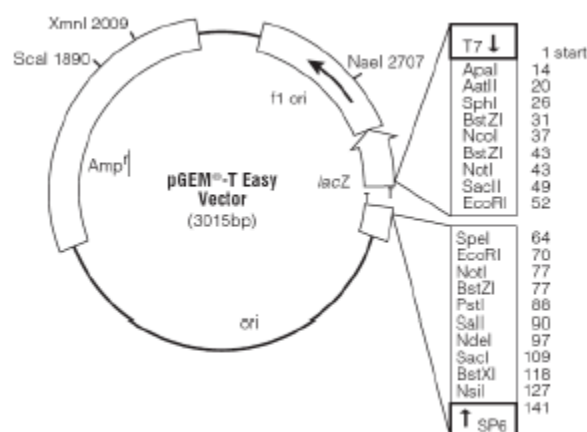
Figure 41: pGem-T-Easy plasmid. This plasmid (3015 bp) is a cloning vector used for subcloning of connexins into pIRES2-EGFP. It has an ampicillin resistance and a lacZ gene for blue/with selection (Promega).

6.3 Used protocols

6.3.1 RNA isolation

Kit: NuceloSpin RNA II (Machery – Nagel)

- preparation of carp eye
- extraction of the retina
- homogenisation of two retinae in 650 µL RAI and 7 µL ß-Mercaptoethanol with a
  20G injection (10 ups and downs)
- 50 µL RAI was used to wash the injection and added to the sample
- homogenate was pipette in violet column
- zentrifugation: 1 min; 11000 x g; RT
- flow through mixed with 700 µL 70% EtOH
- add to blue column
- zentrifugation: 30 sec; 11000 x g; RT
- flow through discarded
- a new 2 mL tube was used
- 350 µL MDB added to column
- zentrifugation: 1 min; 11000 x g; RT
- 95 µL DNase Reaction mixture were added to column
- incubated for 15 min at RT
- 200 µL RAII were added to column
- zentrifugation: 30 sec; 11000 x g; RT
- 600 µL RAIII were added to column
- zentrifugation: 30 sec; 11000 x g; RT
- 250 µL RAIII were added to column
- zentrifugation: 30 sec; 11000 x g; RT
- a new 1,5 mL Tube was used
- for elution 65 µL RNase free water were added to column
- zentrifugation: 1 min; 11000 x g; RT
- 40 µL of flow through were added again to column
- zentrifugation: 1 min; 11000 x g; RT
- 1 µL RNasin was added to elution

after isolation RNA was treated with DNase I (Invitrogen)

reaction: RNA [4 µg]   ?

                        RNasin   1.0 µL

                        DNase buffer   4.0 µL

                        DNase I   4.0µL

                        water   added to 40 µL

- short zentrifugation to collect all contents

- incubation: 15 min at RT

- 4 µL EDTA were added and mixed

- incubation: 10 min at 65°C

RNA was stored at -80°C.

6.3.2 Reverse transcription

SuperScript™ III Reverse Transcriptase (Invitrogen) was used

Reaction: RNA [2µg]   ?

                        Oligo (dt) primer   1.0 µL

                        dNTPs   1.0 µL

                        water   added to 30 µL

- ingredients were mixed

- incubation: 5 min at 65°C, then 1 min on ice

- short zentrifugation

- the following solutions were added:

                        5x first strand buffer   6.0 µL

                        0.1 M DTT   1.5 µL

                        RNasin   1.0 µL

                        Superscript III   1.0 µL

- short zentrifugation

- incubation: 5 min at 25°C

                   50 min at 50°C

                   15 min at 70°C

cDNA was stored at -80°C.

6.3.3 Transformation of One Shot^{TM} TOP10 E.*coli* cells

LB medium	LB agar plates
25g Luira Bertani medium	32g Lennox LB Agar
1 L water	1 L water

- 1 µL ligation mix was added to 50 µL competent cells

- incubation: 30 min on ice

                   1 min at 42°C

                   10 min on ice

- 150 µL LB was added

- incubation: 1h at 37°C on a shaker

- transformed cells were plated on plates with the respective antibiotic

6.3.4 DNA isolation

For a low amount of DNA, a minipreparation was performed by using Miniprep Kit I (PeqLab).

- 5 mL overnight culture was applied

- zentrifugation: 10 min; 5000 x g; RT

- 250 µL of Solution I was added a the pellet resuspended

- 250 µL of Solution II was added at the reaction converted 5 to 10 times

- 350 µL of Solution III was added at converted 3 times

- zentrifugation: 15 min; 11000 x g; RT

- sample was loaded on column

- zentrifugation: 1min; 11000; RT

- 500 µL HB buffer was added to column

- zentrifugation: 1 min; 11000 x g; RT

- flow through discarded

- 750 µL 100% EtOH was added to column

- zentrifugation: 1 min; 11000 x g; RT

- flow through discarded

- zentrifugation: 1 min; 11000 x g; RT

- elution: 50 µL EB was added to column

- zentrifugation: 1 min; 11000 x g; RT

DNA was stored at -20°C.

For a high amount of DNA, a midipreparation was performed, using PureYield™ Plasmid Midiprep System (Promega).

- 200 mL overnight culture was applied
- bacteria were pelleted by 5000 x g for 10 minutes
- 6 mL of Resuspension Solution was added to resuspend the bacteria
- 6 mL of Cell Lysis Solution was added and inverted 5 times
- incubation: 3 min at RT
- 10 mL of Neutralization Solution was added and inverted 3 times
- a blue Clearing Column was placed on top of a white Binding Column onto a
  vacuum manifold
- sample was added to the Clearing column and vacuum was applied
- Clearing column was discarded after the sample has passed
- 5 mL of Endotoxin Removal Solution was added to the column and vacuum was
  applied
- 20 mL Column Wash Solution was added to the column and vacuum was applied
- 30 seconds after the sample has passed the vacuum was slowly released
- for elution: 600 µL water was added to the column and zentrifugated in and
  swinging bucket rotor
- zentrifugation: 5 min; 2000 x g; RT

DNA was stored at -20°C.

6.3.5 Transfection of N2A cells

N2A cells were cultured at 37°C, 5 % CO2 und 95 % relative air humidity in DMEM (Penicillin/Streptomycin, 10 % FCS). One day before transfection cells were planted on either coverslips (50000 cells) for immunocytochemical analysis or on 6 cm dishes (500000 cells) for protein biochemical analysis. After 24 h cells were transfected. For coverslips 60 µL DMEM (without additives) was used and 1 µL Attractene (Qiagen) and 0.4 µg DNA was added. The mixture was incubated for 10 to 15 minutes and then added to the cells. 24 h after transfection the medium was changed. After another 24 h cells were analyzed by immunocytochemistry or protein biochemistry.

6.3.5.1 Immunocytochemical analysis

<u>0.2 M PB</u>   <u>4% PFA</u>

0.2 M Na_2HPO_4 1 g paraformaldehyde

0.2 M NaH_2PO_4 25 mL 0.1 M PB

→ mix to pH7.4   1M NaOH till solution gets claer

- coverslips were washed with 0.1 M PB (pH 7.4)

- incubation steps (at RT):

 - 500 µL 4% PFA; 30 min

- 3 x 10 min in 1 mL 0.1 M PB

- 1h in 1 mL blocking solution (0.1 M PB, 0,5% Triton-X 100, 10% normal goat serum)

- 200 µL primary antibody (diluted in 0.1 M PB, 0.5% Triton-X100) over night at 4°C

- 3 x 10 min in 1 mL 0.1 M PB

- 2h in 200 µL secondary antibody (diluted in 0.1 M PB, 0.5% Triton-X100)

- 3 x 10 min in 0.1 M PB

Coverslips were embedded in Vectashield and stored at 4°C.

6.3.5.2 Protein biochemical analysis

<u>HP2</u>   <u>TBST</u>   <u>SDS running buffer (2 L)</u>

50 mM Tris/HCl pH 7.4   20 mM Tris/HCl   28,8 g glycine

2 mM EGTA pH 7.4   150 mM NaCl   6 g Tris/HCl

2 mM EDTA pH 7.4   0.2% Tween-20   2 g SDS

1 mM DTE   → adjust pH 7.4

1mM PMSF

2 µg/µL leupeptine   <u>SDS sample buffer (10mL)</u>

5 µg/µL aprotinine   3 mL glycine

0.1 M orthovanadate   0.3 mL ß-mercaptoethanol

                         0.9 g SDS

<u>Strip Solution 1</u>   3.75 mL 0.5 M Tris buffer (pH 6.8)

0.01 M Tris/HCl   add water up to 10 mL

1% SDS

10 mM ß-mercaptoethanol

Strip solution 2

0.1 M Tri-natriumcitrate dihydrolate

1% SDS

Transfer buffer (2 L)   10 mM ß-mercaptoethanol

6 g Tris/HCl   → adjust pH 3.0

28.8 g glycine

10% SDS

Crude subcellular fractionation

- homogenisation of cells of one 6 cm dish in 100 µL HP2 with a glass potter (10 ups and downs)
- two identical transfected dishes were fused
- 25 µL of the total homogenate (TH) was separated and stored at -20°C
- zentrifugation: 10 min; 1500 rpm; 4°C
- the soluble fraction (SF) was transferred into a new 1,5 mL tube
- the pellet was resuspended in 30 µL HP2 and zentrifugated for 10 min at 1500 rpm at 4°C
- the soluble fraction was added to SF
- the pellet (P1) was resuspended in 60 µL HP2 and stored at -20°C
- SF was zentrifugated for 1 h at 14000 rpm at 4°C
- the soluble fraction (CF) was transferred into new 1.5 mL tube and stored at -20°C
- the pellet (P2) was resuspended in 60 µL HP2 and stored at -20°C

SDS-PAGE

- proteins of the fractions were separated by SDS gel for 120 min at 160 V.

Western blot

- protein were transferred from SDS gel onto a nitrocellulose membrane overnight at 40 V in a blotting tank

ECL

incubation steps:
- 3 x 10 min in TBST

- 1 h in TBS with 5% milk powder

- primary antibody diluted in TBST with 0,2% milk powder over night at 4°C

- 3 x 10 min in TBST

- 2h secondary antibody conjugated in HRP diluted in TBS

- 3 x 10 min in TBST

- 800 µL of both solution in the ECL kit were mixed, disposed onto the blot and incubated for one minute

- light response was measured on a radiographic film

6.3.6 Production of DIG labeled RNA probes

preparative restriction

probe	antisense	sense
DNA	11 µg	11 µg
Restriction buffer	10 µL	10 µL
Restriction enzyme	5 µL	5 µL
water (RNase free)	added up to 100 µL	added up to 100µL

- incubation: 2,5 h at 37°C

- control of restriction on agarose gel

- DNA purification (elution in 30 µL EB)

in vitro transcription

probe	antisense	sense
linear DNA	1.0 µg	1.0 µg
10x Transcription buffer	2.0 µL	2.0 µL
RNasin	1.0 µL	1.0 µL
10x DIG-Mix	2.0 µL	2.0 µL
RNA-Polymerase	1,5 µL	1,5 µL
water (RNase free)	added up to 20 µL	added up to 20 µL

- incubation at 37°C overnight

- 1 µL DNase I was added

- incubation: 15 min; 37°C

- 2 µL 0.5 M EDTA (pH 8.0) was added

precipitation of RNA

- 2,5 µL 4 M LiCl and 75 µL 100% EtOH (-20°C) were added and mixed

- incubation: 1h at -80°C

- zentrifugation: 15 min; 13000 rpm; 4°C

- soluble fraction was discarded

- pellet was resuspended in 50 µL 70% EtOH (-20°C)

- zentrifugation: 10 min; 13000 rpm

- soluble fraction was discarded

- pellet was dried 30 min at RT

- pellet was resuspended in 100 µL water (RNase free)

- 1 µL RNasin was added

- RNA probes were stored at -80°C

6.3.7 *In situ* hybridization

Carbonate buffer (pH 10.2)
60 mM Na_2CO_3
40 mM $NaHCO_3$

0.1 M HCl
4.1 mL HCl (38 %)
495.9 mL H_2O

10x PBS (pH 7.4)
87.6 g NaCl
2.25 g NaH_2PO_4
14.4 g Na_2HPO_4
add to 1 L with H_2O

1x PBS (pH 7.4)
100 mL 10x PBS pH 7.4
900 mL H_2O

4% PFA
8 g paraformaldehyde
180 mL 1x PBS pH 7.4 (60°C)
x drops of 1 M NaOH
add to 200 mL with 1x PBS pH 7.4

20x SSC (pH 7.4)
87.65 g NaCl
36.47 g tri-Natriumcitrat
add to 500 mL H_2O

acetic anhydride/triethanolamine (pH 8,0)

3 g triethanolamine

180 mL H_2O

0.5 mL acetic anhydride

add to 200 mL with H_2O

0.2x SSC (pH 7.4)

10 mL 20x SSC

990 mL H_2O

prehybridization buffer

30.5 mL H_2O

5 mL 50x Denhardt´s solution

5 mL 1 M Tris (pH 7.5)

5 mL 0.5 M EDTA

2.5 µL tRNA (10 mg/mL)

2 mL 1 M NaCl

50 mL formamide

storage at -20°C

10x hybridization buffer

2.8 mL H_2O

2 mL 50x Denhardt´s solution

2 mL 1 M Tris (pH 7.5)

200 µL 0.5 M EDTA

2 mL tRNA (25 mg/mL)

1 mL poly-A (10 mg/mL)

storage at -20°C

1x hybridization buffer

25 mL formamide

5 mL 10x hybridization buffer

3.33 mL 5 M DTT

10 mL dextran sulphate (50 %)

3.765 mL H_2O

storage at -20°C

50x Denhardt´s solution

25 mL H_2O

0.5 g BSA

0.5 g Ficoll

0.5 g polyvinylpyrollidin (PVP)

add to 50 mL with H_2O

storage at -20°C

50% formamide/0.1x SSC

300 mL 0.2x SSC

300 mL formamide

P1 buffer (pH 7.5)

100 mL 1 M Tris (pH 7.5)

30 mL 5 M NaCl

add to 1 L with H_2O

P3 buffer (pH 9.5)

25 mL 1 M Tris (pH 9.5)

5 mL 5 M NaCl

12.5 mL 1 M MgCl2

add to 250 mL with H_2O

P4 buffer (pH 8.0)

2.5 mL 1 M Tris (pH 8.0)

0.5 mL 5 M EDTA

add to 250 mL with H_2O

MBM

400 mL P1 buffer (60°C)

4 g Blocking Reagent

2 g BSA Fraktion V

storage at -20°C

50% dextran sulphate

5 g dextran sulphate

10 mL H_2O

dissolved in water bath

storage at -20°C

Developer

10 mL P3 buffer (pH 9.5)

35 µL NBT (100 mg/mL)

35 µL BCIP (50 mg/mL)

10 µL levamisole (250 mg/mL)

storage at 4°C, light protected

- 20 µm cryosections were prepared and dried on a warm plate for 20 min

- glass slides were placed into glass cuvettes

- incubation steps:

- 30 min in 4% PFA at 4°C

- change of cuvettes

- 3 x 10 min in 1 x PBS

- 5 min in 70% EtOH

- 2 x 10 min in water

- 5 min in 0.1 M HCl

- change of cuvettes

- 3 x 10 min in 1 x PBS

- 20 min in 0.25% acetic anhydride / 0.1 M triethanolamine

- change of cuvettes

- 3 x 10 min in 1 x PBS

- 5 min in 70% EtOH

- 5 min in 80% EtOH

- 5 min in 95% EtOH

- sections were dried for 1h

- sections were revolved with a pap pen and put in a humid chamber

- sections were covered with 200 µL prehybridization buffer and incubated for 3h at 37°C

- RNA probes were diluted in hybridization buffer [1 ng/µL]

- 150 µL hybridization-mix were used to cover the sections

- incubation at 55°C overnight in a humid chamber

- sections were placed in cuvettes

- 1 min in 0.2 x SSC at 55°C

- 2 x 30 min in 0.2 x SSC at 55°C

- 3 x 60 min in 0.1 x SSC with 50% formamide at 55°C

- change of cuvettes

- 10 min in 0.2 x SSC at RT

- 10 min in P1 at RT

- 30 min in MBM at RT

- sections were placed in a humid chamber

- sections were covered with 150 µL of in MBM diluted (1:500) anti-DIG AP (Roche)
  and incubated overnight at 4°C

- sections were placed in cuvettes

- 2 x 15 min in P1 at RT

- 5 min in P3 at RT

- section were placed in a humid chamber and covered with 300 µL developer

- signal development lasted 45 min to 5h

- 15 min in P4 at RT

- 5 min in water

- sections were embedded with Fluoromount

6.3.8 Fluorescence ISH

<u>TNT</u>   <u>2% H_2O_2</u>

0.05 % Tween-20   13 mL H_2O_2 (30 %)

in P1 buffer (pH 7.5)   187 mL 1x PBS (pH 7.4)

- see ISH till washing with 0.1 x SSC with 50% formamide at 55°C

then

- 10 min in 1 x PBS at RT

- 15 min in 2% H2O2 in PBS at RT

- 30 min in MBM

- sections were placed in a humid chamber

- sections were covered with 150 µL of in MBM diluted (1:500) anti-DIG POD
  (Roche) and incubated overnight at 4°C

- sections were placed in cuvettes

- 3 x 10 min in TNT

- signal development by TFA System

      - 100 µL of a 1:50 dilution of Fluorescin in 1x Amplification Diluent were used

      - signal development lasted 7 minutes

- 3 x 10 min in TNT

- sections were embedded with Vectashield

6.3.9 Immuno-FISH

- after microscopic analysis of FISH cover glasses were removed from the sections

- 3 x 10 min in 0.1 M PB

- 1h in 0.1 M PB with 10% NGS or DKS and 0.3% Triton-X100 at RT

- primary antibody diluted in 0.1 M PB with 0.3% Triton-X100 overnight at 4°C

- 3 x 10 min in 0.1 M PB

- secondary antibody diluted in 0.1 M PB with 0.3% Triton-X100 at RT

- 3 x 10 min in 0.1 M PB

- sections were embedded in Vectashield

Acknowledgements

First of all I have to thank Apl. Prof. Dr. Ulrike Janssen-Bienhold, who gave me the opportunity to work on this interesting project and patiently guided my work and helped me to improve my research skills with suggestions and ideas. It was always a pleasure to discuss my work with her.

Many thanks go to Dr. Karin Dedek for the adoption of the second certificate and for correcting this work before.

I would like to thank Prof. Dr. Reto Weiler for the opportunity to complete my master thesis in the Department of Neurobiology.

Big thanks go to Regina Herrling, Petra Bolte and Helena Greb, who could always find the time for discussions or explanations and therefore improve my work. Thank you for your patience and to Regina, thanks correcting this work before.

I am thankful to Susanne Wallenstein, Bettina Kewitz, Dr. Konrad Schultz and Hoto Meyer for their support and helpfulness during my laboratory work.

I thank all members of the Department of Neurobiology, particularly Nadine Mellies, Katharine John, Nina Hoyer, Birthe Dorgau, Sebastian Hermann, and Katharina Schmidt for a friendly working atmosphere, their support and motivation.

I cordially thank my mother, Ulrike Seggewiß, who has supported me throughout my studies, both morally and financially, and without whom this study would not have been possible.

Finally, special thanks to my boyfriend, Timur Schipper for his moral support and his motivation and encouragement during my work.

Erklärung

Hiermit versichere ich, dass ich diese Arbeit selbstständig verfasst und keine anderen als die angegebenen Quellen und Hilfsmittel benutzt habe. Außerdem versichere ich, dass ich die allgemeinen Prinzipien wissenschaftlicher Arbeit und Veröffentlichung, wie sie in den Leitlinien guter wissenschaftlicher Praxis der Carl von Ossietzky Universität Oldenburg festgelegt sind, befolgt habe.

. . . .

Nicole Seggewiß